Funded by
the European Union

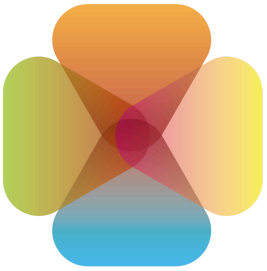

ACCREU
Assessing
Climate Change
Risk in EUrope

Impacts on Ecosystems & Biodiversity

GA number: 101081358; Funding type: HORIZON-CL5-2022-D1-07-two-stage

Deliverable number (relative in WP)	D2.4
Deliverable name:	Impacts on ecosystems & biodiversity
WP / WP number:	WP2
Delivery due date:	Project month 25 (June 2025)
Actual date of submission:	15 July 2025
Dissemination level:	Public
Lead beneficiary:	IIASA
Responsible scientist/administrator:	Gemma Gerber (IIASA); Amanda Palazzo (IIASA)
Contributor(s):	**IIASA**: Amanda Palazzo Andre Nakhavali Gemma Gerber Juliana Arbelaez-Gaviria Martin Jung **DTU**: Martin Drews Ophélie Georgina Marie Meuriot Jorge Soto Martin; **GCF**: Sebastiano Bacca Jochen Hinkel Daniel Lincke
Internal reviewer:	Francesco Bosello

Funded by the European Union. Views and opinions expressed are however those of the author(s) only and do not necessarily reflect those of the European Union. Neither the European Union nor the granting authority can be held responsible for them.

Changes with respect to the DoA

There are no changes with respect to the description of work outlined in Task 2.4 of the ACCREU Grant Agreement.

Dissemination and uptake

The findings and methodologies from this deliverable can directly inform ecosystem-based adaptation strategies within ACCREU's WP3 adaptation case study CS3.2 and provide essential inputs to WP4 macro-economic models, creating an integrated assessment framework across work packages.

Beyond the project, our results offer valuable evidence for EU-level biodiversity policy development, protected area planning, and agricultural adaptation strategies that balance productivity with pollinator conservation.

Additionally, our novel modeling approaches and economic valuation frameworks will benefit researchers across disciplines, including environmental economists, conservation biologists, agricultural scientists, and government agencies implementing the EU Biodiversity Strategy and Climate Adaptation policies.

Short summary of results

See a full summary of all chapters under “Executive Summary” on pages 5-7.

Evidence of accomplishment

Published Manuscripts

- ACCREU D2.1 Impacts on infrastructure and built environment https://www.accreu.eu/wp-content/uploads/2025/01/D2.1_Impacts-on-infrastructure-and-built-environment.pdf
- ACCREU D2.2 Impacts on food, energy, and water https://www.accreu.eu/wp-content/uploads/2025/01/D2.2WaterEnergyLand.pdf

Published Datasets & Code

- **Code**: Bacca, S. (2025). SebastianoBacca/Coastal-Wetlands-Economic-Valuation: Coastal wetlands valuation toolkit (v1.0.0). [**Code**]. Zenodo. https://doi.org/10.5281/zenodo.15536288
- Meuriot, O.G.M., Martin, J.S. (2025). DTU Wildfire Modelling Suite for ACCREU. GitHub. [**Code**]. https://github.com/ophme/DTU_wildfire_modeling
- Gerber, G. (2025). Wildfire and Biodiversity Meta-Analysis Dataset (European Forests) (1.0) [**Dataset & Code**]. Zenodo. https://doi.org/10.5281/zenodo.15800907
- Nakhavali M.A. (2025). [**Code**] EU Crop-Area, Grassland, Production & Revenue Dataset https://github.com/andrenakhavali/ACCREU (https://doi.org/10.5281/zenodo.15878951)

Manuscripts in Preparation

- Gerber, G. et al. Variable effects of wildfires on European forest species: evidence from a systematic review and meta-analysis.
- Bacca, S. et al. Valuing global coastal wetlands loss: A comparison of benefit transfer and biophysical production function methods.
- Palazzo, A. et al. Assessing the Economic Impacts of Sea-Level Rise on Agricultural Land Use

Other (web links, etc)

- Nakhavali M.A., Gerber G., Palazzo A., Arbelaez-Gaviria J., Wogerer M. (2025) EU Crop-Area, Grassland, Production & Revenue Dataset. [Data hosted temporarily on IIASA's Accelerator platform until such time it can be made publicly available https://accelerator.iiasa.ac.at/] https://doi.org/10.5281/zenodo.15878951
- Gerber, G. (2025) EU Crop Pollination Flow (Physical and Monetary) for 2020-2050 at NUTS0, NUTS1, NUTS2, and NUTS3 classifications. [Dataset]. [Data hosted temporarily on IIASA's Accelerator platform until such time it can be made publicly available https://accelerator.iiasa.ac.at/]

Table of Contents

Executive Summary

The purpose of this task and deliverable is to report the work conducted and progress made towards achieving the objectives of ACCREU's Task 2.4 Impacts on ecosystems & biodiversity. Specifically, we present a **comprehensive assessment of European ecosystem and biodiversity impacts across the terrestrial and coastal ecosystems and species distribution at a 10 km^2 resolution, including the impacts of wildfires**.

This report presents an overview of our results and the significant advancements in modelling the projected impacts of climate change and land use (**ACCREU Deliverable 2.2**) on the ecological and economic dimensions of **biodiversity and ecosystem services**. We provide future assessments aligned with the ACCREU-defined scenarios. To expand on the novelty of this work, we incorporated the impacts of wildfires (**M2.1**) and sea level rise on biodiversity and ecosystem services.

For this report, our biodiversity analysis focused on target species (e.g., Birds and Habitats Directive species, pollinators). For ecosystem services, we concentrate on both use and non-use services, including crop provision, crop pollination, and coastal protection. Our analysis may serve as the basis for informing ecosystem-based adaptation and conservation strategies, including linkages to **WP3** adaptation case study CS3.2 and inputs to macro-economic models (**WP4**).

The Task 2.4 consortium conducted several interlinked research subtasks addressing different facets of the Task 2.4 objectives (**Appendix A**). These are presented in this deliverable as five separate chapters. Detailed methodologies and further results are described in the report and several technical appendices.

Chapter 1: Coastal wetlands & protection services

In Chapter 1, we addressed Task 2.4's objective of estimating wetland area changes and the resulting economic benefits from coastal protection services. We developed a comprehensive economic valuation framework that quantifies how coastal wetlands (mangroves, salt marshes, and tidal flats) protect European coastlines from erosion, flooding, and storms. Our approach combined two complementary valuation methods (replacement cost and avoided damage) to assess the full spectrum of economic benefits these ecosystems provide across different climate change and wetland loss scenarios through 2100.

Our analysis revealed that coastal wetlands currently deliver protection benefits exceeding USD 10 billion annually across Europe. The United Kingdom shows the highest replacement cost benefits (USD 4.2 billion in sea-dike construction savings), while the Netherlands experiences the greatest avoided damage benefits (USD 2 billion). Most notably, replacement costs consistently exceed avoided damages by a factor of 2-3, demonstrating that nature-based solutions provide equivalent protection at substantially lower costs than engineered alternatives. However, these benefits decline significantly under scenarios of 10-30% wetland loss, highlighting the economic consequences of allowing these ecosystems to degrade. By framing wetland conservation in economic terms, our work strengthens the case for investing in natural infrastructure as a cost-effective adaptation strategy that becomes increasingly valuable as sea levels rise and coastal development intensifies.

Chapter 2: Wildfire Risks & Impacts

In Chapter 2, we address Task 2.4 objective of comprehensively assessing wildfire impacts across European ecosystems. We developed advanced wildfire risk projections by integrating the ForeFire-Climate model with Fire Weather Index metrics, creating spatially explicit risk maps under three climate scenarios (RCP2.6, RCP4.5, RCP7.0) through 2100. This novel methodology allowed us to quantify both direct fire impacts and secondary ecological consequences.

We incorporated the wildfire risk projections into the GLOBIOM-G4M forest sector model to assess the effect of fire events on harvest wood supply, biomass and carbon emissions. Our analysis revealed that climate-driven wildfire impacts will be substantial but heterogeneous across Europe. Southern European countries face the greatest biomass losses, with approximately 90% of total losses concentrated in Spain, Italy, France, and Greece.

These impacts extend beyond direct burning effects on forests, as our meta-analysis of 2016 effect sizes from 36 studies demonstrated striking taxonomic-specific responses to fire. Most taxa showed a significant decline in abundance after fire, whereas beetles and reptiles showed increased abundance. Fire severity emerged as a critical determinant of outcomes, with several taxa showing positive responses to low-severity fires but negative responses to high-severity fires. Our findings highlight the urgent need for further research on wildfire impacts on biodiversity, particularly in southern Europe, where economic and ecological impacts are projected to be most severe.

Chapter 3: Impacts of sea-level rise on crop and grassland provision and opportunity cost for sustainable land management and conservation

In Chapter 3, we assessed the impacts of sea-level rise on agricultural land availability as well as the economic and environmental impacts of adopting more conservation-focused land management policies across Europe. Building on adaptation scenarios quantified by the economic land use model GLOBIOM developed in ACCREU project Task 2.2 and presented in **ACCREU Deliverable 2.2**, we examined how rising sea levels may reduce cropland and grassland in low-lying areas, impacting crop production and livestock feed availability. We then evaluated the foregone agricultural benefits when these lands are not available for agricultural production. Our analysis found that sea-level rise poses a risk to coastal agricultural and forest areas, leading to production and revenue losses and increasing pressure on inland ecosystems. Our analysis shows that Germany, Italy and the Netherlands are the most affected by the coastal flooding on agricultural lands. The grass production gap, unsatisfied local demand for grass for livestock, is non-negligible in coastal areas which can have a significant impact on the profitability of livestock farmers in these areas.

In this task we also integrated novel biodiversity-conservation policies aligned with the global “bending the curve” strategy by Leclère et al. (2020) into the adaptation scenarios developed and quantified in Task 2.2 of the ACCREU project. The conservation scenarios prioritize areas with high biodiversity value and restoration potential and apply strict land-use protections within EU countries. The ACCREU scenario framework integrates climate impacts, mitigation, and adaptation dimensions. Our analysis from Deliverable 2.2 showed that mitigation assumptions significantly influence the future development of the agricultural sector, while higher warming levels exert varying pressures across different regions of Europe. In this analysis, we find that conservation policies further compound these land-use pressures but

contribute to gains in biodiversity intactness and restoration area expansion. We report changes in both the Biodiversity Intactness Index (BII) and economic welfare, including net revenues and value added for producers, under ACCREU scenarios with and without the conservation-focused scenarios.

Our findings underscore the complex trade-offs between maintaining agricultural output and achieving biodiversity goals under climate change. By combining economic and environmental perspectives, this chapter provides insights into how integrated land-use strategies can support sustainable food systems, climate adaptation, and ecosystem protection in Europe.

Chapter 4: Impacts of global change on habitat suitability

In Chapter 4, we addressed Task 2.4 objectives of evaluating combined climate and land-use impacts on European species habitat suitability. Using the ibis.iSDM modeling tool, we projected habitat suitability for species listed in the EU Birds and Habitats Directives across different climate scenarios (RCP2.6, RCP4.5, RCP7.0) and agricultural adaptation pathways through 2050. We further expanded our analysis to include impacts of wildfire and sea level rise to account for multiple threats to habitat suitability.

Our analysis revealed that most taxonomic groups will face declining suitable habitats by 2050, with impact patterns varying significantly across taxa and increasing with emission intensity. We found that strategies to maintain agricultural productivity often increase habitat losses, particularly for pollinators like bees and butterflies. This is concerning given pollination's essential ecosystem service value. The varied responses across taxonomic groups indicate that effective conservation planning must incorporate taxonomic differences in climate sensitivity and responses to agricultural practices. Our findings provide evidence that biodiversity-friendly agricultural adaptation approaches are urgently needed, especially for species showing high sensitivity to intensive farming practices, creating a scientific foundation for developing targeted conservation strategies that reconcile agricultural adaptation with biodiversity protection in a changing climate.

Chapter 5: impacts on non-market ecosystem services: the case of crop pollination

In Chapter 5, we build upon the SDMs presented in **Chapter 4** to assess how global change impacts European pollinators and crop pollination services. This directly addresses Task 2.4 objectives of evaluating non-market ecosystem service values. We used an integrated assessment framework that connects changes in pollinator habitat suitability to agricultural outcomes, combining habitat projections for 153 pollinator species with crop distribution data across multiple climate scenarios and adaptation pathways. This supply-demand approach simultaneously models changes in both pollinator habitat and crop distributions, allowing for the identification of potential spatial mismatches.

Our analysis revealed a concerning "double pressure" on European crop pollination through 2050. High-quality pollinator habitat in Europe is projected to decline by 12-18%. At the same time, pollinator-dependent crops show mixed responses: highly dependent crops like sunflower decrease substantially, and moderately dependent crops like soybean increase. Our methodology estimated the current economic value of crop pollination services to be approximately **5.2 billion USD in 2020**. However, note that this is an underestimation given our model's lack of fruit and vegetable crops. Our crop pollination estimates will decline to 2.2-3.8 USD billion by 2050 with geographic variability. While Central European agricultural regions face substantial service losses, countries like Ireland and Greece

could see dramatic increases under specific adaptation scenarios. These findings highlight the need for regionally tailored strategies that balance agricultural adaptation with pollinator conservation, ensuring this critical ecosystem service continues to support European agriculture in a changing climate.

1 Coastal wetlands & protection services

1.1 Introduction

In this chapter, we address Task 2.4's objective of estimating wetland area changes **and the resulting economic benefits from coastal protection services**. Coastal wetlands such as mangroves, salt marshes, and tidal flats support nature and coastal communities. These ecosystems help regulate the climate by storing carbon and act as natural barriers that protect coastlines from erosion, flooding, and storms. (Howard et al., 2017; Mcleod et al., 2011; Schuerch et al., 2018; Taillardat et al., 2020; van Zelst et al., 2021). For example, mangroves are estimated to protect around 15 million people from coastal flooding each year. (Menéndez et al., 2020).

Despite their value, coastal wetlands are disappearing at an alarming rate. In the past, they were often seen as unproductive land and were drained or developed for farming, housing, and industry. (Davidson, 2014; Fluet-Chouinard et al., 2023). Today, they are being lost even faster than tropical rainforests (Davidson et al., 2018; Newton et al., 2020), with significant impacts on biodiversity, coastal resilience, and human well-being. Climate change, particularly sea-level rise (SLR), is worsening the situation, but it is not the primary driver of global wetland loss. The main cause is anthropogenic pressure, especially the expansion of the built environment, such as roads, buildings, and seawalls, that obstructs the natural biophysical processes wetlands rely on to adapt to rising seas. Under natural conditions, wetlands can migrate inland in response to SLR. However, this adaptive mechanism is increasingly being blocked or "squeezed" by human development along coastlines, preventing this essential landward migration (Schuerch et al., 2018; Spencer et al., 2016). As a result, it is the combined effect of climate-induced SLR and human-induced landscape modification that is driving the ongoing and projected global loss of wetlands throughout the 21st century (Schuerch et al., 2018).

To effectively protect coastal wetlands, it is crucial to understand and measure the benefits they provide. In environmental economics, ecosystems are regarded as natural capital assets that generate valuable services over time (Dasgupta, 2021; Krutilla, 1967; OECD, 2018). By assigning economic value to these services, we can more clearly assess the costs of ecosystem loss and strengthen the case for their conservation (Barbier, 2013). Given the growing threats to these ecosystems, there is increasing recognition of the need to evaluate their contributions to human well-being. From this perspective, the loss of wetlands constitutes a depreciation of the natural capital and a loss of future service flows, reframing ecological decline as a form of economic loss (Barbier, 2013; OECD, 2018).

1.2 Methods

Our methodology follows two main steps (Figure 1). In step 1, we build a global database that includes coastal wetlands, floodplains, and their socio-economic features (Appendix B Table B1). This database serves as the foundation for the next step. In step 2, we construct two models to measure the benefits of wetlands in reducing flood risk and infrastructure costs. One model called avoided damage (AD) calculates the avoided flood damage by having wetlands attenuating extreme water level events. In contrast, the other, called replacement cost (RC), estimates how wetlands reduce the cost of building and maintaining sea dikes. Both these models quantify the coastal protection service provided by wetlands.

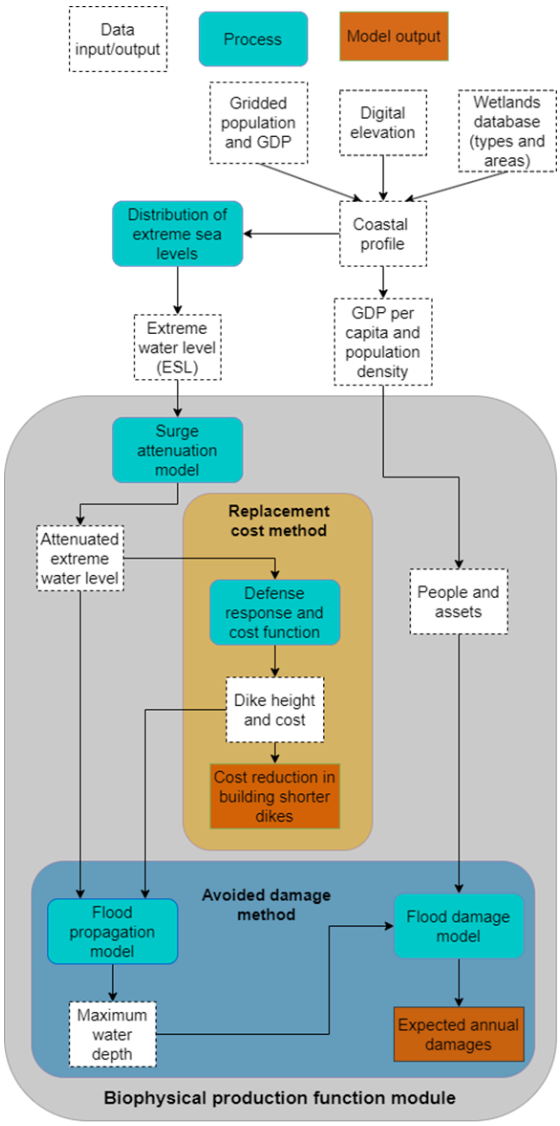

Figure 1: Flowchart showing the processes and module interactions in DIVA modeling framework and the ecosystem services valuation modules: the biophysical production function module composed by the avoided damage and replacement cost models.

We then compare the results from these models under different scenarios: the current extent of wetlands (the 'Actual Wetlands' scenario) and three future scenarios where wetland areas are reduced by 10%, 20% and 30% by the year 2100. These reductions are based on projections from Schuerch et al. (2018), which calculates that up to 30% could be lost by 2100 without more space for wetlands to expand.

Our coastal wetlands database is based on the approach of Vafeidis et al. (2008), but we improve it using higher-resolution spatial data (**Appendix B Table B1**) and a more accurate method to define coastal floodplains as in **ACCREU D2.1 Impacts on infrastructure and built environment**. In our method, the world is divided into nearly 138,000 coastal floodplains. A floodplain is a low-lying area connected to the sea and located below the local 1-in-100-year extreme sea level. These levels are taken from COAST-RP surge data (Dullaart et al., 2022) and we also consider administrative boundaries in our definitions.

To assess flood exposure in each floodplain, we overlay elevation data from MERIT-DEM (Yamazaki et al., 2017) With population data from the Global Human Settlement Layer (Schiavina et al., 2023).

We estimate the value of assets at risk by converting the exposed population into economic terms. This is done by multiplying the population by the country's GDP per capita data. (Kummu et al., 2018) and then scaling it using a 'produced capital to GDP' ratio calculated in Hallegatte et al. (2013). This study found a strong correlation between GDP and produced capital. Based on their findings, we use a global average ratio of 2.8, applied uniformly across countries:

$$Assets = GDP_{pc} * Pop * 2.8 \#(1.1)$$

To estimate the cost of sea-dike construction and maintenance, we follow the approach of Nicholls et al. (2019), which uses cost data from the Netherlands (Jonkman et al., 2013) and adjusts it to each country using a country cost factor (*CCF*) based on expert assessments. Sea-dike unit costs represent the cost of building one kilometre of dike raised by one meter. For each country, we use the lower-end Dutch rural cost for rural sea-dikes and the upper-end Dutch urban cost for urban sea-dikes elsewhere in the world, reflecting the higher flood protection standards and costs in the Netherlands. These costs are converted into US dollars (in 2011 PPP terms) and adjusted using each country's *CCF*.

The total cost of sea-dike protection includes the investment cost plus an annual maintenance cost of 1% of the investment:

$$S = h * L * C_i * (1 + 0.01) \#(1.2)$$

Where *S* is the total cost of the sea-dike, *h* is the dike's height, *L* is the length of coastline protected, and C_i is the unit cost for country *i*.

To map global coastal wetlands, we use a k-nearest neighbors (KNN) algorithm to map spatial data on mangroves. (Bunting et al., 2022), salt marshes (Mcowen et al., 2017) and tidal flats (Murray et al., 2019) To our floodplains in DIVA. This mapping is done using the DIVACoast library GIS functionalities.

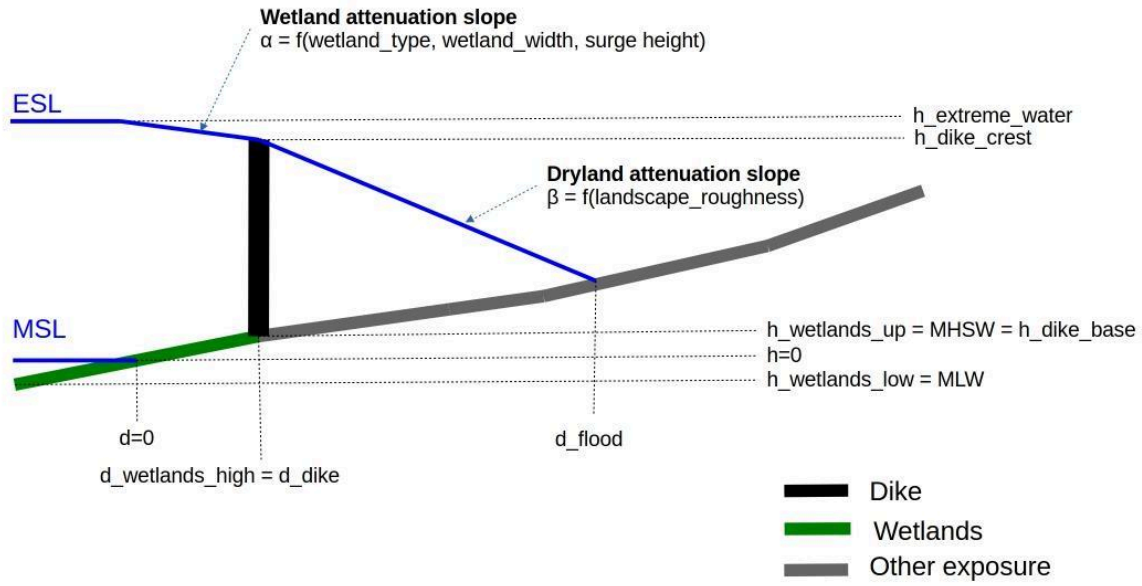

Figure 2: Wetlands and downward sloping propagation (attenuation) of extreme water levels in DIVA.

Vertically, coastal wetlands are positioned between the mean low water (MLW) level and the mean high water spring (MHWS) level (Figure 2), representing the typical tidal elevation range in which these ecosystems exist. Extreme sea level (ESL) events, driven by storm surges, tides, and sea-level rise, are assumed to be attenuated as they pass over wetlands. The degree of attenuation depends on the wetland width (*w*), the height of the ESL, and the wetland type (attenuation coefficient *a*). We model this attenuation process using a static, type-specific (*j*) attenuation coefficient *a*, whereby ESL height is linearly reduced across the wetland surface. The attenuation height Δx for each segment is defined as:

$$\Delta x = w * a_j \#(1.3)$$

where *w* is the wetland width, calculated by dividing the wetland area from our spatial wetlands database by the length of the coastline segment it occupies and a_j is the attenuation coefficient for each wetland type *j* taken from Vafeidis et al. (2019). This approach allows us to account for the protective function of wetlands against ESL events within each floodplain, linking their spatial characteristics directly to flood attenuation potential.

Figure 3 and Figure 4 show sample regions from the resulting global wetland dataset and Figure 5 the European distribution of coastal wetlands (salt marshes and tidal flats).

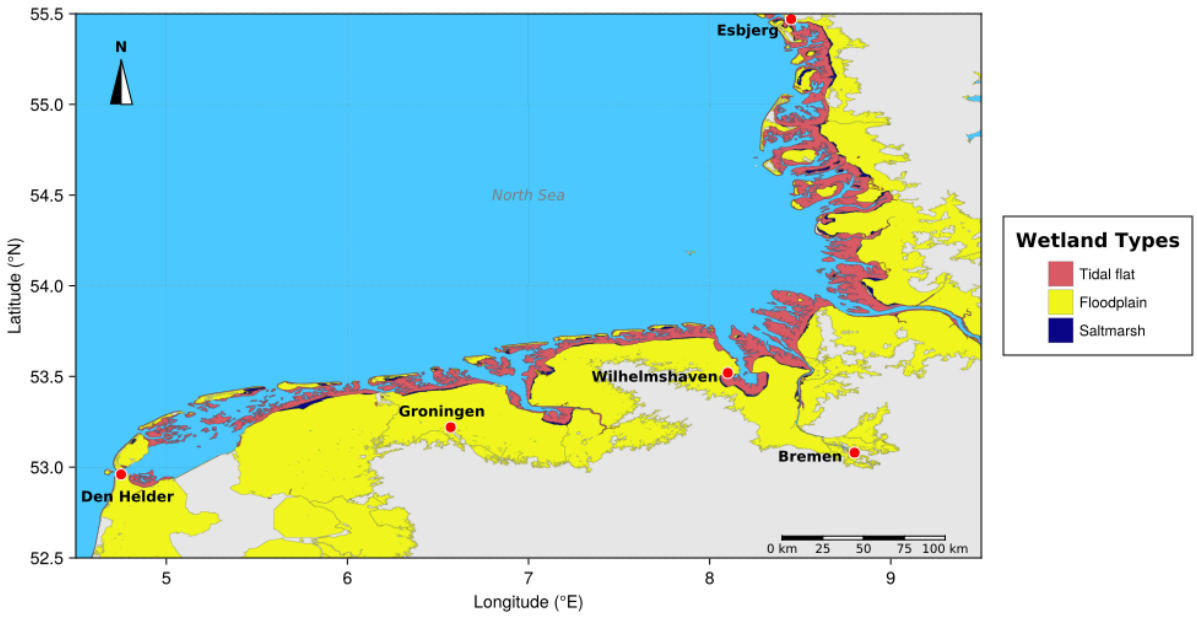

Figure 3: Map showing the coastal wetlands between the Netherlands and Germany along the North Sea coast. Floodplains are highlighted in yellow, tidal flats in orange and salt marshes in dark blue.

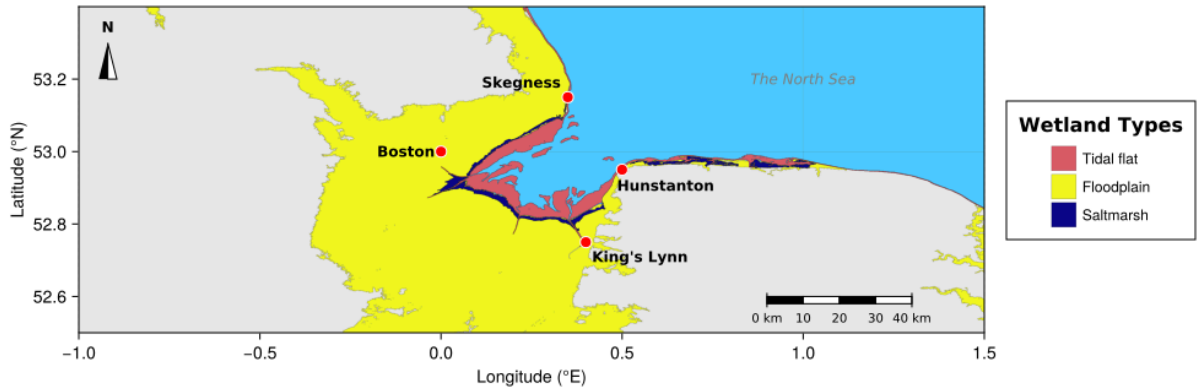

Figure 4: Map showing the coastal wetlands in The Wash, UK. Floodplains are highlighted in yellow, tidal flats in orange and salt marshes in dark blue.

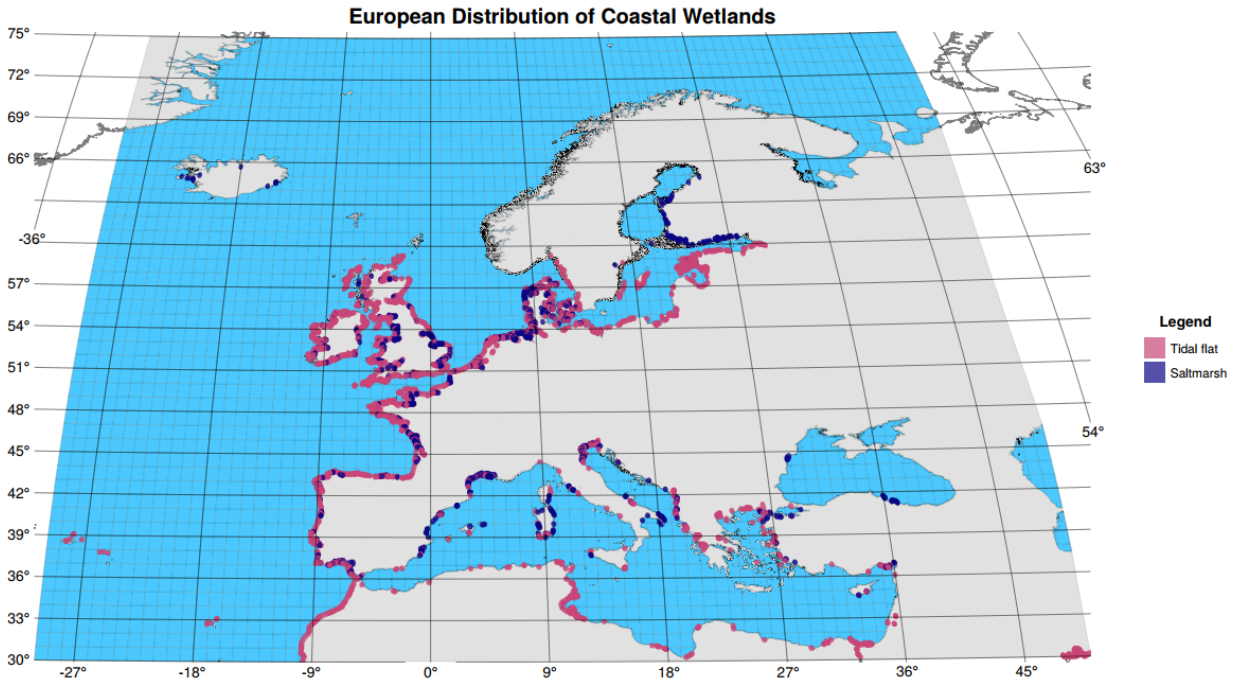

Figure 5: European wetlands (salt marshes in blue and tidal flats in pink) distribution.

The DIVACoast.jl library is available in the GitHub repository at the following link: https://github.com/GlobalClimateForum/DIVACoast.jl.git. The wetlands change economic valuation code is available at the Zenodo repository https://doi.org/10.5281/zenodo.15536288.

1.2.1 Coastal wetland change

Coastal wetland change is primarily driven by two interlinked factors: sea-level rise and land-use change. While earlier global assessments highlighted the overwhelming influence of SLR on the loss of wetlands, more recent regional and local case studies suggest that these impacts may be overstated. Previous research demonstrates that many coastal wetlands, including marshes and mangroves, are capable of maintaining or even exceeding vertical accretion rates in response to historical SLR, thanks to sediment accumulation and biophysical feedback mechanisms (Kirwan et al., 2016; Sasmito et al., 2016). These studies emphasize that vulnerability assessments often fail to account for these processes and the capacity for inland migration, leading to exaggerated projections of wetland loss.

A significant advance in reconciling these divergent perspectives (Schuerch et al., 2018) integrates the DIVA model with a biophysical feedback module that incorporates both vertical and horizontal wetland adaptability. This model introduces the concept of "accommodation space," the land available for wetlands to migrate inland in response to rising sea levels. Their findings indicate that the true limiting factor is not SLR per se, but rather the presence of human infrastructure that blocks inland migration pathways. In scenarios with sufficient sediment supply and available accommodation space, SLR can even enhance sediment deposition and support wetland expansion. Conversely, where horizontal space is constrained by development, wetlands face severe loss.

Land-use change further exacerbates this problem. In the absence of effective mechanisms to value natural ecosystems, decisions frequently favor development over conservation. The conversion of coastal wetlands into agricultural, industrial, or urban land results in the irreversible loss of ecosystem services. Previous research has emphasized that without policies that reflect the full value of these ecosystems, exploitation remains the default outcome (Costanza et al., 2014; de Groot et al., 2012).

Building on a previous modeling framework (Schuerch et al., 2018), we apply a scenario-based approach to evaluate the potential future loss of global coastal wetlands under the assumption that no additional accommodation space is made available. We define three loss scenarios representing 10%, 20% and 30% reductions in global wetland area by the year 2100. These scenarios reflect increasing severity in land-use pressure and infrastructure development, which block inland migration and reduce the adaptability of wetland systems. Finally, in these scenario-based runs, we do not consider future SLR projections but the current distribution of extreme water levels as a test-simulation of the model.

1.2.2 Coastal ecosystem services

Two main classes of methods have been developed to estimate the non-market value of ecosystem services (ESS) at regional and global scales. The two classes of methods are the benefit transfer methods and the biophysical production function methods. Benefit transfer methods estimate ESS values at policy sites by adapting values derived from existing studies at comparable locations (Rosenberger and Loomis, 2017). These include unit value transfer, which applies average monetary values per unit area, and value function transfer, which adjusts estimates using statistical models such as meta-regression (Brander et al., 2012; Rosenberger and Loomis, 2017). However, the accuracy of benefit transfer is often limited by regional data gaps and difficulties in accounting for ecological and socio-economic variability (Brander et al., 2012; de Groot et al., 2012; Ghermandi and Nunes, 2013; Rao et al., 2015).

Biophysical production function methods, on the other hand, derive values from ecological processes that underlie the ecosystem service provision. These methods are particularly useful for estimating services with direct use value, such as coastal protection. The avoided damage method evaluates the reduction in potential damage to people, infrastructure, and property due to the presence of wetlands (Barbier, 2016, 2013; Menéndez et al., 2020; Reguero et al., 2020, 2018), while the replacement cost method estimates the cost of replicating these services through artificial means (Barbier, 2016; van Zelst et al., 2021). However, these cost-based approaches often equate avoided costs with economic value, potentially overstating benefits by not directly measuring changes in welfare.

In this model simulation, we assess the coastal protection benefits of wetlands using two biophysical production function valuation methods: avoided damage and replacement cost. In the avoided damage approach, the benefit of coastal wetlands is quantified as the reduction in expected annual damages (EAD) from coastal flooding, due to the attenuation of extreme sea level events (ESL) by the presence of wetlands on the floodplain. In the replacement cost approach, the benefit is framed as the cost savings from constructing lower sea dikes, made possible by the wetlands' ability to reduce water levels before they reach hard defenses. In both cases, the protective function of coastal wetlands translates into measurable economic value, either by reducing direct flood damages or by lowering infrastructure investment requirements (less investment and maintenance costs).

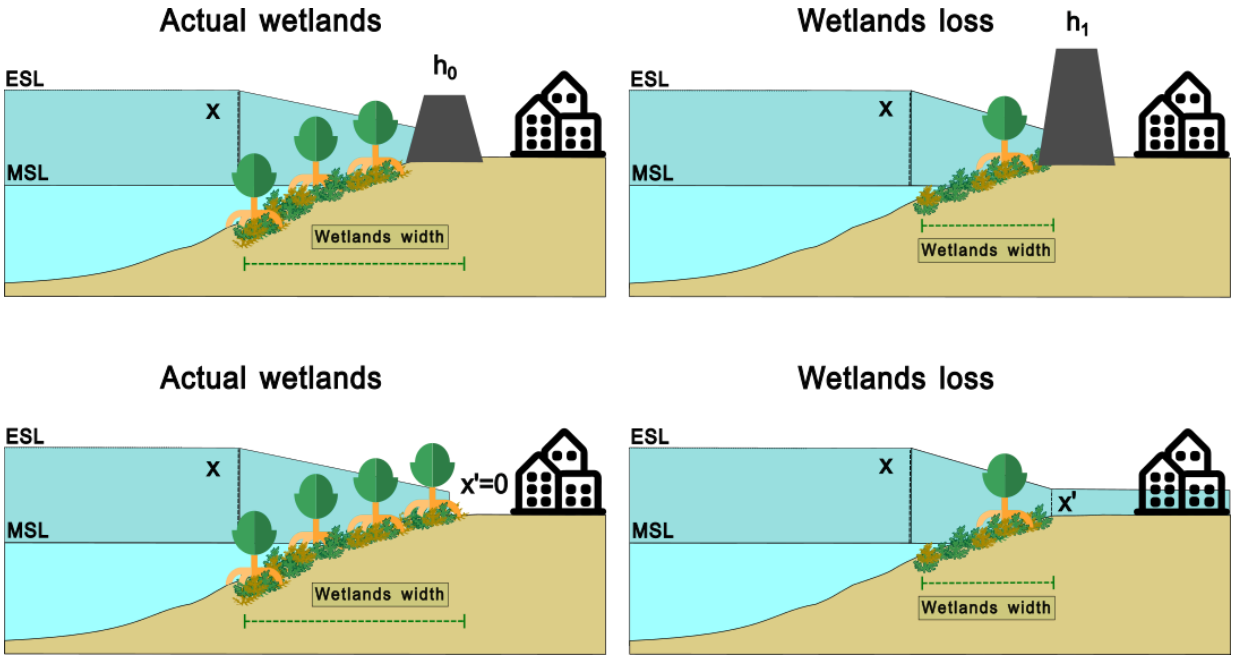

Figure 6: Avoided damage (lower panel) and replacement cost (upper panel) biophysical production function methods used for coastal wetlands coastal protection service valuation. In avoided damage the coastal protection benefit is framed as a reduction in expected annual damages from coastal flooding due to the presence of coastal wetlands on the floodplain. In replacement cost, the coastal protection benefit is framed as a reduction in the cost of building lower sea dikes (cost-saving) because the wetlands attenuate the water level.

1.3 Results & Discussion

1.3.1 Coastal wetland change

In the final DIVA model run for the ACCREU project, results will include global projections of total coastal wetland loss under sea-level rise (SLR) and spatial constraints imposed by the built environment. These unconstrained wetland loss scenarios assume that no additional horizontal accommodation space will be available for inland wetland migration due to the continued expansion of coastal defenses and urban development. Under this assumption, wetlands are unable to retreat landward and are considered lost once their elevation falls below the 1-in-1-year flood return level, consistent with previous outlined approaches (Nicholls et al., 2011). This modeling framework represents a worst-case scenario where the natural adaptive capacity of wetlands is severely impeded.

In the test simulation presented in this deliverable, we apply a simplified version of this framework by modeling three fixed scenarios of global wetland loss 10%, 20%, and 30% by the year 2100 (Table 1), without incorporating future SLR projections. These hypothetical loss levels reflect the increasing severity of spatial constraints and policy inaction. We then compute the resulting economic impacts in terms of lost coastal protection benefits, specifically focusing on avoided flood damages (using AD) and replacement costs (using RC) of artificial protection (e.g., sea dikes). This test provides an initial assessment of the magnitude of economic losses associated with declining wetland extent.

At this preliminary stage of the analysis, we apply fixed global wetland loss scenarios (10%, 20%, 30%) by 2100 to isolate and illustrate the sensitivity of economic impacts to declining wetland extent under increasing spatial constraints. This approach reflects the growing severity of non-climatic drivers, particularly the continued expansion of coastal infrastructure and urban development, which increasingly prevent inland wetland migration. As explained in Subsection 1.2.1, the presence of such hard coastal defenses is a major contributor to wetland loss, as it restricts the horizontal accommodation space required for natural adaptation (Schuerch et al., 2018). Therefore, this simplified framework allows us to benchmark the magnitude of potential losses without introducing the complexity and uncertainty associated with future SLR projections and the wetlands response.

Full integration of climate-based (SSP-RCP based) wetland loss scenarios will be included in the final DIVA model runs, enabling a dynamic coupling between SLR trajectories, wetland migration potential, and socio-economic pathways. However, at this exploratory phase, our goal is to assess the directional economic implications of worsening policy inaction and hard infrastructure expansion, independent of climate forcing uncertainties.

Table 1: Actual global wetlands area (km^2) and global wetlands area loss in the three wetlands loss scenario: 10, 20 and 30%.

Wetlands	Actual	10% loss	20% loss	30% loss
Salt marshes	73,207	65,886	58,566	51,245

Tidal flats	108,006	97,205	86,404	75,604
Mangroves	98,780	88,902	79,024	69,146
Total	279,993	251,993	223,994	195,995

1.3.2 Coastal ecosystem services

The comparison of avoided damage (Table 2) and replacement cost (Table 3) estimates across European countries reveal distinct patterns in the valuation of ecosystem-based coastal protection. Countries with high population density along low-lying coastlines, such as the United Kingdom, Netherlands, and France, consistently show the greatest economic reliance on coastal wetlands protection services, both in terms of reduced flood damages and lower infrastructure expenditure. Replacement cost values are generally much higher than avoided damage values, reflecting the relatively high costs of engineered alternatives like sea dikes compared to the freely available protection offered by natural systems. This gap further supports the notion that nature-based solutions, particularly coastal wetlands, provide protective services at a significantly lower cost than man-made infrastructure. Moreover, the diminishing benefits under progressive wetland loss scenarios (10–30%) indicate a nonlinear decline in protection value, especially for nations with limited room for inland wetland migration (urban and densely populated low-lying coastal areas).

Table 2: Avoided damages coastal protection values for European countries (million USD PPP 2011). The values represent the flood damage reduction across wetlands loss scenarios.

Country	Code	AD Actual wetlands	AD Wetlands loss 10%	AD Wetlands loss 20%	AD Wetlands loss 30%
France	FRA	552.9	508.1	462.8	415.1
Netherlands	NLD	1952.3	1755.0	1561.5	1367.6
United Kingdom	GBR	958.0	863.8	770.0	674.3
Portugal	PRT	11.3	10.2	9.1	8.0
Romania	ROU	20.9	20.9	20.9	20.8
Belgium	BEL	32.7	29.4	26.2	22.9
Norway	NOR	233.7	210.1	186.8	163.0
Italy	ITA	45.8	42.4	41.0	34.3
Albania	ALB	5.9	5.3	4.6	4.1
Greece	GRC	28.2	26.3	24.3	22.0
Lithuania	LTU	2.8	2.6	2.3	2.0
Ukraine	UKR	7.0	6.4	5.8	5.2
Poland	POL	11.1	11.1	9.9	8.7
Montenegro	MNE	1.2	1.1	0.9	0.8
Spain	ESP	238.6	220.2	201.0	180.2
Sweden	SWE	62.8	56.9	51.0	45.0
Turkey	TUR	56.5	53.1	49.1	45.0

Country	Code	AD Actual wetlands	AD Wetlands loss 10%	AD Wetlands loss 20%	AD Wetlands loss 30%
Malta	MLT	0.0	0.0	0.0	0.0
Ireland	IRL	87.8	80.3	72.5	64.5
Slovenia	SVN	7.9	7.1	6.2	5.4
Latvia	LVA	0.8	0.7	0.6	0.5
Denmark	DNK	54.1	49.0	42.1	38.6
Iceland	ISL	29.4	26.5	23.5	20.5
Estonia	EST	0.1	0.1	0.1	0.1
Croatia	HRV	31.9	29.6	27.0	24.3
Bulgaria	BGR	8.7	8.2	7.7	7.1
Finland	FIN	52.0	47.4	42.7	37.6
Germany	DEU	168.3	151.3	134.6	117.9

Table 3: Replacement cost coastal protection values for European countries (million USD PPP 2011). Values represent the cost savings from lower coastal protection constructions across wetlands loss scenarios.

Country	Code	RC Actual wetlands	RC Wetlands loss 10%	RC Wetlands loss 20%	RC Wetlands loss 30%
France	FRA	2514.3	2371.6	2207.2	2099.9
Netherlands	NLD	1462.6	1443.8	1425.0	1406.3
United Kingdom	GBR	4243.3	4127.4	3930.0	3738.4
Portugal	PRT	83.9	80.3	84.3	85.0
Romania	ROU	232.4	240.6	222.4	199.8
Belgium	BEL	186.6	186.1	185.5	185.0
Norway	NOR	1113.7	1090.5	1069.3	1037.5
Italy	ITA	308.6	295.0	284.7	274.2
Albania	ALB	12.5	12.0	11.5	11.0
Greece	GRC	107.3	103.1	97.3	86.7
Lithuania	LTU	21.7	20.4	19.2	17.9
Ukraine	UKR	162.5	150.5	138.4	123.4

Country	Code	RC Actual wetlands	RC Wetlands loss 10%	RC Wetlands loss 20%	RC Wetlands loss 30%
Poland	POL	78.0	76.4	74.8	73.3
Montenegro	MNE	9.7	9.2	8.7	8.1
Spain	ESP	437.7	423.4	405.7	388.3
Sweden	SWE	406.5	383.4	353.4	334.1
Turkey	TUR	129.6	122.3	113.5	102.5
Malta	MLT	0.7	0.7	0.6	0.6
Ireland	IRL	642.2	643.5	556.4	537.7
Slovenia	SVN	4.1	3.9	3.6	3.4
Latvia	LVA	104.0	103.0	61.3	60.1
Denmark	DNK	540.2	518.9	495.1	464.4
Iceland	ISL	158.5	141.4	133.4	127.0
Estonia	EST	18.1	17.4	16.7	16.0
Croatia	HRV	71.7	68.5	66.0	63.5
Bulgaria	BGR	43.0	39.8	36.5	33.3
Finland	FIN	188.4	177.8	167.8	166.7
Germany	DEU	888.3	872.5	856.7	820.8

1.4 Conclusion/Key takeaways

The analysis of European-level protection benefits reveals significant economic value derived from coastal wetlands, both through avoided flood damages (avoided damage) and reduced infrastructure costs (replacement cost). Among European countries, the United Kingdom exhibits the highest cost savings in sea-dike construction, estimated at USD 4.2 billion annually, due to its long, densely populated coastline and extensive built environment. Conversely, the Netherlands leads in terms of avoided expected annual damages (USD 2 billion), reflecting its exposure as a low-lying country with highly developed flood protection systems. Countries like France, Germany, and the Nordic nations also show substantial benefits. Under current conditions, total European coastal protection benefits exceed USD 10 billion annually. However, these benefits decline significantly under scenarios of 10–30% wetland loss by 2100, reinforcing the vulnerability of coastal protection services when wetlands are spatially constrained and adaptive capacity is lost.

A consistent finding across all wetland loss scenarios is that replacement cost values are 2–3 times higher than avoided damage estimates. This underscores a fundamental economic insight: nature-based solutions, such as wetlands, could provide equivalent protective benefits at a substantially lower cost than engineered alternatives. Unlike dikes or sea walls, which require high upfront capital and ongoing maintenance, wetlands offer passive, self-reinforcing protection that scales with environmental change, making them more cost-effective over time for rural and low-populated areas. These findings highlight the urgent need for proactive investment in conserving and restoring coastal wetlands. Protecting existing natural infrastructure is not only ecologically sound but also economically rational, especially as the cost of relying solely on engineered defenses continues to escalate in the face of rising sea levels.

2 Wildfire Risks & Impacts

2.1 Introduction

European forests provide crucial ecosystem services, including timber production, carbon sequestration, and recreational opportunities. However, these forests face mounting threats from wildfires, with many regions experiencing increases in burned area over the past few decades (Fernandez-Anez et al., 2021). This trend is expected to intensify as climate change brings warmer, drier conditions to many European regions previously unaffected by significant fire activity.

The ecological impacts of these changing fire regimes are complex and taxon-specific. Some species thrive in post-fire landscapes, e.g., fire-adapted plants that require heat for seed germination and dispersal. (García-Duro et al., 2019), and certain birds that exploit newly available resources in burned areas (Brotons et al., 2008; Versluijs et al., 2020). Conversely, other species suffer from increased fire frequency and intensity, directly through increased mortality or indirectly through increased fire. (Kim and Holt, 2012; Sgardelis et al., 1995), or indirectly due to loss of habitat (Puig-Gironès et al., 2023), and key food resources (Franklin et al., 2022), leading to overall reductions in species abundance and diversity (Rey et al., 2019). With increasing annual fire-related damages to European forests and significant biodiversity implications, a comprehensive assessment of wildfire risks and impacts is essential for effective climate adaptation planning.

To address this critical need, we pursued three complementary research objectives that directly speak to **ACCREU Task 2.4** of ***estimating the impact and risk of wildfires across terrestrial and coastal ecosystems***.

1. First, to understand the risks of European wildfires now and in the future, we built upon ACCREU Milestone 2.1 and developed advanced wildfire risk mapping and projections by combining the ForeFire-Climate model with the Fire Weather Index system. We aimed to create spatially explicit wildfire risk maps under different climate scenarios (RCP2.6, RCP4.5, RCP7.0) for 2020-2100.
2. Second, we conducted a forest sector impact assessment to quantify impacts on European forest carbon stocks, harvested wood supply, and forest sector GHG emissions.
3. Third, we performed a biodiversity impact analysis through a systematic literature review and meta-analytical modeling of taxa-specific responses to fires of different extents and severities, allowing us to disentangle how different taxonomic groups respond to varying fire regimes.

Integrating these three components provides a holistic assessment of wildfire risks and impacts across European landscapes.

2.2 Methods

2.2.1 Wildfire Risk

A modular wildfire modeling suite was developed to assess wildfire risk under historical and future European climate conditions. The simulations focus on the fire season (June to October) and rely on multiple climate data sources, including the ERA5-Land reanalysis (2008–2023) for historical validation and bias-corrected CLIMEX2 projections (1991–2010 and 2021–2100) for future scenario analysis.

The methodology's core is a machine learning (ML) based fire probability model trained using observed fire events from the EFFIS dataset and 23 predictors, including climate, land cover, topography, and human activity. A Random Forest algorithm was selected as the best-performing model. This ML model generates daily fire risk maps, which are subsequently used to estimate ignition points and simulate fire spread. The main steps of the modelling suite (Figure 7) include:

- **Bias correction** of CLIMEX2 data using linear scaling and quantile mapping to address model biases.
- **Fire risk mapping** through the ML model produces daily fire risk probabilities.
- **Ignition point selection,** based on the relationship between historical events and model-derived probabilities.
- **Future scenario scaling,** to account for missing years and align data with SSP2 scenario conditions.
- **Fire spread simulations** with ForeFire and WindNinja used to downscale wind fields (the primary driver of fire spread) and simulate dynamics at an effective resolution of 50 meters.

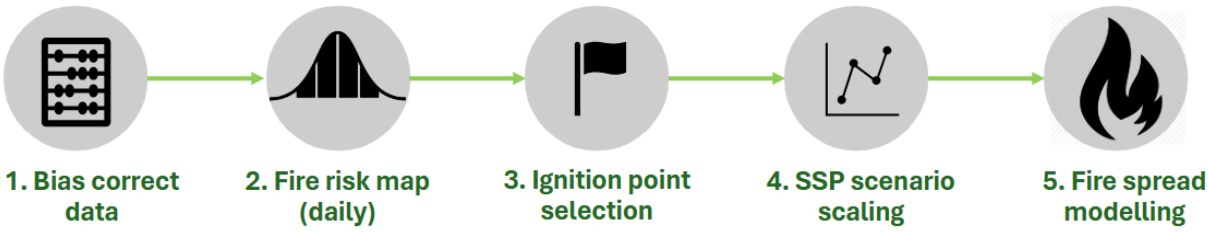

Figure 7: Overview of DTU wildfire modeling methodology.

All spatial data is provided in the ETRS89 / LAEA Europe projection (EPSG: 3035). Simulation outputs include daily time series of burned areas, enabling comparative assessments across different climate scenarios. For a more detailed and technical description of the methodology, including the whole modeling workflow and underlying assumptions, see **Appendix C**. The complete code and implementation of the modeling suite are in the GitHub repository: https://github.com/ophme/DTU_wildfire_modeling.

2.2.2 Impacts of wildfire risk on forest sector

To quantify the impacts of wildfires on European forest carbon dynamics, biomass stocks, and harvested wood supply, burned area estimates from the DTU Wildfire Model (ForeFire) were integrated into the GLOBIOM-G4M modeling framework, which provides a consistent, spatially explicit representation of forest growth, management, and land-use change under different climate and policy scenarios.

GLOBIOM (Global Biosphere Management Model) is a global, partial equilibrium model that captures the competition for land among agriculture, forestry, and bioenergy sectors (Havlík et al., 2011). G4M (Global Forest Model) is a spatially explicit forest growth and management model designed to estimate forest biomass development, harvested wood potential, and greenhouse gas (GHG) emissions and removals from forests, including the effects of climate change and natural disturbances such as wildfires (Augustynczik et al., 2025; Kindermann et al., 2008). The two models operate in a linked framework. GLOBIOM provides G4M with projections of changes in land cover and land use, including deforestation, carbon prices for GHG emissions, and harvested wood demand consistent with socioeconomic scenarios and climate policy pathways. G4M simulates forest growth, management decisions, and the impacts of disturbances such as wildfires. It operates at a spatial resolution of 0.5 degrees globally, with detailed forest structure, age distribution, and species-specific biomass characteristics for each grid cell.

This task aggregated burned area estimates from ForeFire to 0.5-degree resolution and aligned with G4M's forest sector spatial structure. Within each affected grid cell, burned area is distributed across five forest types, reflecting the heterogeneity of forest composition. The allocation follows a random sequence that allows for variability in which forest types are affected, recognizing uncertainty in fire spread patterns within landscapes.

The translation of burned area into biomass damage depends on multiple factors:

- The area of each forest type affected by fire within the grid cell;
- Standing biomass per hectare, specific to forest type and age;
- The proportion of trees vulnerable to fire, based on species composition;
- The age structure of the forest, determining which cohorts are impacted by fire;
- Species-specific mortality rates applied post-fire, accounting for differences in fire susceptibility.

Previous studies have demonstrated how G4M accounts for spatial heterogeneity in forest structure, species composition, and management, allowing for differentiated fire impacts on biomass and carbon dynamics (Gusti, 2010; Gusti et al., 2020).

Forest recovery after fire is modeled based on both management regime and site productivity. Actively managed forests undergo salvage logging, with an assumed recovery rate of 54% of damaged biomass, based on the CBM database and expert consultation (Blujdea, personal communication, 26 July 2023). These burned areas are then promptly replanted. In contrast, unmanaged or protected forests regenerate

naturally, which generally results in slower biomass recovery. Site productivity further influences regrowth rates, with more productive locations experiencing faster regeneration.

The timing of fire events is also considered, as earlier fires provide more time for biomass accumulation and recovery within the simulation period, whereas later fires result in higher net biomass losses due to limited recovery time.

By comparing scenarios with only climate change impacts to scenarios that include both climate change and fire disturbances, the model isolates the additional GHG emissions attributable to fires. With this approach we can assess wildfire impacts on forest carbon stocks, harvested wood supply, and forest sector GHG emissions. The framework also allows for targeted analysis of fire impacts on forests likely to be under natural regeneration only, providing insight into the greater vulnerability of unmanaged or protected forest areas under future climate and disturbance conditions.

2.2.3 Impacts of wildfire risk on local plant & animal communities

Here, we aim to estimate the average impact of wildfires across Europe on forest species from reported literature via a meta-analytical approach. This is the first step in deriving empirical evidence to use in later spatial assessments of the impacts of wildfire on forest biodiversity. We use taxa abundance as a biodiversity indicator, as this allows us to account for potentially varying responses of different species to fire (e.g., Mason et al. 2021; Bieber et al. 2023). Our objectives included fitting the best possible model of the measured effects of forest wildfire on taxa abundances, deriving *in situ* quantitative data from the literature.

To fit a quantitative model of the effects of fire on species abundances, we first conducted a systematic literature review following scientifically established frameworks (Cummings et al., 2013; Mattos and Ruellas, 2015; Page et al., 2021). We considered studies eligible for inclusion in our meta-analysis if (1) the study was conducted within European forested areas, (2) mean taxa abundances, sample sizes, and preferably standard deviation, were compared before and after fire in the same area, or between a burned and unburned area of similar vegetation, land-use, and climatic conditions, and (3) the abundances were measured < 10 years after the fire, accounting for 'shorter' term impacts. We conducted an initial literature search of the Scopus database and combined this with additional reference articles from previous meta-analyses. We screened the database, removing any duplicates, retracted articles, and those that did not meet our eligibility criteria. From the eligible studies, we manually extracted and collated data pertaining to study design, site, and fire characteristics that could significantly influence taxa abundance (Mason et al., 2021). We extracted means and variances of taxa abundances (species-specific, where possible) from reported results, supplementary material, or digitized from figures using plotdigitizer https://plotdigitizer.com/app (e.g., Fayt, 2003; Nunes, 2006).

We categorized all effect sizes (ES) into 11 broad taxon groups, two categories of fire severity (low-medium, and high), and two postfire assessment categories (0-5 years; 5-10 years). Thereafter, we performed meta-analyses on the effect sizes by fitting multivariate mixed-effect linear models using the restricted maximum likelihood (REML) method (Viechtbauer, 2010). As there was no significant difference between the two postfire assessment categories (p = 0.20), we omitted this factor from the model and refitted the model with 'broad taxa group' and 'fire severity' only. Thereafter, we calculated the modelled predicted ES per taxon group, per fire severity (Viechtbauer, 2010). Further technical details regarding the

methodology and statistical analyses performed are in **Appendix C**. The full dataset and code are available on Zenodo https://doi.org/10.5281/zenodo.15800907 (Gerber, 2025).

2.3 Results & Discussion

2.3.1 Wildfire Risk

2.3.1.1 Simulation and Validation Approach

The results are presented as a daily series of burned areas. To first validate the ignition point selection component of our methodology, the observed number of ignitions from the EFFIS database (Figure 8a) is compared with the ignitions predicted by our ML model (Figure 8b), assessing whether the ignition points estimated by the model have a similar spatial distribution to the historical ignitions. Both maps show the number of ignitions per 10×10 km grid cell.

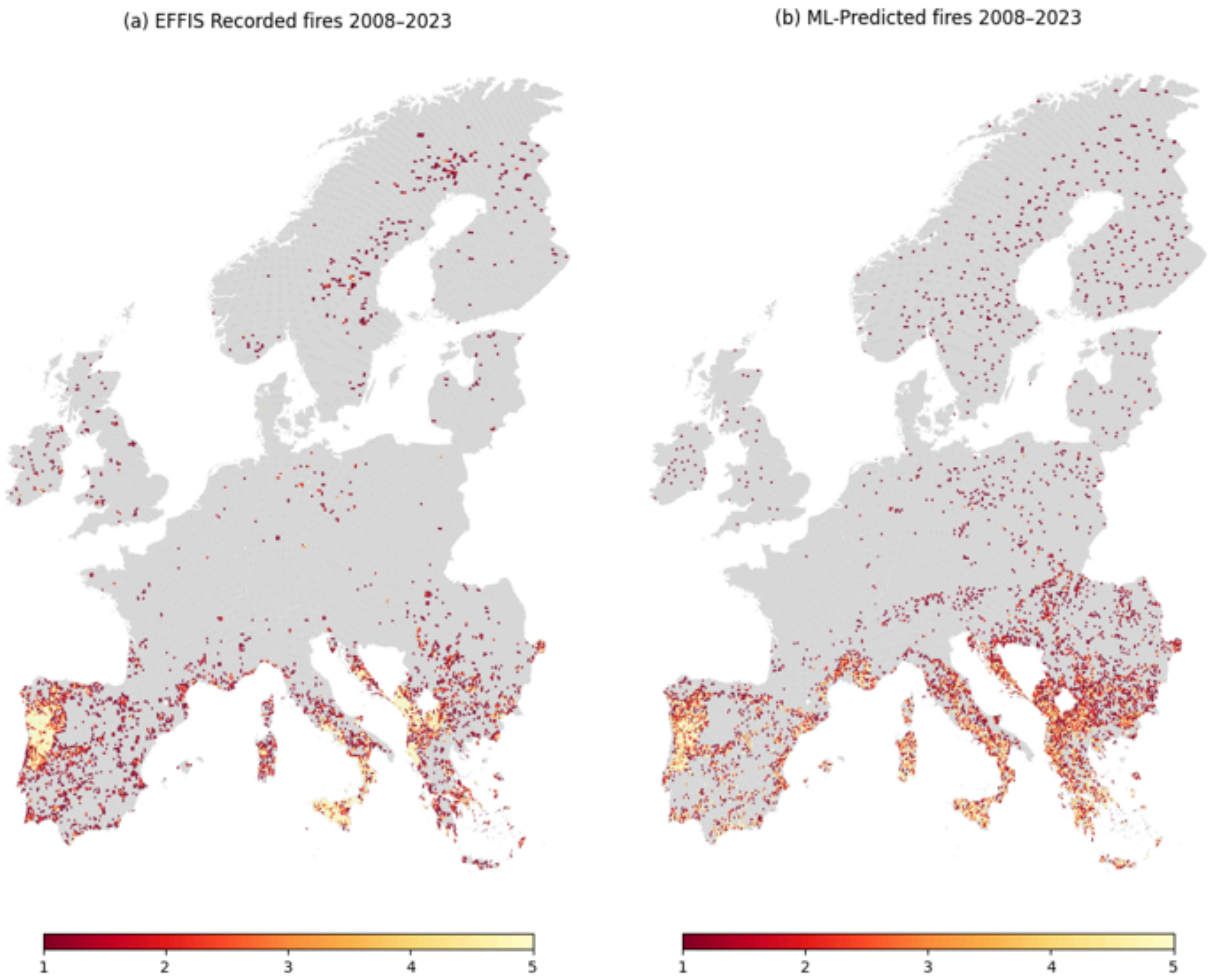

Figure 8: Number of fires per grid cell (a) from the historical record (b) from the ML probabilities using ERA5-land.

The spatial distribution of ignitions in both datasets reveals strong agreement in Southern Europe, where fire activity is more frequent. High ignition densities are consistently captured across the northwest part of Portugal and Spain, as well as the southwest of Italy and large parts of Greece, demonstrating the model's ability to identify these hotspot areas. Over Central and Northern Europe, ignition densities are lower, again reflecting the spatial patterns observed in the historical dataset. However, our ML model shows a wider spread of ignitions across these regions compared to the historical EFFIS ignitions.

The next step is to assess the ability of the fire spread model to capture the burned area across Europe, also considering its interannual variability. Figure 9 shows a comparison between the annual total burned area recorded in the EFFIS database and the values simulated by ForeFire for the period 2008–2019.

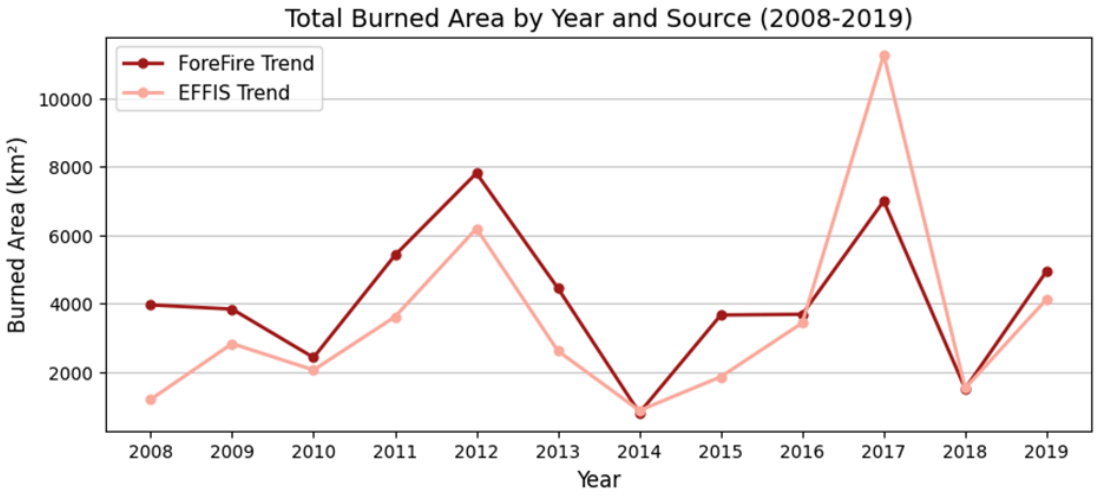

Figure 9: Comparison of total annual burned area in Europe between ForeFire simulations and EFFIS observations for the period 2008–2019.

Overall, the ForeFire spread model exhibits a good ability to capture the interannual variability of the fire activity. It identifies years of high fire occurrence, such as 2012 and 2017, and reflects the year-to-year fluctuations in the burned area. Although the magnitude of the burned area sometimes differs from observations, the temporal alignment indicates that the model is sensitive to fire-prone conditions, despite occasional under- or overestimation in certain years.

2.3.1.2 *Projected Burned Area Under Future Climate Scenario*

Building on the validated performance of our fire ignition and spread model, the analysis is extended to explore how wildfire activity may evolve throughout the 21st century. Using climate projections based on three scenarios (SSP2-RCP2.6; SSP2-RCP4.5; SSP2-RCP7.0), the daily burned areas across Europe from 2021 to 2100 are simulated. Figure 10 presents the total annual burned area for each scenario from the fire spread simulations. Similarly, Figure 11 shows the cumulative burned area for four 20-year periods: 2021–2040 (near future), 2041–2060 (mid-century), 2061–2080 (far future), and 2081–2100 (end-of-century) for the different scenarios.

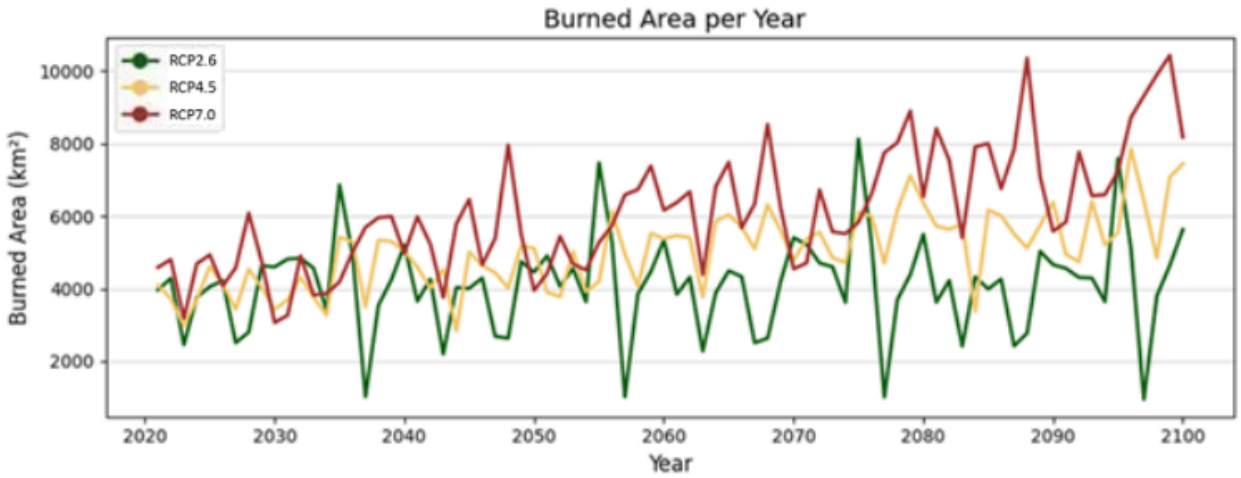

Figure 10: Annual projected burned area across Europe from 2021 to 2100 under three climate scenarios.

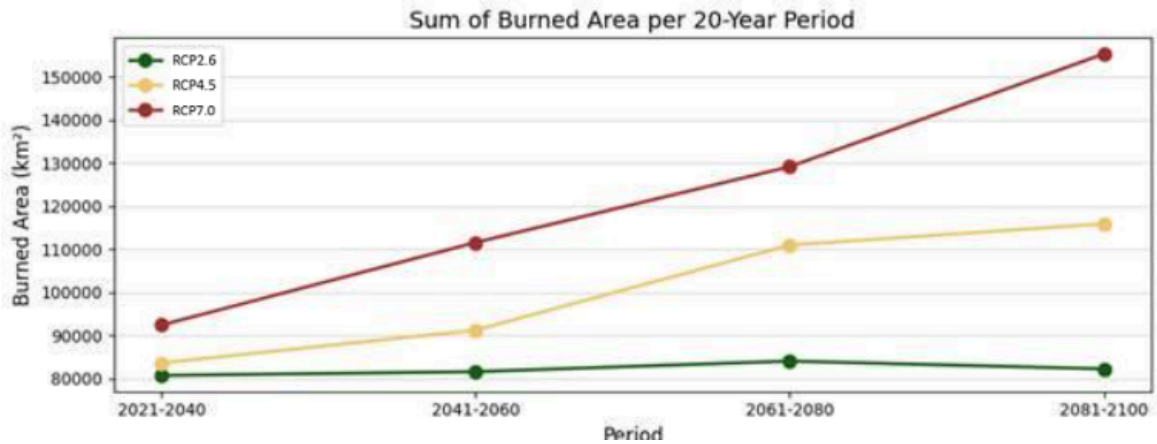

Figure 11: Cumulative burned area for four future periods (2021–2040, 2041–2060, 2061–2080, and 2081–2100) under three different climate change scenarios.

Both Figure 10 and Figure 11 illustrate both the long-term trends and interannual variability of burned area projections under different climate scenarios. While interannual fluctuations persist throughout the century in all scenarios, a clear underlying trend can be seen. Under RCP2.6, burned areas gradually decrease by the end of the century (2081–2100) compared to the near future (2021–2040), reflecting a more sustainable pathway with effective climate mitigation. In contrast, RCP4.5 and especially RCP7.0 show substantial increases in burned area over time, with RCP7.0 exceeding 150000 km² by the end of the century.

2.3.2 Impacts of wildfire risk on forest sector

The integration of burned area projections from the DTU Wildfire Model into the GLOBIOM-G4M framework allows us to make a detailed assessment of the impacts of wildfires on European forests under different ACCREU/climate scenarios. The results presented in this section illustrate both the spatial extent of burned areas across Europe and the associated impacts on forest carbon losses and greenhouse gas (GHG) emissions.

Figure 12 provides a map of the total burned area extent used within G4M, including historical observations, ERA5 reanalysis, and future climate scenarios, aggregated to 0.5-degree resolution. The spatial patterns reflect both regional differences in projected fire activity and the underlying forest structure simulated within G4M.

Once integrated into G4M, the burned area projections are translated into biomass damage and carbon losses, accounting for the heterogeneity of forests and management practices within each affected grid cell. Burned area is distributed across five forest types within each cell using a randomized selection process, which reflects differences in forest composition, protection status, and management intensity. The extent of biomass loss depends on several factors, including the standing biomass per hectare for each forest type, species composition, site productivity, and the vulnerability of individual tree species to fire. Species with higher susceptibility to fire contribute disproportionately to overall biomass losses (Table 4).

In the scenarios presented here, the G4M model relies on the underlying land-use scenario data produced by the GLOBIOM model as part of **ACCREU Deliverable 2.2**. Specifically, GLOBIOM provided consistent projections of land cover and biomass demand under the ACCREU scenario protocol which considers *adaptation*, *climate impact*, and *mitigation policy* scenarios. According to the ACCREU scenario protocol, the socioeconomic drivers (GDP, population growth, food demand projections) are held the same across all scenarios and follow the SSP2 middle-of-the-road assumptions. The climate impacts on the mean annual increment of forest growth were also taken from the forest growth model 3PGmix (also conducted under the **ACCREU Task 2.2**). These projections serve as key drivers for G4M, allowing for a detailed analysis of future forest dynamics and biomass supply under climate change.

To assess the impacts of fire on forest dynamics and biomass supply, we build incrementally on our ACCREU reference scenario. First, we add the effects of climate change on forest growth and then a second step, we include both climate change impacts and burned areas from fire events. This approach allows us to isolate and compare the influence of each factor. For consistency, the same RCPs are used for both the climate impacts on forest productivity and the burned area projections. Mitigation policies influence the biomass demand, and therefore we keep biomass demand pathways consistent across all the climate impact and fire scenarios for clarity. This ensures that any observed changes in future biomass supply can be attributed directly to climate and fire impacts, rather than to differences in demand.

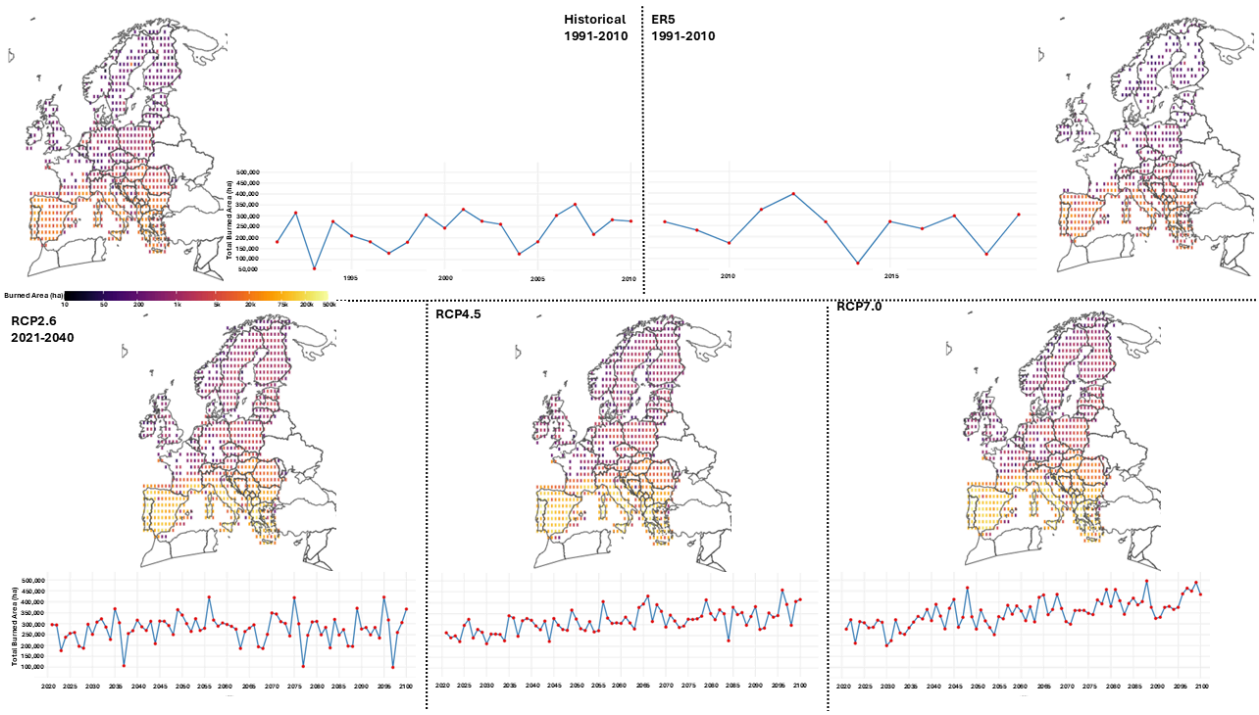

Figure 12: Burned area extent (ha) over time period as modeled by ForeFire and used within G4M, including historical observations, ERA5 reanalysis, and future climate scenarios

Table 4: Applied mortality rates for different species groups following fire events, based on expert judgment and data from Portugal's National Inventory Document (NID, 2025; Table 6-19).

Species/Forest Type	Applied Mortality Rate After Fire
Pinus pinaster	70%
Pinus pinea	30%
Other coniferous	70%
Eucalyptus spp.	50%
Quercus suber	30%
Quercus rotundifolia	10%
Quercus spp. (other oaks)	30%
Other broadleaves	30%
Shrublands	90%

The age structure of the forest further influences fire damage, with different age cohorts experiencing varying levels of impact depending on their developmental stage. Following fire events, regeneration in G4M depends both on the forest management and local conditions. Actively managed forests typically undergo salvage logging followed by immediate replanting with the assumed recovery share set at 54%, based on expert consultation with the developers of the Carbon Budget Model (CBM) (Blujdea, personal communication, 26 July 2023). However, protected forests are left to regenerate naturally, following the natural forest succession cycle. The underlying productivity of the cell also influences recovery rates, as more productive areas tend to exhibit faster regrowth. Through this mechanism, G4M translates spatially explicit burned area from the DTU fire model into biomass losses and recovery dynamics that reflect both ecological conditions and forest management practices.

Figure 13 shows the estimated losses in aboveground biomass carbon supply due to fires in all forested areas. The estimates are measured in 1000 tons of carbon (t C), under the three different climate impact scenarios: RCP2.6, RCP4.5, and RCP7.0. For each country, the bars show the magnitude of change in the total accumulated aboveground biomass carbon (expressed in 1000 tons of carbon) which are attributable to fire by 2050, the solid bars indicate that the accumulation results in a loss while the hatched bars indicate that the accumulation ends in a positive biomass accumulation. The overlaid points indicate the cumulative burned forest area (in 1000 hectares) over different time periods (2020-2030: white, 2020-2040: grey, 2020-2050: black). Facets are ordered so that countries with the largest absolute differences in biomass accumulation appear first, moving left to right, top to bottom. The biomass accumulation shown in the figure is relative to the total biomass that would accumulate in these forests under the corresponding climate scenario without fire disturbance. It is important to note that the impacts of climate change on biomass accumulation (e.g., mean annual increment) may be positive under higher RCP scenarios in some regions, due to CO_2 fertilization or longer growing seasons. However, in most cases, the occurrence of fire leads to reduced biomass accumulation within these forested areas, regardless of the underlying climate-driven productivity trends. It is also important to note that the timing of fire events influences biomass dynamics, as fires in the earlier years of the period allow more time for recovery before the end of the period.

The largest biomass losses are primarily found in southern European countries, Spain, Italy, France, Greece which account for almost 90% of the total biomass loss due to fire. The total burned areas are highest under RCP 7.0 and at a regional level the total biomass loss is highest under that RCP as well. In general, more burned areas across all forested areas results in higher losses in biomass, however there are notable exceptions. Since the spatial distribution of fires varies across the RCP scenarios, and owing to the differences in forest age structure and biomass stocks, some countries can experience positive gains in biomass accumulation over the period less burned area (e.g., Czech Republic) or in the case more mature forests being replaced by younger regenerating forests resulting in increased biomass accumulation after fire (e.g., Ireland).

Figure 13: Magnitude of change in above ground biomass after fire for all forested areas in 2050 under MPI GCM scenario under different representative concentration pathways (1000 t C, bars, primary axis) and cumulative burned areas at different time intervals in the fire scenarios (1000 ha, points)

Unmanaged forests, particularly those under protection or set aside for conservation purposes, are generally more susceptible to biomass losses following fire events due to their limited natural regeneration. By our estimates, under all RCP scenarios a third of the biomass losses occur in the unmanaged forested area, because unlike managed forests, where salvage logging and active replanting can accelerate regeneration and partially mitigate fire impacts, unmanaged forests rely solely on natural regeneration processes for recovery. This lack of intervention, combined with the fact that many of these forests are older, more mature stands, makes them especially vulnerable to persistent biomass losses when fires occur. Figure 14 specifically highlights the biomass losses in these forest areas classified as unmanaged and potentially protected, which are assumed to regenerate only through natural processes after fire events. These areas play a critical role in biodiversity protection and carbon storage, but their limited regenerative capacity after disturbances such as fire means that biomass losses can be more severe and persist for longer periods. Additionally, the age structure and biomass density of these forests contribute to the variability in losses, with mature forests often experiencing disproportionately high carbon losses when burned. Most of the unmanaged forest biomass losses are concentrated in southern European countries (70-75%). Between 20-25% of the losses are split between western Europe and central and eastern European countries.

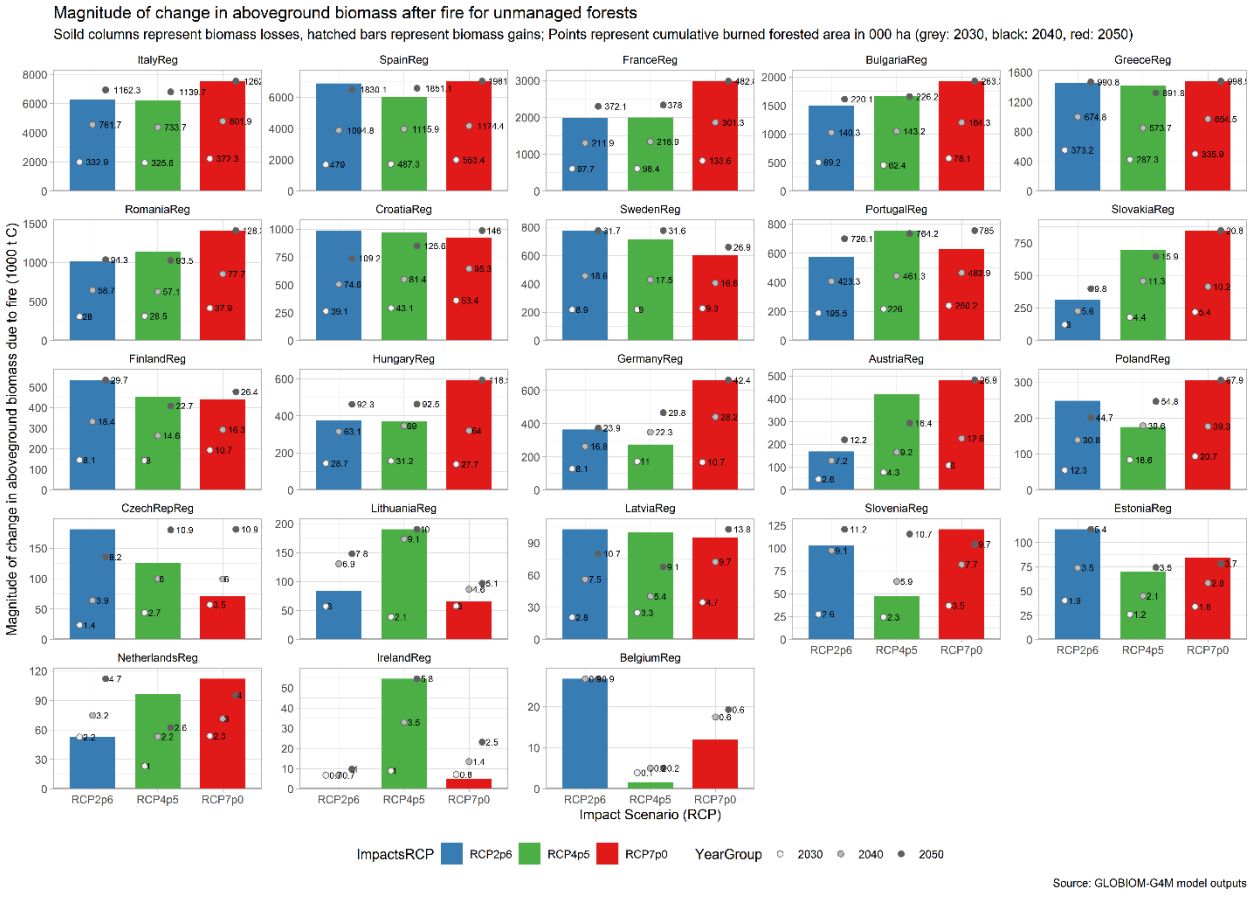

Figure 14: Magnitude of change in above ground biomass after fire for unmanaged forested areas in 2050 under MPI GCM scenario under different representative concentration pathways (1000 t C, bars,

primary axis) and cumulative burned areas at different time intervals in the fire scenarios (1000 ha, points)

Fire-related carbon dioxide emissions from European forests are projected to increase under future climate scenarios, reflecting both greater fire occurrence and higher biomass losses in vulnerable regions. Historical estimates from the Global Fire Emissions Database (GFED4.1s) suggest that between 2000 and 2016, the average annual CO2 emissions from fires in Europe were approximately 7 Mt CO2 per year, with substantial year-to-year variability driven by extreme fire seasons, particularly in Southern Europe (van der Werf et al., 2017). In comparison, our model results from the ACCREU scenarios presented here estimate that, by 2050, annual fire-related CO2 emissions from forests in Europe could reach 11.86 Mt CO2 per year under RCP2.6, increasing to 12.86 Mt CO2 per year under RCP4.5, and 14.55 Mt CO2 per year under RCP7.0. These estimates indicate a potential doubling of average fire emissions relative to recent historical levels under higher warming scenarios, underscoring the increasing role of wildfires as a source of greenhouse gas emissions in Europe's forest sector. To isolate the emissions specifically attributable to fire events, we compare two sets of model runs: the first incorporates only the impacts of climate change on forests, and the second includes both climate change impacts and the additional burned areas from fire events. By subtracting the emissions from the climate-only scenarios from the emissions in the combined climate and fire scenarios, we can estimate the net additional greenhouse gas emissions that are directly linked to fire events. The difference in the total fire-related emissions is presented in Figure 15 which provides a comprehensive view of how forests contribute to or mitigate climate change. The emission estimates include emissions and removals from multiple components of the forest sector, such as afforestation, dead organic matter, deforestation, forest management, deadwood, and litter.

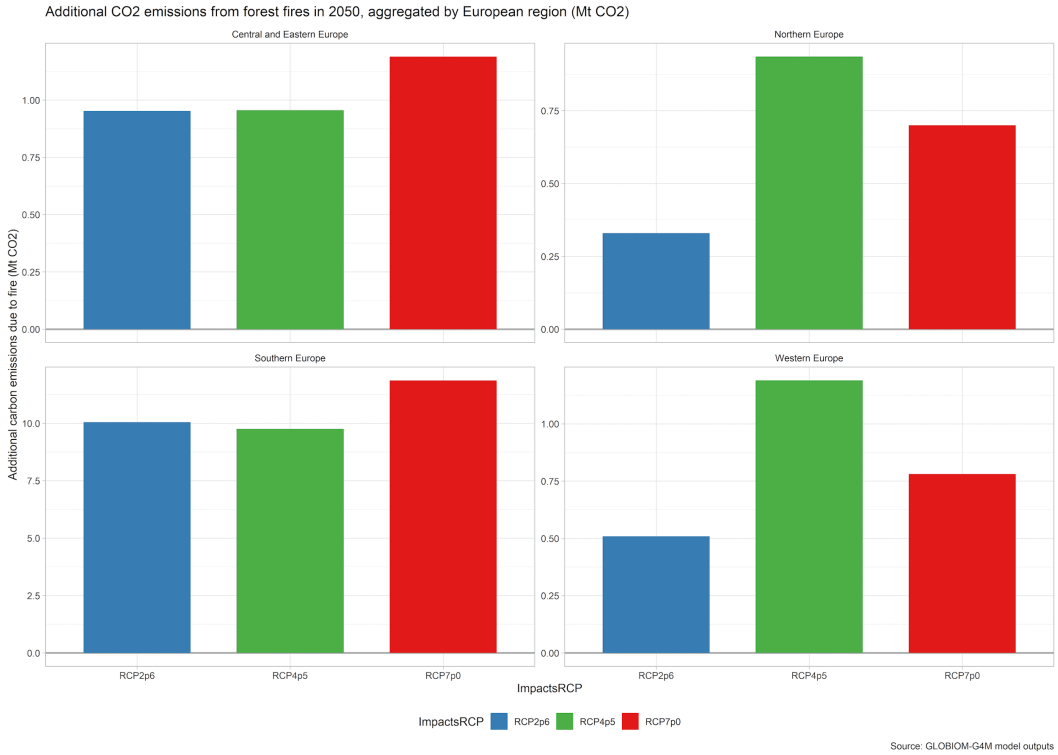

Figure 15: Estimated additional carbon emissions attributed to the forest sector from forest fires events for different major European regions in 2050, expressed in million tons of carbon (Mt C), under three different climate impact scenarios (RCP2.6, RCP4.5, RCP7.0).

The country-level impacts of fire-related carbon emissions are presented in Figure 16, providing a more detailed view of how fire affects forest carbon dynamics across different European countries, the figure is ordered such that the countries with higher emissions appear in the upper left of the figure. Southern Europe is the most affected region, with by far the highest additional CO2 emissions from forest fires across all climate scenarios. Central and eastern Europe have the second most significant CO2 emissions from fires though the model results highlight the strong spatial variability in fire-related emissions especially for RCP 4.5 and suggest that the relationship between fire risk and carbon emissions is not uniform across Europe.

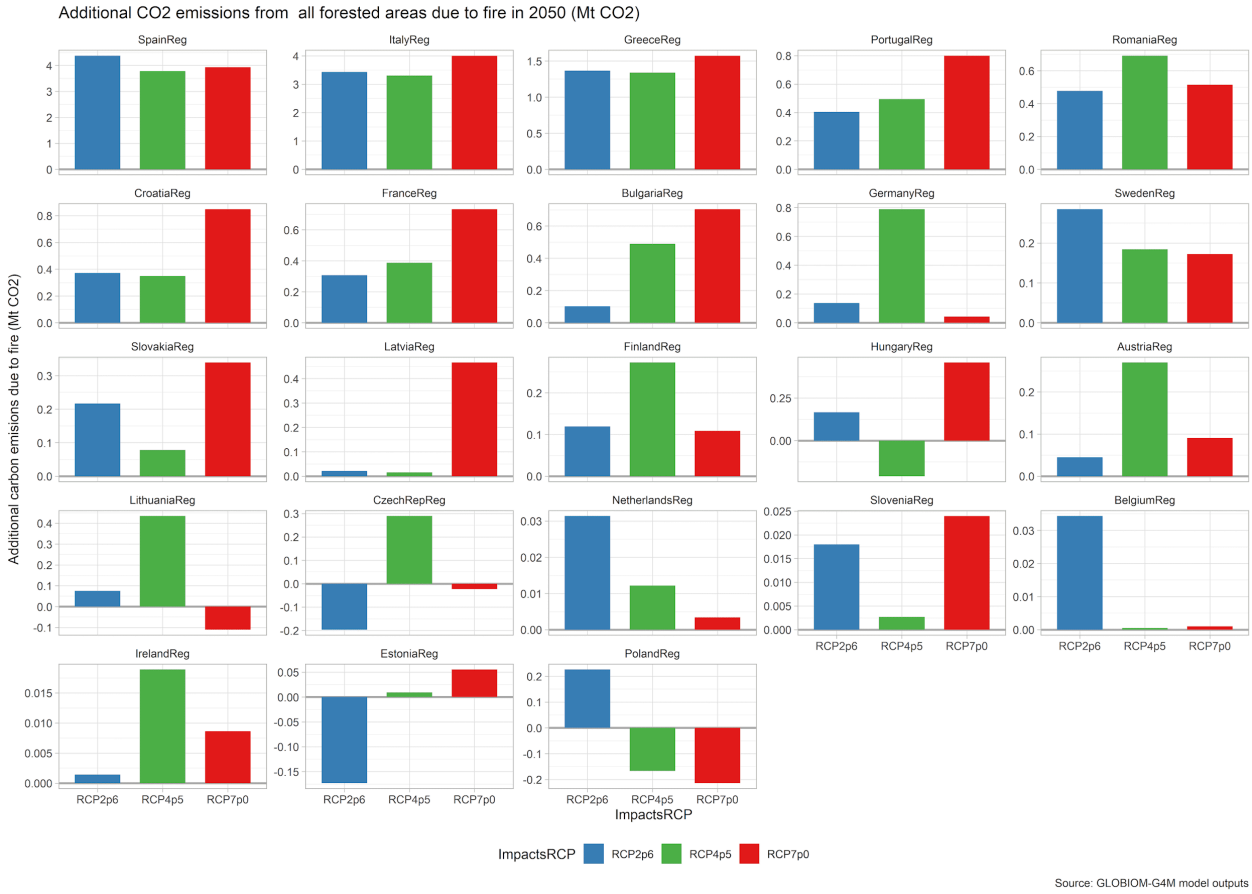

Figure 16: Estimated additional carbon emissions from the forest sector from forest fire events in 2050 at the country level, expressed in million tons of carbon (Mt C), under three different climate impact scenarios (RCP2.6, RCP4.5, RCP7.0).

As noted before, after fire events burned or damaged trees under forest management can be recovered and harvested which we refer to as salvage harvest. Planned harvest is the regular, scheduled forest management based on the long-term for growth cycles and management. Figure 17 presents the projected change in harvested wood supply across European countries from wildfire events occurring between 2020 and 2050. The figure distinguishes between the two types of harvested wood, salvage wood (hatched bars), and planned harvested wood (solid bars). Our results show that salvage operations can partially offset wood supply losses from a fire event but the total harvested wood over the long-term may fall below pre-fire expectations. This is because salvage only recovers a fraction of the biomass that would have been available under normal management and because the timing of salvage harvesting is likely suboptimal relative to the management plans and forest growth cycles. Owing to this, fire events not only reduce standing biomass but also interfere with optimal harvest scheduling, which can lead to a reduction in both economically optimal harvested wood supply in many cases.

Figure 17: Estimated difference in harvested wood supply due to fires in 2050 at the country level, expressed in 1000 m3 (Mt C), under different harvesting types (salvage and planned harvesting) under three different climate impact scenarios (RCP2.6, RCP4.5, RCP7.0).

2.3.3 Impacts of wildfire risk on local plant & animal communities

We calculated 2016 unique effect sizes of the effect of fire on local taxa abundances from 36 studies, covering four European forest biomes (Mediterranean Forests, woodlands and scrubs; Temperate broadleaf and mixed forests; Temperate Coniferous Forest, and Boreal forests/Taiga) and 15 ecoregions (Olson et al., 2001). Our data set had 1068 unique plant and animal species (or the closest possible taxonomic classification), which we grouped into one of 11 broad taxon categories. This data set allows us to quantitatively explore the effects of fire on various European taxa and provides the foundation for robust predictions of taxon-specific local abundance responses to future forest fires in Europe.

Our overall meta-analysis model that pools all effect sizes together showed a non-significant, small positive association between fire and taxa abundances (effect size = 0.07; 95 % Confidence Intervals CI -0.10, 0.24; p = 0.43). Our subgroup analysis, accounting for taxa-specific responses and fire severity, revealed that the **effect of fire on taxa abundances was significantly different between broad taxa groups and between fires of different severity** ($p < 0.001$). Notably, local abundances of arachnids, other arthropods, birds, insects, and molluscs significantly decreased after fire ($p < 0.05$) (Figure 18). Non-significant overall declines in abundance after fire were shown for mammals, plants, pollinator insects, and springtails ($p > 0.05$). In contrast, beetle and reptile abundances significantly increased after fire of any severity ($p < 0.05$). Increases in beetle abundances after fire have previously been attributed to patch moisture (Toivanen, 2014), and vegetation (Santos et al., 2014). Habitat homogenization, reptile thermal preferences by open areas, has been suggested as a reason for reptile abundance increase after fire (Ferreira et al., 2017). However, this has also been shown to be species-specific (Ferreira et al., 2016).

Interestingly, within some taxonomic groups, while fires of high severity led to a decrease in abundance, fires of low-medium severity led to an *increase* in abundance. This was particularly apparent for pollinator insects, plants, mammals, and springtails. Positive associations between pollinator insect (butterflies, bees, hoverflies) abundances and lower severity fires have previously been explained by trait diversity, increased plant survival compared to high severity fires, and local habitat modification (Mason et al., 2021). For example, increased bee abundances after lower severity fire have been attributed to increased abundance and accessibility to nesting sites (in deadwood or underground) after fire (Mason et al., 2021; Passovoy and Fulé, 2006). Butterfly abundance increase after lower severity fires may be related to increased survival of plants during these events, thereby increasing food resources and refugia (Swengel and Swengel, 2007). Mammal abundances have previously been noted to increase in recently-burned sites of lower intensity, often attributed to higher abundance of preferred regrowth vegetation in those sites (Chard et al., 2022; Driscoll et al., 2024).

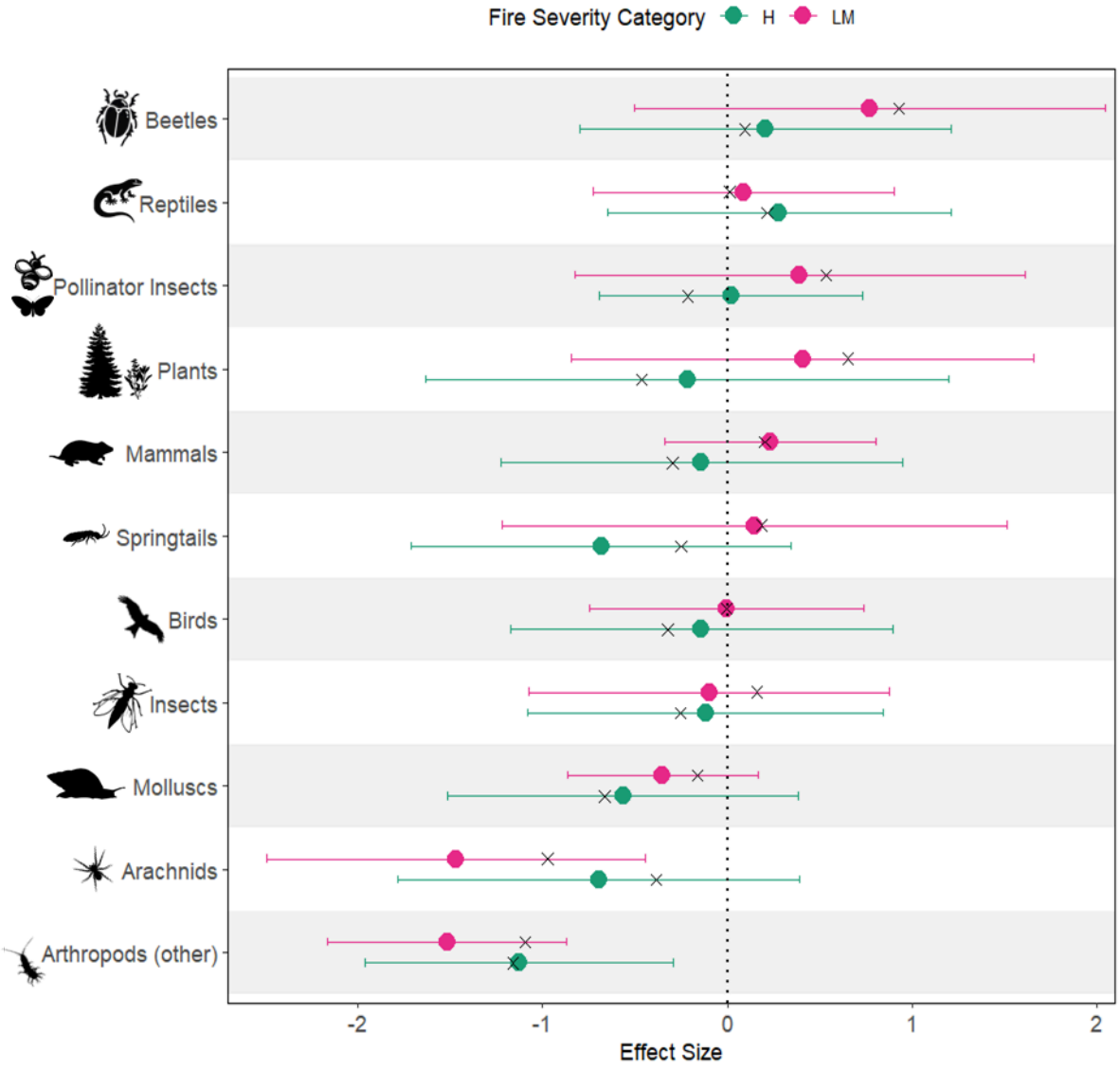

Figure 18: Mean observed effect sizes for European forest taxa, per broad taxon group, for two fire severity categories (H = high, LM = low-medium) (n = 2016) from 36 in situ European forest studies, covering four forest biomes and 15 ecoregions. Error bars depict ± 1 SD. The black vertical dotted line indicates an effect size of zero. The black crosses (×) depict the meta-analysis model predicted effect sizes.

Our meta-analysis represents a significant step toward empirically modeling taxon-specific responses to wildfire in European forests. The results demonstrate divergent abundance responses across taxonomic groups under the same fire scenarios, with some taxa increasing while others decline. Our results corroborate the consistently contrasting responses of abundances to fire in previous research (Driscoll et al., 2024; Giorgis et al., 2021; González et al., 2022; Mason et al., 2021), and adds evidence to the general scientific consensus that biotic community responses (e.g., taxa abundances) to fire are complex. Previous work shows that such responses are dependent on at least (1) underlying climatic and site condition e.g., biome (Moyo, 2022) and prevailing climate (Giorgis et al., 2021); (2) fire characteristics, e.g., severity, frequency, and time since fire (Grau-Andrés et al., 2024); and (3) species/taxa-specific ecological and functional traits (Bieber et al., 2023; Moyo, 2022; Santos et al., 2014).

This heterogeneity underscores the necessity of multi-taxa approaches in biodiversity impact assessments rather than relying on surrogate taxa to estimate ecosystem-wide effects. While we aimed to integrate these empirical effect sizes with projected wildfire scenarios, our meta-analysis revealed that **fire severity, rather than simply fire extent**, is a critical determinant of ecological impacts for most taxa. This creates a fundamental limitation, as current wildfire projections in Section 2.3.1 report only on the extent of the fire without characterizing its severity.

It should be noted that fire intensity and fire severity represent distinct concepts that should not be conflated in ecological modeling. Fire intensity refers to the energy released during combustion (typically measured in kW/m^2) (Rossi et al., 2020). Fire severity describes the ecological impact on vegetation, soils, and ecosystem structure (Hardy, 2005). Although related, the relationship between intensity and severity is highly context-dependent, influenced by factors such as fuel structure, vegetation type, soil moisture, and seasonal timing. This complexity prevents us from making ecologically meaningful projections based solely on fire frequency and extent data without accompanying severity information.

We recommend that future integrated assessment of wildfire impact on biodiversity should (1) focus on species/taxa, or similar functional groups, rather than overall biodiversity, as our study taxa show different responses to fire than the 'overall' predictions, (2) account for wildfire characteristics (e.g., severity, extent, frequency) as these can have significant effects on biodiversity measures, and (3) account for the type of forest ecosystems, its management and ecological intactness. Further, we recommend that future fire projection models include severity metrics alongside extent and frequency projections to incorporate wildfire impacts into biodiversity impact modelling effectively.

2.4 Conclusion/Key takeaways

We developed a **modular wildfire modeling suite** to assess wildfire risk across Europe under historical and future climate conditions. The modeling framework integrates multiple climate data sources, including ERA5-Land reanalysis for historical validation and bias-corrected CLIMEX2 projections for future scenarios. This approach provides the foundation for quantitative assessment of fire impacts, though the effectiveness of management interventions requires further investigation.

Integrating **wildfire projections into forest modeling** reveals significant spatial heterogeneity in biomass losses, with southern European countries (Spain, Italy, France, Greece) bearing approximately 90% of total biomass losses. Fire impacts are amplified under higher emission scenarios, with RCP7.0 showing the greatest burned area and biomass loss at the regional level. Management practices significantly influence post-fire recovery trajectories: (1) managed forests benefit from salvage logging and replanting (54% recovery rate); (2) unmanaged/protected forests rely solely on natural regeneration, making them disproportionately vulnerable (accounting for one-third of biomass losses despite smaller spatial extent). Wildfire-related CO_2 emissions from European forests are projected to increase substantially by 2050. These projections represent a potential doubling of fire emissions compared to recent historical levels. Salvage harvesting can partially offset immediate wood supply losses but typically results in suboptimal timing and volume compared to planned management, reducing long-term harvested wood supply.

We used a meta-analytical approach to **investigate the empirical impacts of fire on biodiversity**. Our meta-analysis of 2016 effect sizes from 36 studies demonstrates that wildfire impacts on biodiversity are highly taxon-specific and severity-dependent. We found that different taxonomic groups show contrasting responses to fire: (1) Significant decreases: arachnids, arthropods, birds, insects, molluscs; (2) Significant increases: beetles, reptiles; and (3) variable responses based on fire severity: pollinators, plants, mammals, springtails. Fire severity emerges as a critical determinant of ecological outcomes, with several taxa showing positive responses to low-medium severity fires but negative responses to high-severity fires. The current wildfire modelling that quantifies only extent and frequency, without characterizing severity, is insufficient for robust biodiversity impact assessment. From our findings, we make several recommendations for future integrated assessments: (1) focus on species/taxa or functional groups rather than generalized biodiversity metrics; (2) account for multiple fire characteristics (severity, extent, frequency); (3) consider forest ecosystem type, management practices, and ecological intactness; and (4) incorporate severity metrics alongside extent and frequency in projection models

The combined modeling approaches demonstrate that complex interactions will mediate climate change impacts on European forests between fire regimes, forest management practices, and taxonomic responses. While projected increases in fire activity will generally reduce forest carbon stocks and increase emissions, outcomes are highly context-dependent and vary significantly across regions, management regimes, and biodiversity components. A more integrated approach linking fire severity predictions with taxa-specific response models is needed to develop effective adaptation strategies that balance carbon sequestration, timber production, and biodiversity conservation objectives.

3 Impacts of Sea-Level Rise on Crop and Grassland Provision and Opportunity Cost for Sustainable Land Management and Conservation

3.1 Introduction

This chapter explores the economic implications of policies to promote conservation and restoration efforts under climate change and climate adaptation scenarios in Europe. Additionally, we assess the provisioning service of European ecosystems to provide crop and livestock products by examining how these services are impacted by change in land for the agriculture and forestry sector due to 1) sea-level rise impacts, and 2) conservation and restoration policies. Rising sea levels are expected to reduce the extent and productivity of low-lying agricultural and forest lands, leading to potential production and revenue losses and increased pressure on inland ecosystems. At the same time, protecting biodiversity and ecosystem integrity requires careful consideration of potential trade-offs with land allocated to agricultural production.

This chapter builds on the adaptation scenarios developed in **Task 2.2** of the ACCREU project. We introduce additional policies targeting land conservation and ecosystem restoration. These policies are consistent with the global strategy developed by Leclère et al. (2020) to "bend the curve" of biodiversity loss. We evaluate the outcomes in terms of Biodiversity Intactness Index (BII), and economic welfare impacts, reporting changes in consumer and producer surplus under conservation and restoration-enhanced scenarios relative to adaptation-only baselines. The assumptions for conservation and restoration follow the global strategy in Leclère et al. (2020) and include spatial prioritization of areas for conservation based on biodiversity value and restoration potential as well as the expansion of protected areas, with strict limits on land conversion in biodiversity-rich regions. As the focus of the ACCREU project is on Europe we have applied the biodiversity policies to EU countries only. By combining economic and ecosystem service perspectives, this analysis provides insights into trade-offs and synergies between land-based mitigation, adaptation, and production goals in Europe.

3.2 Methods

This section describes the methodological approach used to assess the economic implications of conservation and restoration policies, as well as the impacts of sea-level rise (SLR) on the provisioning ecosystem services of crop and grassland production in Europe. The analysis is carried out using the Global Biosphere Management Model (GLOBIOM), a global, partial equilibrium model developed by the International Institute for Applied Systems Analysis (IIASA).

GLOBIOM is a global partial equilibrium model that is used to model the supply and demand of agricultural products at a high spatial resolution in an integrated approach that considers the impacts of global change (socioeconomic and climatic) on food, feed, and fiber markets (Havlík et al., 2011). GLOBIOM models the supply and demand for various agricultural and forestry products using regional level and spatially explicit data inputs (Figure 19). In GLOBIOM, land is allocated or converted to production activities in the agricultural and forestry sector in order to maximize the sum of producer and consumer surpluses, subject to market equilibrium and resource, technological, and policy constraints. The equations of the model are linear or have been linearized so that the model can be solved using a

linear programming method. The model is recursive-dynamic and runs on ten year time steps, meaning that endogenous model solutions depend on the solutions found for the previous period.

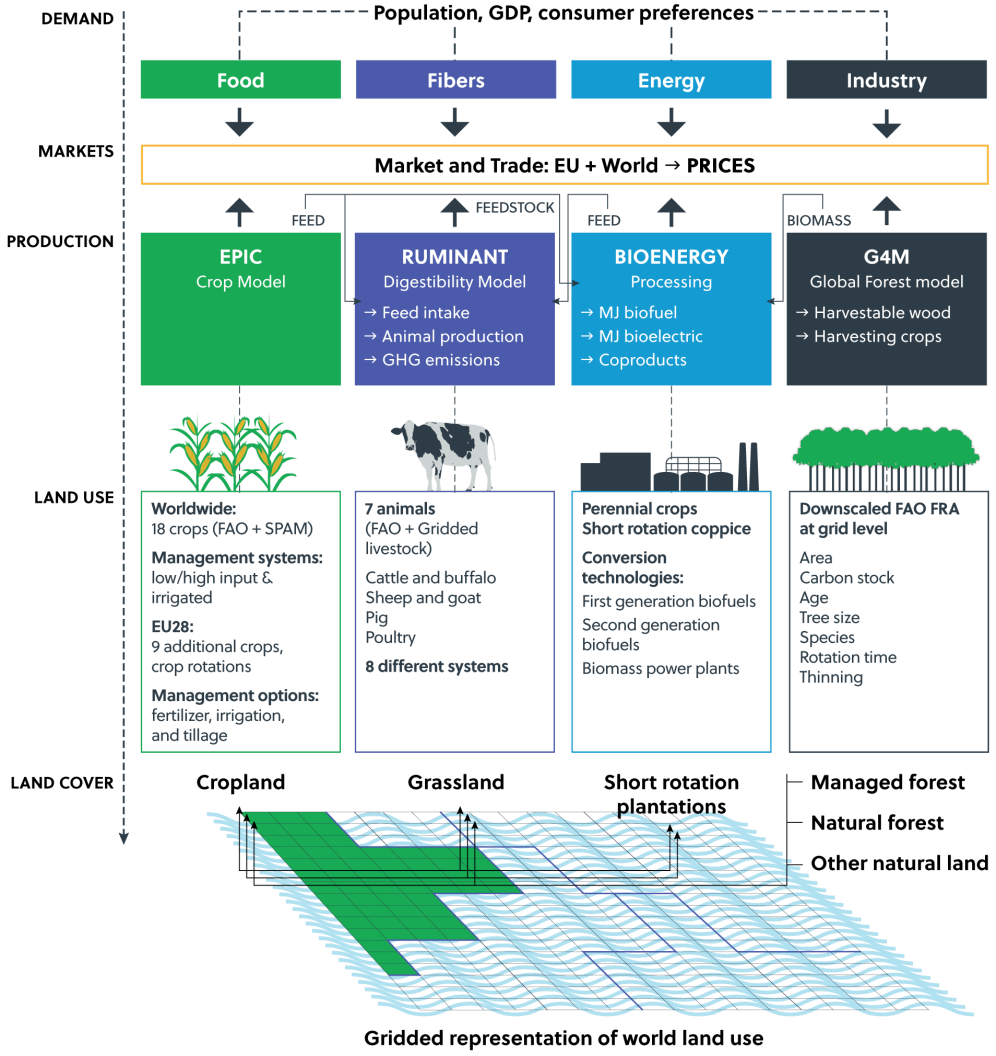

Figure 19: Illustrative representation of the bottom-up structure of GLOBIOM (Source: updated from Havlík et al. (2011) and GLOBIOM.org)

3.2.1 Restoration and conservation policies for biodiversity protection

For the ACCREU analysis, we examined the economic and biodiversity impacts of increased conservation and restoration efforts. To do this, we relied on three different measures for conservation and restoration. The first was the expansion of protected areas (PA) aligned with the work from Leclère et al. (2020). In this approach, spatial layers at 30-arcminute resolution were developed, which represent both the extent of protected area expansion and the possible land-use change restrictions within them. The expanded protected areas were created by combining information from three global datasets: the World Database of Protected Areas (for existing protections), the World Database on Key Biodiversity Areas (priority conservation areas), and wilderness areas as of 2009 (identified for their ecological integrity). These were first mapped at 5-arcminute resolution and then aggregated to 30-arcminute resolution to calculate the proportion of applicable land in each grid cell. These were then aggregated to the GLOBIOM land units to be used in the economic land use modeling.

The second type of expansion of protected areas is more aligned with the concept of Other Effective Area-Based Conservation Measures (OECMs) than with traditionally protected areas. This approach was also used by Leclère et al. (2020) to determine where land-use change should be restricted and prohibited if it led to a negative effect on biodiversity, as indicated by the Biodiversity Intactness Index (BII) modeled using the PREDICTS database. These layers were then used in the land-use change modeling to constrain how land could change in areas under the scenario assumptions. For unmanaged land (e.g., natural land and primary forests), conversion is fully restricted, consistent with strict protection. For managed land within these areas, existing land uses are permitted, and a shift towards land uses more favorable to biodiversity are allowed. These conservation modeling assumptions do not guarantee biodiversity improvement, but rather they aim to prevent further degradation through restrictions on land use change.

The third type of policy is considered a restoration policy which follows the methodology from Leclère et al. (2020) which developed a spatially explicit biodiversity value score (BV) at a 30-arcminute resolution. This score estimates the relative biodiversity importance of each grid cell based on land use. It combines (i) a regional, pixel-specific species richness index weighted by range rarity (RRRWSR), (ii) the biodiversity intactness (BII) associated with each land-use type and pixel, and (iii) the proportion of land area covered by each land use in each pixel. The RRRWSR score was calculated from species range maps covering a wide range of taxonomic groups (e.g., mammals, birds, amphibians, plants), and provides a measure of the contribution each pixel makes to regional biodiversity. This information was then used within GLOBIOM to identify priority areas for conservation and restoration outside of existing protected areas. Restoration-focused scenarios explicitly introduce a new land use class (RstLnd) which represents restored areas, alongside a biodiversity-weighted subsidy or tax that influences land use change decisions to favor restoration or less intensive land uses.

The ACCREU modeling framework aims to examine conservation and restoration lines with global biodiversity targets, though within a shorter timeframe than the original 'Bending the Curve' framework proposed by Leclère et al. (2020), which assessed biodiversity pathways to 2100. In the results section of this chapter, we provide an assessment of the impact these policies have on different biodiversity indicators as well as how the policies impact the supply of different crop and livestock provisioning ecosystem services (e.g., crop production and grassland fodder).

3.2.2 SLR impacts on agricultural production and revenues

We further examine how different crop and livestock provisioning ecosystem services are affected within a context of shrinking land availability due to sea-level rise. This analysis assesses the potential economic impacts of sea level rise (SLR) on agricultural systems by overlaying spatial projections of SLR exposure with land use outputs from GLOBIOM under the ACCREU climate adaptation scenarios. We estimate the changes in crop and grassland production and associated revenues, comparing the indicators with and without SLR-induced coastal flooding.

Flood hazard risk areas were identified using a high-resolution, country-specific SLR inundation model based on the MERIT DEM (Yamazaki et al., 2017). This model applied a 10 km coastal buffer, excluded permanent water bodies, and incorporated national-level relative SLR projections from the DIVA model. The resulting binary flood maps were aggregated to 10 x 10 km fractional inundation grids, aligned with the spatial structure of the ACCREU land-use scenarios.

We spatially overlaid these projected inundation extents with downscaled land-use data that categorize agricultural and natural land into detailed management classes. For each polygon (SimUID), we used zonal statistics to calculate the share of each land-use type affected by flooding. These flooded land-use fractions were then used to estimate impacts on crop and grassland provisioning. Our method does not make a distinction with the different hazard types stemming from sea-level rise including saltwater intrusion and coastal flooding/erosion.

Economic impacts were calculated by comparing production and revenue under baseline and SLR-affected conditions. For cropland, we estimated total production and revenue by crop using area, yield, multicropping index (MCI), and price data. Losses due to SLR were derived by subtracting the SLR-affected values from the baseline. For grassland, similar calculations were used to assess total grass production and the shortfall resulting from inundation, which was then compared to livestock feed demand to estimate the grass production gap.

This integrated approach enables us to quantify both the direct land loss and the indirect consequences for crop and feed production and the resulting economic implications in terms of lost revenues and feed gaps. For more detailed information on the methods used to examine the impacts of coast flooding please refer to Annex D.

3.2.3 Scenario protocol

The scenario protocol for this analysis builds on three dimensions previously explored and assessed in **ACCREU Deliverable 2.2**. In that analysis the protocol explored the biophysical *climate change impact* scenarios representing four levels of warming (No climate change/reference climate, RCP 2.6, RCP 4.5, RCP 7.0 based on four CMIP6 GCMs) as well as three different *mitigation policy pathways*, and the *ACCREU adaptation scenarios* (Reference, High, and Low). We hold *socioeconomic assumptions* constant across all scenarios by using the SSP2 narratives and drivers for GDP and population growth, as well as SSP2 diets and demand for other products. In our analysis, we distinguish between the *mitigation policy* scenarios, which assumes different carbon pricing for AFOLU emissions and biomass demands, and scenarios that include *climate impacts*. This separation is important because mitigation policy and climate change impacts influence the AFOLU sector through fundamentally different mechanisms.

Mitigation affects profitability via policy-driven shifts such as increased biomass demand and GHG emissions taxes, while climate impacts affect productivity and resource availability (via yields and water availability) through biophysical changes in temperature, precipitation, and radiative forcing.

In the results presented here, we have presented the scenarios of the protocol that link the climate impacts with their corresponding mitigation pathways (e.g., RCP2.6 impacts with RCP2.6 mitigation). However, for comparison, we chose to focus on how the ACCREU adaptation scenarios (which include both climate and mitigation effects) behave relative to a *reference adaptation* scenario with no climate change and no mitigation policy so we can see the incremental and combined effects. The analysis for this deliverable extends this scenario protocol to assess the economic and biodiversity implications of increased *conservation and restoration policy scenarios* for Europe. We run the GLOBIOM model with model-enforced restrictions on biodiversity-detrimental land use change (which we refer to as increased conservation) and restoration in addition to the ACCREU scenario protocol from D2.2 which includes the *ACCREU adaptation, climate impacts, and climate mitigation policy* scenarios.

The adaptation scenarios refer to the following levels of agricultural sector adaptation to changing environmental conditions (See **ACCREU Deliverable 2.2**):

- The high adaptation scenario represents a future where farmers have a high adaptive capacity to climate change. Significant investments are made to reduce the vulnerability of agricultural systems to climate impacts, including proactive measures and advanced technology to increase yields under climate change, more efficient irrigation systems, expansion of sustainable irrigation, and increased trade from less climate-affected areas
- The reference scenario represents the medium adaptation scenario that aligns with the underlying assumptions for the development of the agriculture and forestry sector under the socioeconomic pathway SSP2.
- The low adaptation scenario represents a future where farmers have less access to technical options and therefore, the agricultural sector has limited adaptive capacity to climate change. In this scenario, irrigation systems are poorly maintained, which lowers their efficiency. Crop switching and land use adjustments happen slowly and on a smaller scale.

3.3 Results & Discussion

3.3.1 Conservation and restoration scenarios

This section presents the results of the conservation and restoration policies applied to the economic land use model GLOBIOM under the ACCREU scenario framework. It includes an assessment of biodiversity outcomes (Biodiversity Intactness Index, BII) and land use change, changes in net revenues from agricultural and forest production which can offer an indication of potential economic trade-offs from prioritizing biodiversity and finally the impacts of these policies on the crop and livestock provisioning services provided by European ecosystems.

The Biodiversity Intactness Index (BII) represents the average abundance of originally present species across terrestrial ecosystems relative to pre-disturbance conditions. Values closer to 1 indicate higher biodiversity intactness, with lower values signaling increased biodiversity loss. BII was calculated using the methodology established by Leclère et al. (2020) to assess biodiversity responses under different land-use, climate, and conservation scenarios. In this section, we will examine three levels of climate impacts: RCP2.6, RCP 4.5, and RCP 7.0. We would like to note that this scenario dimension for climate impacts, as presented in the figures of this analysis, reflects the average of the modeling results obtained using general circulation model (GCM) specific model inputs. The average of model results (in this case 4 GCMS) is not an average of the climate inputs themselves. Each biophysical input is specific to each GCM scenario and was run separately with its own distinct climate inputs, and the resulting impacts were run in GLOBIOM over the time period and then averaged to provide a representative mean outcome of the climate impact. For more information on how the climate impacts were included in GLOBIOM, please reference the **ACCREU Deliverable 2.2**.

Figure 20 shows the projected BII outcomes for Europe in 2050 based on the ACCREU scenarios for adaptation under climate impacts and mitigation assumptions. In the figure, the solid black horizontal line represents the baseline BII under the reference scenario with reference adaptation, no climate change impacts, no mitigation, and no conservation action. The dotted green line shows the BII for the reference scenario (no climate impacts, no mitigation, reference adaptation) but with conservation and restoration policies implemented. Our findings show that the conservation and restoration policies increase the BII across all scenarios. Increased mitigation efforts (e.g., moving from RCP 7.0 to RCP2.6) result in increased BII for Europe as a region. The BII is highest under the Low Adaptation scenario with conservation and restoration policies. This reflects perhaps a trade-off where poor adaptation capacity and lower agricultural productivity result in greater land abandonment, which can indirectly benefit biodiversity.

These findings illustrate that while weak adaptation limits farmer resilience to climate change, it may also create conditions favorable for biodiversity recovery, highlighting the complex interactions between adaptation, land use, and ecosystem outcomes.

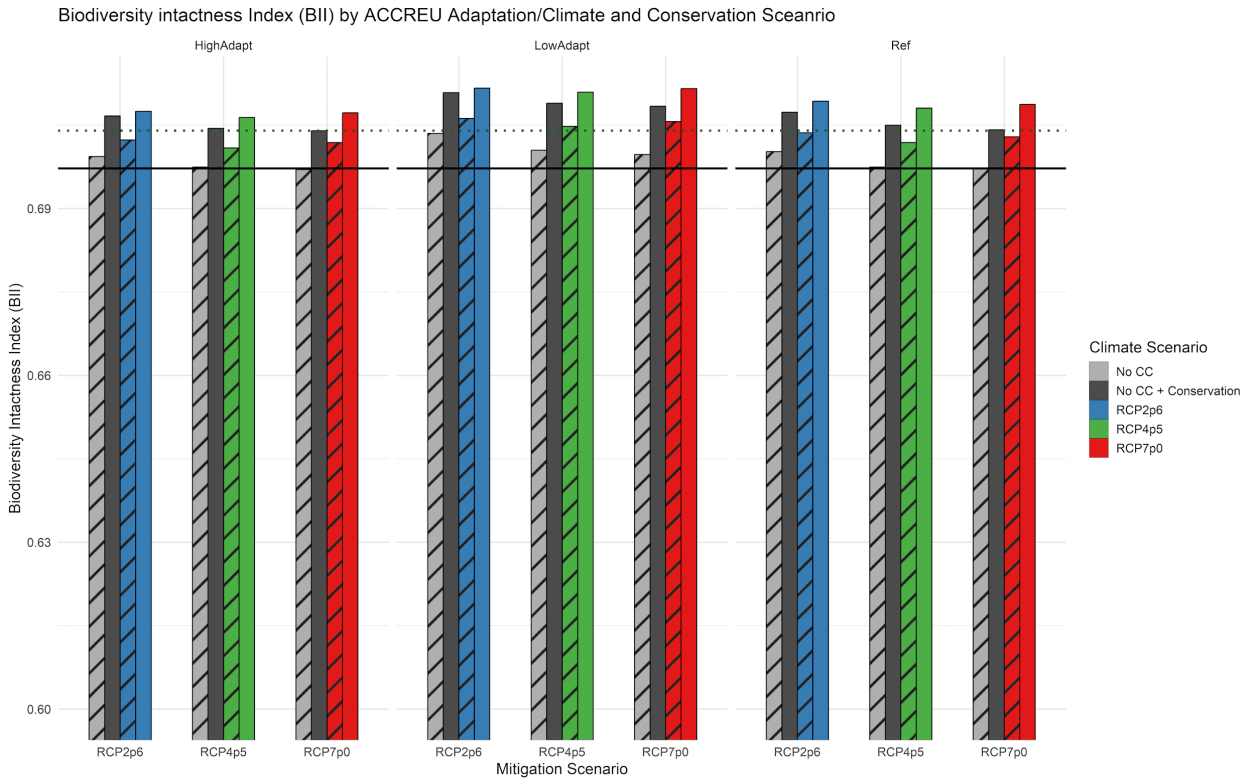

Figure 20: Biodiversity Intactness Index (BII) in 2050 for Europe under combined adaptation, conservation, climate, and mitigation scenarios using the ACCREU framework. Bars represent BII outcomes for different mitigation pathways (RCP2.6, RCP4.5, RCP7.0) across adaptation scenarios (High Adaptation, Low Adaptation, Reference Adaptation). Bar colors indicate climate impact scenarios, while hatching indicates scenarios with the absence of conservation and restoration actions. The solid black lines indicate the baseline BII for the scenario with reference adaptation, reference climate and no mitigation and no conservation), while the dotted green lines show the BII for the same scenario but with conservation policy.

When we look at the impact of the conservation and restoration scenarios at a more regional scale, we can see that for all regions, the reference scenario with reference adaptation, no climate impacts, and no mitigation the BII is the lowest (Figure 21). The conservation and restoration policy assumptions in all regions result in a higher BII. Under climate impacts for the most part the impacts are quite small but there are slight increases in the BII likely due to shifts in agricultural areas that result in land abandonment.

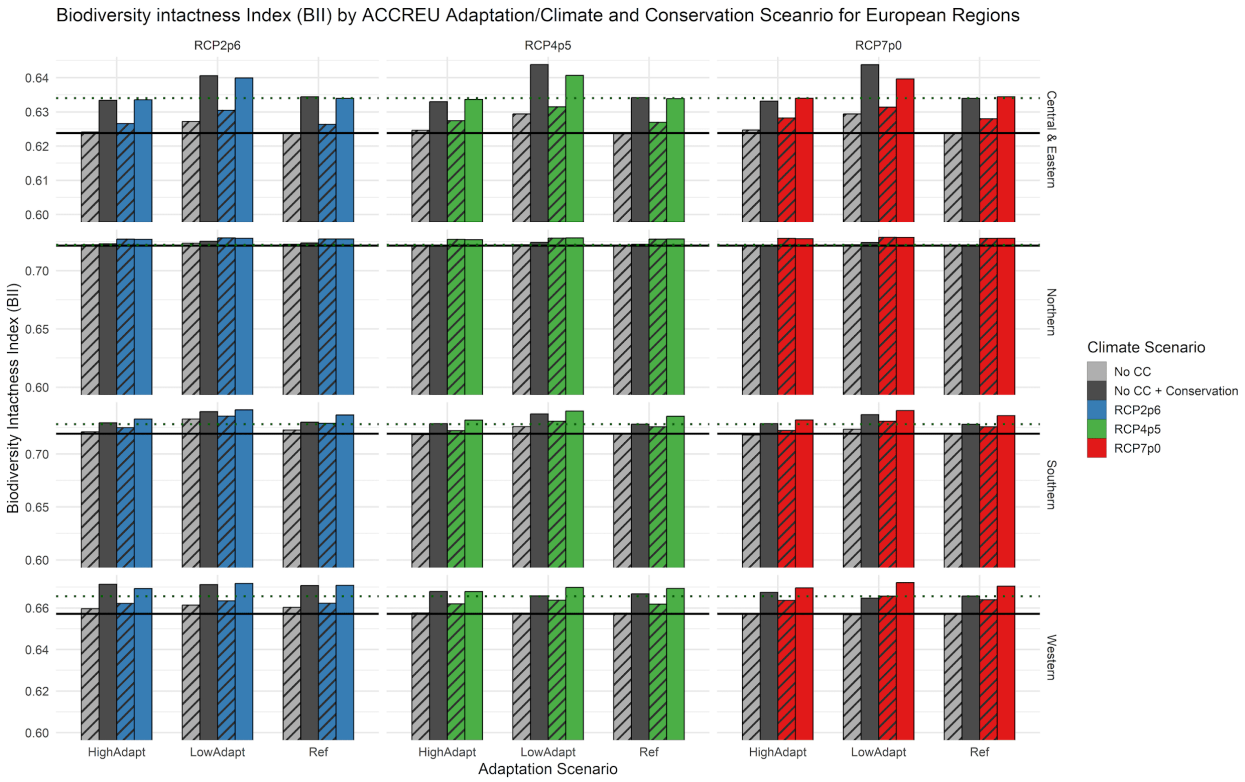

Figure 21: Biodiversity Intactness Index (BII) in 2050 for European regions under combined adaptation, conservation, climate, and mitigation scenarios using the ACCREU framework. Bars represent BII outcomes for different mitigation pathways (RCP2.6, RCP4.5, RCP7.0) across adaptation scenarios (High Adaptation, Low Adaptation, Reference Adaptation). Bar colors indicate climate impact scenarios, while hatching indicates scenarios the absence of conservation and restoration actions. The solid black lines indicate the baseline BII for the reference scenario (reference adaptation, reference climate and mitigation, no conservation), while the dotted green lines show the BII for the reference scenario with conservation.

To look at the impact conservation and restoration policies have on the livelihoods of agricultural producers we examined the changes in the production volumes across the scenarios. Production net revenues reflect the total economic output of the agriculture and forest sector commodities, calculated using the endogenous commodity prices and taking into account the carbon tax payments attributed to agricultural and forest production (Figure 22). In the figure the bar colors indicate average of the GCMs under different warming levels, while hatching indicates scenarios in absence of conservation and restoration actions. The solid black lines indicate the baseline production volume for the reference scenario (reference adaptation, no climate change, no conservation), while the dotted green lines show the production volume for the reference scenario with conservation. Our results show the clear impact of mitigation policy on the revenues for producers with higher mitigation scenarios (e.g. Mit2p6 having lower net revenues compared to Mit7.0). The results show that adaptation plays a critical role in sustaining farmer livelihoods under climate change. We find that the high adaptation scenario can likely offset the negative impacts from climate change and potentially buffer the economic trade-offs of land use policies that aim to shift land away from agriculture. Furthermore, our results show that low

adaptation leaves producers more vulnerable under higher warming levels and under conservation policies. Figure 23 also shows production across the same set of scenarios but this figure is in tons of dry matter production for the crop sector. While the climate effect on production volumes in metric tons is stronger with higher warming levels having the biggest losses in production (-11% less under low adapt, -9% in reference adapt, and -3% in high adapt), the conservation policy effect results in losses of consistently around 3% for the lowest warming levels across adaptation scenarios and 3.5% for the higher warming levels. Low adaptation has the highest losses compared to the other adaptation scenarios under the conservation scenarios with and without climate impacts considered. Implementing conservation and restoration policies consistently lowers production volumes as well as revenues compared to scenarios without such policies.

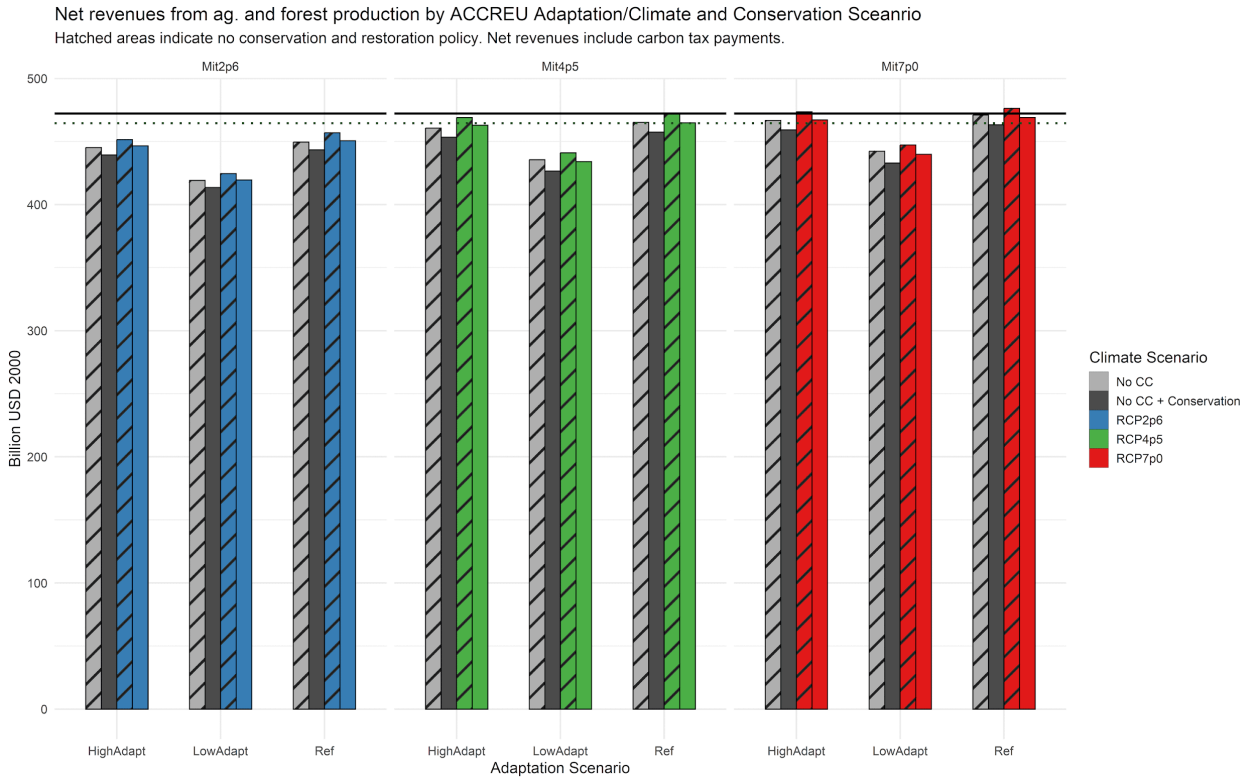

Figure 22: Net revenues agriculture and forest products (Billion USD 2000) in 2050 for Europe under combined adaptation, conservation, climate, and mitigation scenarios using the ACCREU framework. Bars represent production revenues less carbon tax payments for different mitigation pathways (RCP2.6, RCP4.5, RCP7.0) across adaptation scenarios (High Adaptation, Low Adaptation, Reference Adaptation). Bar colors indicate the GCM average of the climate impact scenarios, while hatching indicates scenarios absence of conservation and restoration actions. The solid black lines indicate the reference adaptation scenario production volume for the reference climate and mitigation and no conservation), while the dotted green lines show the production volume for the reference scenario under reference climate and mitigation with conservation.

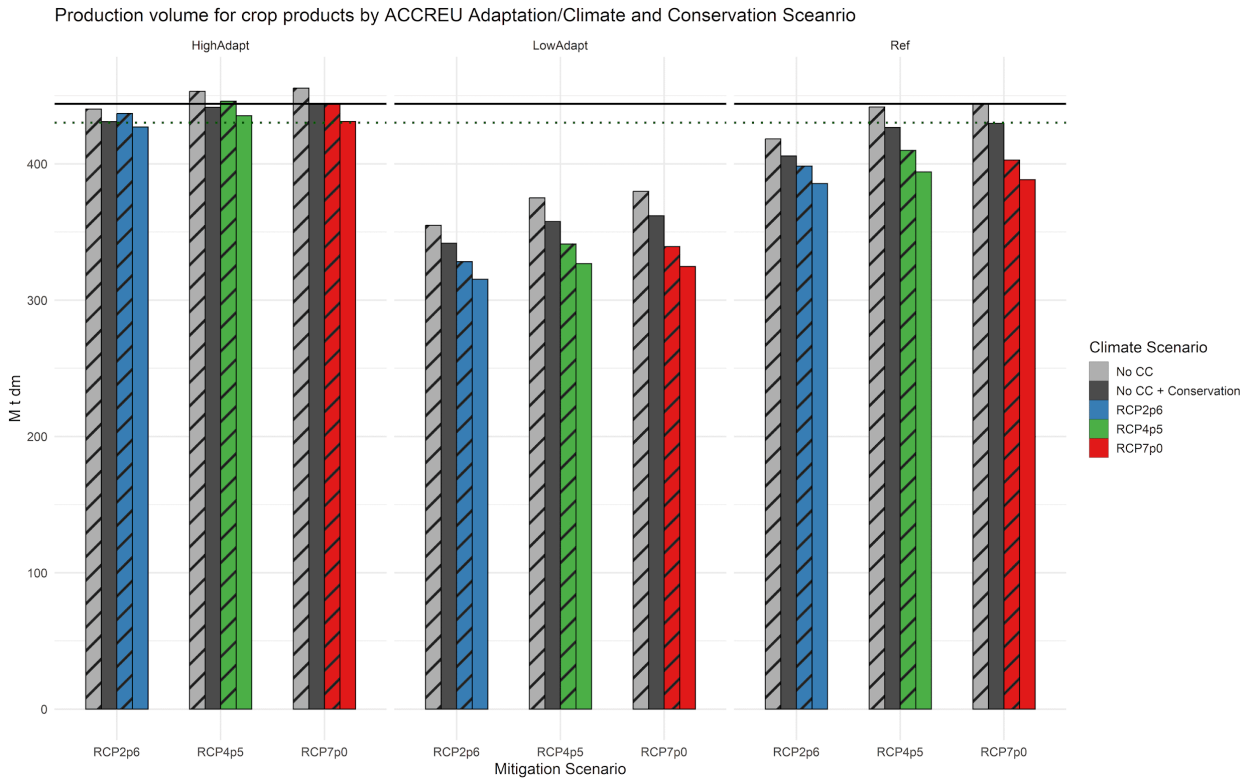

Figure 23: Production volume for crop products (Mt dry matter) in 2050 for Europe under combined adaptation, conservation, climate, and mitigation scenarios using the ACCREU framework. Bars represent production volume for different mitigation pathways (RCP2.6, RCP4.5, RCP7.0) across adaptation scenarios (High Adaptation, Low Adaptation, Reference Adaptation). Bar colors indicate climate impact scenarios, while hatching indicates scenarios absence of conservation and restoration actions. The solid black lines indicate the reference adaptation scenario production volume for the reference climate and mitigation and no conservation), while the dotted green lines show the production volume for the reference scenario under reference climate and mitigation with conservation.

Provisioning services, specifically the production of food, are a vital ecosystem service which contributes to human well-being and socioeconomic stability. We examine the tradeoffs with the food provisioning services of European ecosystems under the conservation and restoration policies. Figure 25 presents the estimated percent change in key agricultural provisioning indicators in Europe by 2050, relative to the ACCREU scenario with reference climate and mitigation and no additional conservation measures. The indicators include cropland area, crop yield, total crop production value in USD (considering changes in prices), grassland area, ruminant livestock numbers and livestock production value for ruminant and dairy (considering changes in prices). The size of the symbols indicates the presence of additional conservation and restoration assumptions, with larger symbols representing the biodiversity-focused conservation and ecosystem restoration scenarios. Results are shown across the different climate mitigation pathways (RCP2.6, RCP4.5, and RCP7.0) and the different ACCREU adaptation scenarios (HighAdapt, LowAdapt, and Ref).

Across all scenarios, implementing conservation and restoration policies aimed at biodiversity protection reduces the value of crop production compared to the same scenario without the policies (i.e., big squares compared to small squares). In all scenarios the conservation and restoration protections result in a further decline in crop area (i.e., all circles are less than 0), but in most scenarios there is at the same time an increase in the crop yield compared to the no conservation scenario (e.g., triangles greater than 0). This indicates that farmers employ intensification or abandonment of less productive land to buffer the impacts of the increased warming levels and the protection measures on land. Under the additional conservation policies, grassland areas, livestock production value, and livestock numbers are all lower than in the same scenarios without conservation policies. However, under increasing mitigation (higher carbon prices), the High and Reference Adaptation Scenarios have both a decline in the grassland area and a decrease in the ruminant livestock numbers while also an increase in the livestock production value compared with the ACCREU scenario under reference climate and mitigation for both the conservation and the no conservation scenarios. In these scenarios, the carbon prices on AFOLU emissions drive livestock managers to adopt more GHG-efficient practices, and the additional conservation policies do not significantly limit their ability to adapt in an economically and environmentally sustainable way. The area limited activities livestock managers can employ to buffer the impacts of carbon taxes on AFOLU emissions or biodiversity and conservation policies targeting land. Reducing livestock numbers and increasing the feeding of grains in lieu of grass are some options.

Overall, we find that the provisioning services that ecosystems deliver for food production are not too negatively impacted by conservation and restoration policies as farmers endogenously adapt to land use restrictions and incentives to restore land that may become less productive under higher warming levels. When conservation policies are combined with ag R&D that boost crop yields (HighAdapt), crop areas can be retired or restored to natural lands with minimal losses in the crop production value.

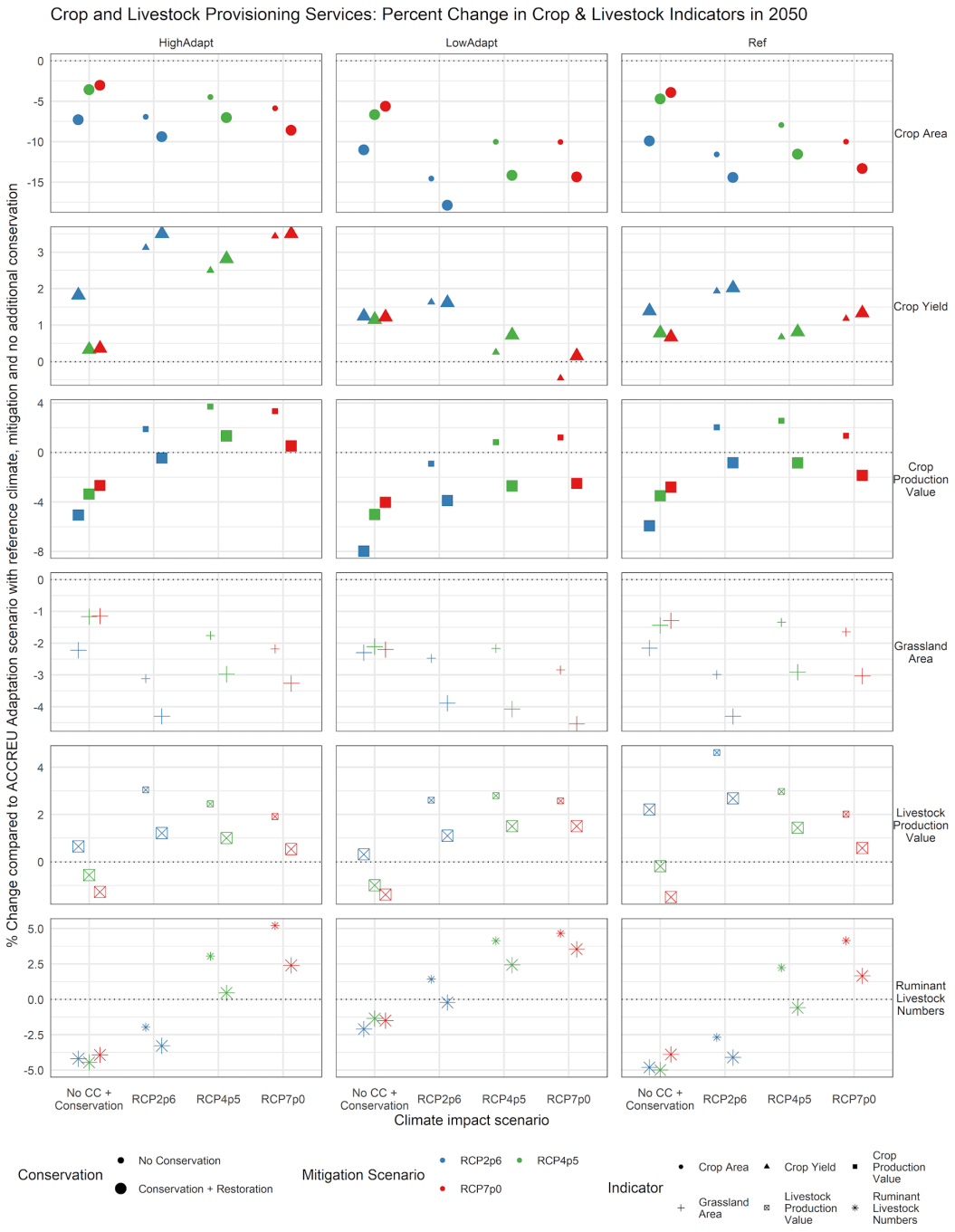

Figure 24: Percent change in crop and livestock provisioning services in 2050 relative to the ACCREU scenario with reference climate, mitigation and no additional conservation interventions. Size of symbols show conservation measures with larger symbols representing scenarios with additional conservation and restoration efforts. Colors indicate the climate mitigation pathways (RCP2.6, RCP4.5, RCP7.0). Panels differentiate the ACCREU Adaptation scenarios: High Adaptation, Low Adaptation and Reference Adaptation.

Under the increased conservation and restoration scenarios there is, by design, an increase in the protected area, firstly by their expansion and secondly, by restricting biodiversity-detrimental land use change within high-biodiversity grid cells. In EU27 countries, by 2050 our results estimate an increase of nearly 13 M ha compared to the ACCREU scenarios without increased conservation. These areas are not different by adaptation scenario or climate scenario as these are strictly enforced protections. The second type of conservation (more aligned with Other Effective area-based Conservation Measures (OECMs)) results in around 92 M ha across EU 27 countries that would be prohibited from further land use conversion that would degrade the biodiversity. The largest share of protected areas occurs in southern Europe with around 42 M ha followed by western Europe with 24M ha. Strong climate mitigation and higher warming levels have very little impact on the overall level of protected areas.

The net change in restoration area under the conservation and restoration scenarios is presented in Figure 25 by major European regions in 2050 under different climate impact and adaptation scenarios. The y-axis shows the difference in restoration area (in million hectares) compared to the Reference baseline scenario without climate impacts, without mitigation and without conservation efforts. Warming levels (i.e., climate impact levels) are presented along the x-axis. The colors of the points distinguish mitigation pathways: blue for RCP2.6, green for RCP4.5, and red for RCP7.0. Different shapes correspond to ACCREU adaptation scenarios: High Adaptation, Low Adaptation, and Reference Adaptation. Across all regions and scenarios the restoration area increases under the restoration scenarios, by design of the scenarios. Western Europe and central and eastern Europe have the largest increase in restoration area by 2050. For most regions, the low Adaptation scenario, which faces limited Ag R&D investment and relatively low crop yield growth, results in the largest restoration area under all climate impacts and mitigation pathways. This indicates that the economic incentive for restoring land is driven by farmers facing low productivity on land. In contrast, in most regions and climate and mitigation scenarios, the restoration area is higher under the reference adaptation scenarios than under the higher adaptation scenarios which faces significantly higher Ag R&D investment and raises the profitability of agricultural land even in the face of higher warming levels. As a result less land is abandoned by agriculture and even less land is economically attractive for restoration which suggests that restoration policies must consider subsidies that are ambitious enough to attract farmers to achieve the restoration targets in the future.

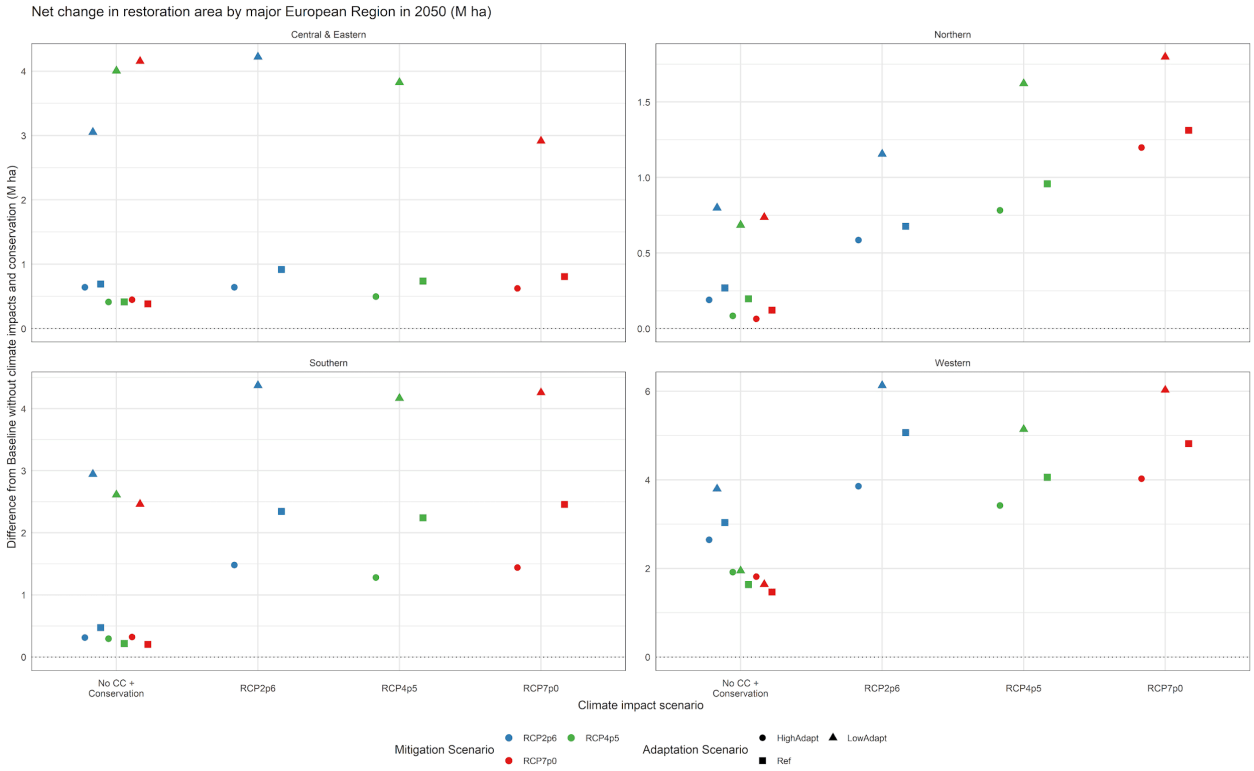

Figure 25: Net change in restoration area for different European Regions in 2050 relative to the baseline without climate impacts or conservation interventions. Symbol shapes differentiate the ACCREU Adaptation scenarios: High Adaptation, Low Adaptation and Reference Adaptation. Colors indicate the climate mitigation pathways (RCP2.6, RCP4.5, RCP7.0). Panels represent different European regions.

3.3.2 SLR impacts on agricultural production and revenues

This section presents the results of the sea level rise impact analysis applied within the ACCREU scenario framework using the economic land use model GLOBIOM. The assessment incorporates the downscaled land cover modeling results from the ACCREU scenarios presented already in ACCREU Deliverable 2.2, which already consider the potential climate impacts from higher warming levels and adaptation to these impacts but the land use scenarios do not include direct adaptation to rising sea levels. The analysis focuses on identifying potentially flooded cropland and grassland areas along Europe's coastlines and estimating the associated economic consequences. Specifically, it examines potential losses in cropland production revenues and the implications of flooded grasslands for meeting livestock grazing requirements, highlighting where sea level rise may further reduce the availability of grazing land and fodder production.

For this work, we required spatial estimates of coastal flooding. The DIVA model deployed in **ACCREU Deliverable 2.1**, and in this **Deliverable 2.4** was not able to provide spatially explicit raster maps of coastal flooding required for our model inputs. To address this limitation, we developed a custom model to generate the required SLR raster maps. Using the identical inputs of relative sea level rise (RSLR) and digital elevation model (MERIT DEM) as per the DIVA model deployment in **Deliverable 2.1**, we developed a modified bathtub model to estimate coastal flooding (fraction of flooded area) per 10x10 km grid cell, accounting for regional differences in RSLR. The full bathtub modelling approach is outlined in **Appendix D**. In our analysis, we focus only on agricultural adaptation to climate change, such as shifts in crop choice, management system, and land use, without taking into account any assumptions about coastal protection adaptation measures. Coastal protections are not included in our current GLOBIOM modeling framework.

Based on the overlaid coastal flooding on the projections of land use from the ACCREU scenarios we estimate that by 2050 nearly 700,000 ha of land area would be flooded. Figure 26 presents the projected flooded areas under different climate scenarios and time periods based on the GCM mean for the reference ACCREU adaptation scenario. The left panel disaggregates the total flooded area by the different European regions (Central & Eastern, Northern, Southern, and Western), while the right panel breaks it down by different land use type. Figure 27 further differentiates the different flooded areas by type and region. Our results show that across all RCPs, the total flooded area increases over time, with Western and Southern Europe consistently accounting for the largest shares of impacted land. In terms of land use, grassland and cropland are the most affected land use types with total flooded areas in excess of 125,000 ha, nearly 75% occurring in Southern and Western Europe, highlighting the vulnerability of productive land to coastal flooding.

a)

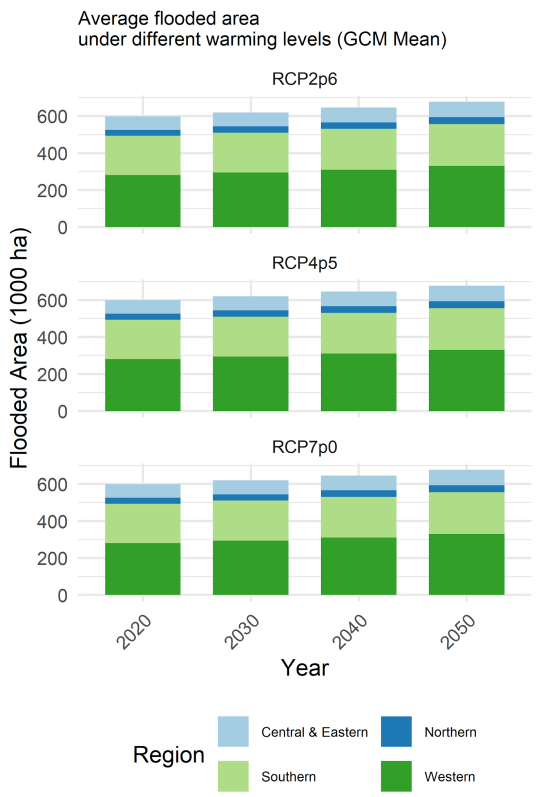

b)

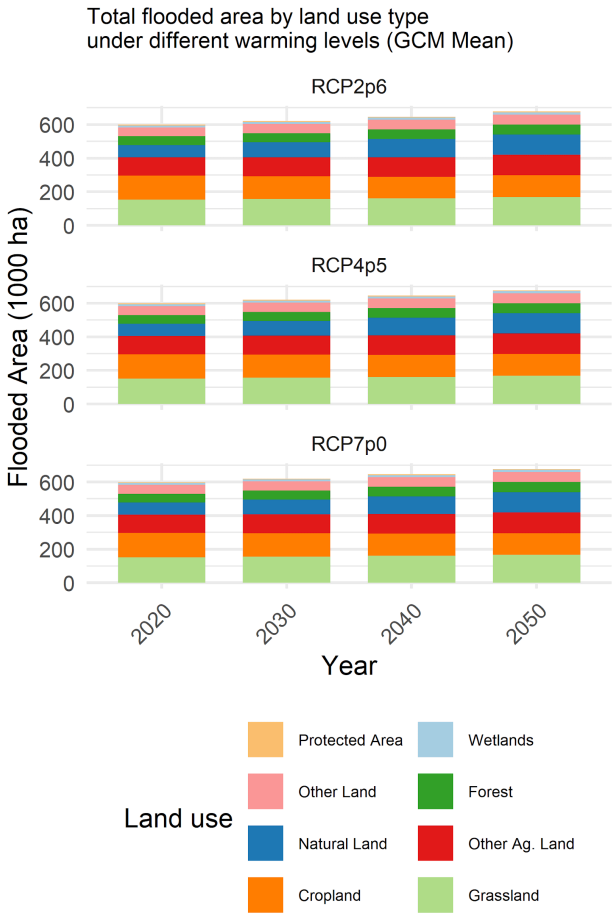

Figure 26: Estimated flooded area under different warming levels for the GCM mean by (a) European region and (b) land use types from 2020-2050 based on land use projections from ACCREU scenarios.

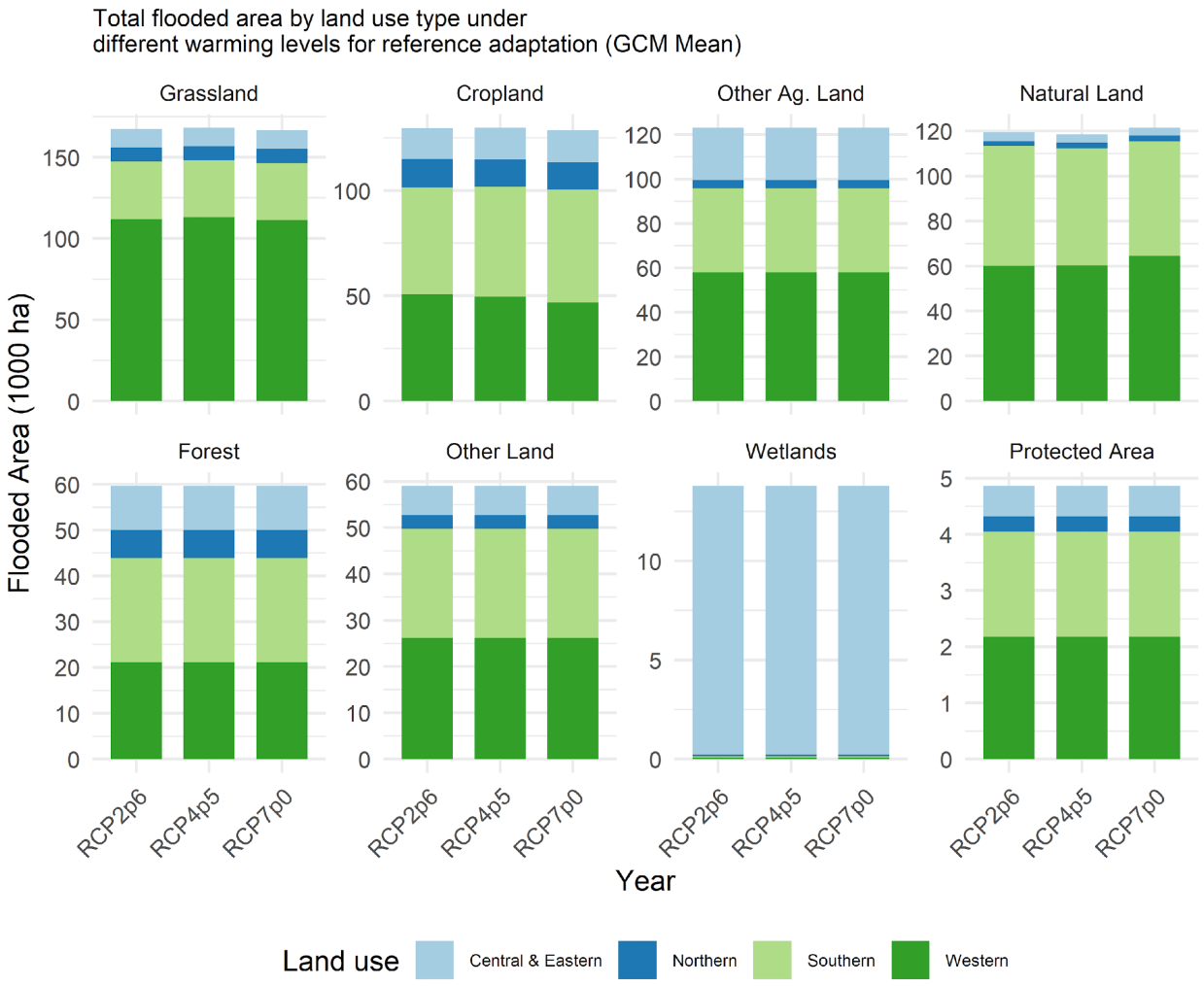

Figure 27: Estimated flooded area under different warming levels for the GCM mean by European region and land use types in 2050 based on land use projections from ACCREU scenarios.

Figure 28 shows the relationship between flooded area and revenue losses from flooded cropland by different European regions in 2050 over the different ACCREU scenarios and climate impact scenarios. For ease of examining the results all scenarios of climate impacts are linked to the associated mitigation pathway. The x-axis shows the total cropland area affected by coastal flooding (in 1000 ha), while the y-axis displays revenue loss (in million USD). We have summed the revenue losses for individual crops based on the crop production associated to each land unit under coastal flooding and the crop price. The figure highlights regional differences in vulnerability and the economic consequences of flooding on agricultural production. We estimate that western Europe has the highest absolute revenue losses due to cropland flooding with values reaching nearly 290 million USD despite a flooded cropland area of around 50,000 ha. Southern Europe has the second highest flooded areas and second highest revenue losses. Under the high adaptation scenario for Western and Southern Europe face more flooded areas compared to the other adaptation scenarios of the same RCP but lower revenue losses.

Under the low adaptation scenario, cropland area is generally lower compared to other ACCREU adaptation scenarios. This is due to less profitable conditions for crop production, which are further exacerbated by climate change at higher warming levels. The reduced profitability leads to higher levels of land abandonment, including in some coastal areas that may already be marginal in terms of productivity. As a result, less cropland remains in coastal zones, and thus, the overall exposure of cropland to coastal flooding is reduced in regions such as Western, Southern, and Central and Eastern Europe. In contrast, Northern Europe shows the lowest levels of flooded area and associated revenue losses from flooded cropland across all adaptation scenarios.

In the higher adaptation scenarios, improved agricultural productivity and profitability keep the land area as cropland, including areas in coastal zones. However, since these scenarios do not include any assumptions about coastal protection measures, this leads to increased exposure of productive cropland to sea-level rise and coastal flooding. The modeling framework used here focuses exclusively on adaptation measures related to agricultural productivity and does not consider coastal protection interventions such as dike construction or managed retreat.

These findings underscore the importance of integrated adaptation planning. While agricultural adaptation can help farmers to maintain cropland productivity under future climate change conditions, without corresponding investments in coastal protection, the benefits of increased productivity may be undermined by growing exposure to coastal flooding hazards. Future scenario development could benefit from explicitly incorporating both agricultural and coastal protection strategies to more fully assess the trade-offs and synergies of adaptation measures.

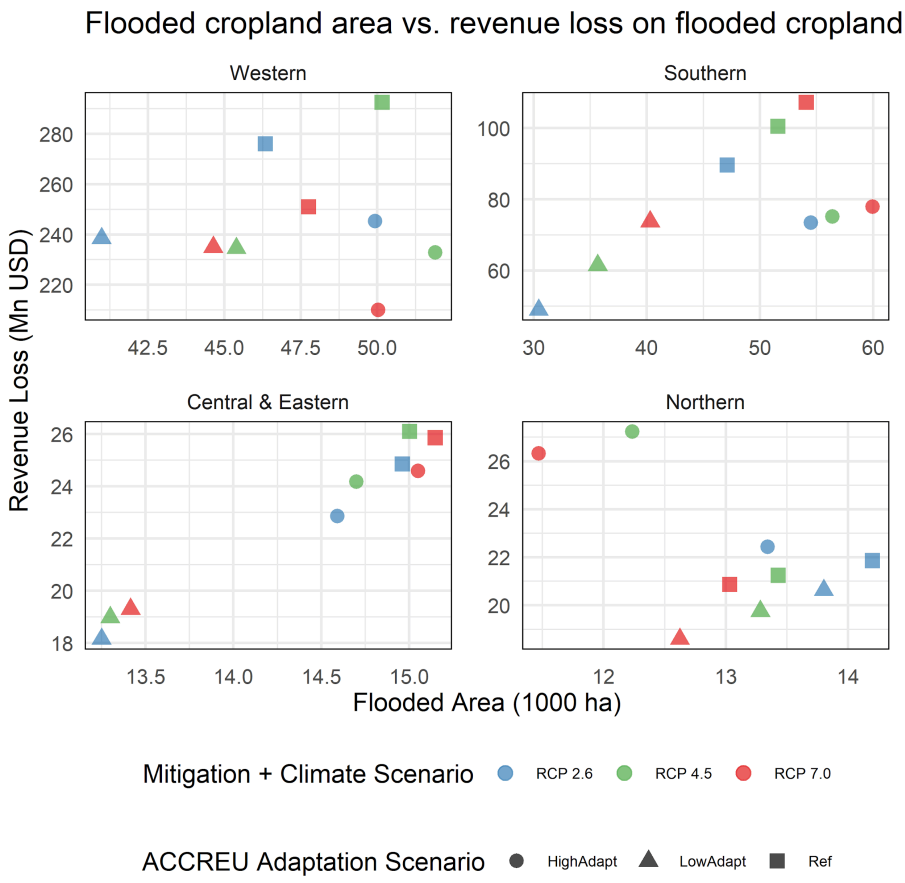

Figure 28: Relationship between flooded cropland area and associated cropland revenue losses by European region under different climate and ACCREU adaptation scenarios in 2050. Each point represents a scenario combination, with color indicating the climate impacts and mitigation pathway (RCP) and shape indicating the adaptation level (ACCREU scenarios).

A strong positive correlation in the reference scenario between flooded cropland area and revenue loss is evident in several countries, such as Italy, Germany, and the Netherlands. Figure 29 presents a cross-country comparison of the relationship between flooded cropland area (in 1,000 hectares) and associated revenue loss (in million USD) for seven European countries with the highest flood exposure. Data points are grouped by ACCREU adaptation scenario (HighAdapt, LowAdapt, Ref) and colored by climate impact and mitigation pathway (RCP 2.6, 4.5, and 7.0). Lines connect points representing the same adaptation scenario, allowing for visual tracking of changes across different climate futures under consistent adaptation conditions. Countries like Denmark and Romania have less flooded area but the variation across the adaptation scenario suggest that there are localized factors like different crop types that impacts the revenue losses. In many countries the High Adaptation scenario is associated with lower revenue losses even at higher flooded area levels suggesting that the adaptation choices (such as moving higher value crops away from less productive coastal areas) have an additional buffering effect. In contrast, the reference adaptation scenarios tend to exhibit the steepest revenue losses compared to the other adaptation scenarios.

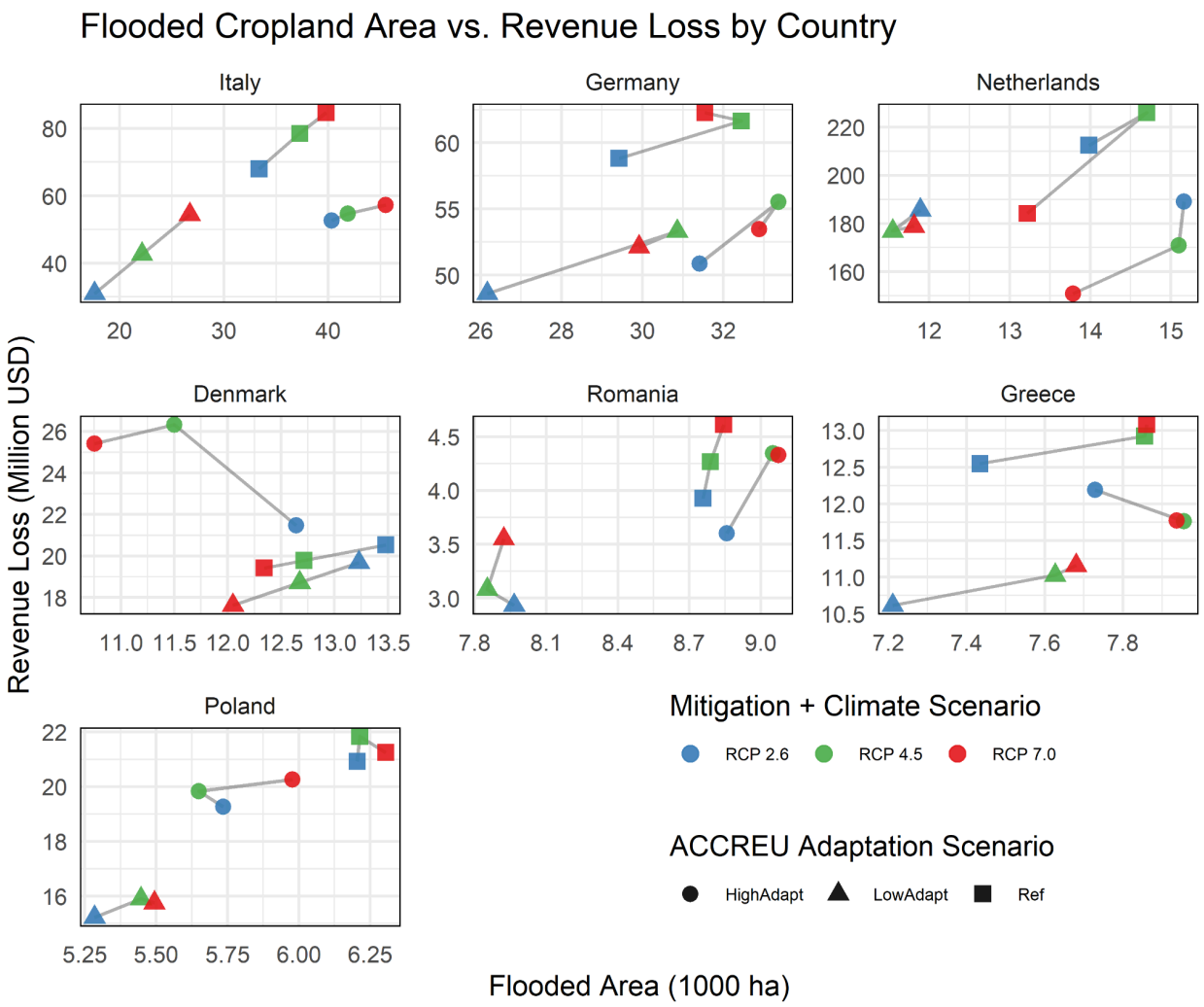

Figure 29: Relationship between flooded cropland area and associated cropland revenue losses by European country under different climate and ACCREU adaptation scenarios. Each point represents a scenario combination, with color indicating the adaptation level (ACCREU scenarios) and the shape indicating the climate impacts and mitigation pathway (RCP).

Grassland production plays a critical role in supporting livestock systems across Europe, particularly in regions where grazing is the dominant form of feed provision. When we look also at the grass production losses due to coastal flooding we find similar patterns to the crop revenue losses that the regions most affected are Western and Southern Europe, in particular Germany, The Netherlands with on average 460,000 tons dry matter and 462,000 tons dry matter lost due to coastal flooding respectively. Italy faces from the highest losses as a share of the total grass production when considered at an national level with around 6% of the total production at risk of loss due to coastal flooding, followed by Germany at 5% and the Netherlands, Poland and Romania at 3%. Unlike global commodity crops that are traded extensively, grass and forage are largely consumed locally due to their perishable nature and high transport costs. Figure 30 presents the relationship between flooded areas and the share of the local land unit grass

production losses due to coastal flooding. Each circle represents a different land unit that has a grass loss which is greater than 0.25% of the land unit's total grass production since the localized losses from grass production can have significant impacts on the local livestock farmers. We can see from this figure that losses in grass production are for the most part a relatively low share of the total land unit, however some land units face significant losses (in particular some in the Netherlands and Italy). We can also see that there is very little difference between the climate impact scenarios and the ACCREU adaptation scenarios likely due to the limited consideration for adaptation measures available for grassland management by the underlying scenarios.

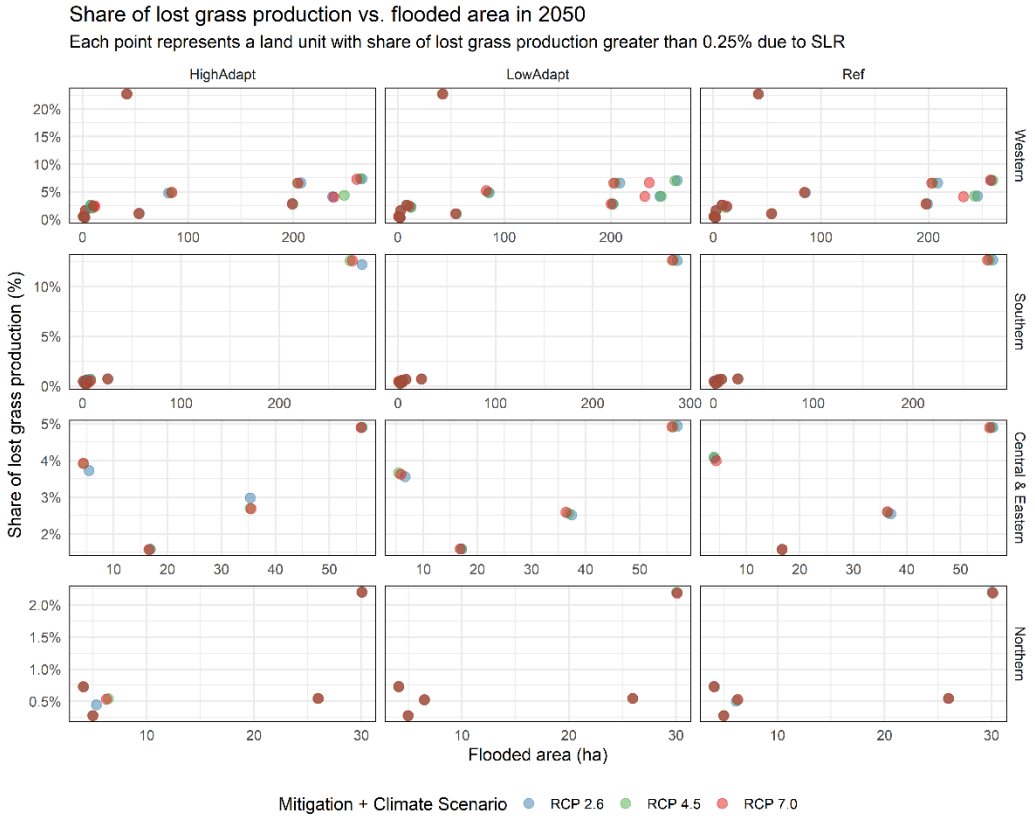

Figure 30: Relationship between flooded grassland area and associated loss in grass production (as a share of the land unit's total production) European regions under different climate and ACCREU adaptation scenarios. Each point represents a land unit under the different scenario combination, with color indicating the climate impacts and mitigation pathway (RCP).

3.4 Conclusion/Key takeaways

We have further expanded our analysis of the ACCREU climate adaptation scenario framework to examine the complex interactions between agricultural livelihoods, climate adaptation, and biodiversity conservation of Europe's land-based sectors. We used our existing modeling framework developed through ACCREU Task 2.2 and presented in **ACCREU Deliverable 2.2** and have conducted additional modeling by expanding the scenario dimensions to consider the impacts of increased conservation and restoration policies.

We have found that implementing conservation and restoration policies aimed to increase the protected and restoration area contributes positively to biodiversity outcomes across Europe, with measurable improvements in the Biodiversity Intactness Index (BII) under such policies. Our findings hold across all scenarios of climate adaptation and impact, both at the European and regional scale, compared to scenarios without conservation action. However, these biodiversity gains come with economic trade-offs, as stricter land-use protections and restoration efforts increase the pressure on the land for crop and livestock production, leading to declines in production volumes and producer revenues compared to scenarios without such policies.

Our findings indicate that conservation and restoration efforts can improve biodiversity and reduce further degradation but without investments in boosting crop yields, such policies can also create trade-offs for the provisioning services that ecosystems deliver, particularly in food production. Our results show that while conservation and restoration policies reduce the total area used for agriculture, both for cropland and grassland, the declines in production volumes for crops and livestock are of a significantly lower magnitude. This intensification effect indicates that the protections aimed at limiting further biodiversity degradation do not prevent farmers from still utilizing the most productive regions to continue the provisioning of food and other agricultural outputs despite reduced land availability. Furthermore, these policies still allow for farmers to engage with the restoration of marginal lands where productivity will be impacted by future climate impacts.

We find that adaptation, as defined by our ACCREU adaptation scenarios, play a critical role in the economic tradeoffs under conservation and restoration policies. Under Low Adaptation scenarios, characterized by limited agricultural R&D and lower productivity, more land is converted away from crop production, creating greater opportunities for restoration. This contributes to higher restoration area and greater BII improvements, but reflects underlying vulnerabilities in the agricultural sector. In contrast, the high adaptation scenarios with strong R&D investments increase yields and raise the economic attractiveness of agricultural land, reducing land abandonment and limiting restoration potential. Ambitious subsidies or restoration incentives would be required to meet restoration targets under such high productivity futures.

Higher levels of climate mitigation (e.g., RCP2.6) when combined with biodiversity-focused land protections, have strong impacts on the net revenues of the agriculture and forestry sectors. Farmers respond through land-use intensification or livestock management shifts, as these conservation policies consistently reduce cropland and grassland area. These findings highlight the complex interactions between climate, biodiversity, and food provisioning goals, underscoring the importance of coordinated policy approaches to balance ecosystem service trade-offs.

4 Impacts of global change on species habitat suitability

4.1 Introduction

Species distributions are increasingly threatened by multiple interacting global change drivers. While climate change directly affects habitat suitability and species distributions through shifting temperature and precipitation patterns (Antão et al., 2022; Gutiérrez-Hernández and García, 2021), secondary impacts like wildfire regimes (Arrogante-Funes et al., 2024) and sea level rise (Ury et al., 2021), alongside human activities (Cimatti et al., 2021) create complex challenges for biodiversity conservation.

Species distribution models (SDMs) traditionally focus on how climate change affects the habitat suitability of individual species. Opposed to combined indices, it can thus reveal greater nuance through both 'winners' and 'losers' of species in response to global change drivers. In previous research, impact analysis on biodiversity, specifically via habitat suitability, has often been limited to investigations of climate change or land use (Amindin et al., 2024; Barras et al., 2021; Fyllas et al., 2022; Gaget et al., 2025; Khan et al., 2022). However, this approach overlooks critical secondary impacts, such as wildfire and sea level rise, that can significantly influence biodiversity outcomes.

Our aim is to investigate the impacts of climate change, land use, sea level rise, and wildfires on biodiversity across Europe. To achieve this aim, we specifically address the following **Task 2.4 objective**: **Assessing the combined effect of climate change and land-use changes estimated in T2.2, using the ibis.iSDM modelling tool, on the suitability of any given land area for European species, specifically those listed in the Habitats and Birds Directive of the EU and for which management-related cost estimates can be made**. Our research introduces wildfires and sea level rise as additional impacts, thereby presenting a more comprehensive picture of the potential compounding impacts on biodiversity.

This integrated approach is particularly important for understanding implications for ecosystem services, including pollination, which directly links wild biodiversity to agricultural productivity (see **Chapter 5**) and food security. By examining how these combined threats reshape potential species distributions across European landscapes, we provide a more comprehensive assessment of biodiversity impacts in a changing world.

4.2 Methods

4.2.1 Overall approach

To capture both climate and land-use change impacts, we applied a hierarchical impact integration approach that estimates first the impact of macroclimate on species (re)distribution, followed by the impact of land use, wildfire, and sea level rise impacts as additional habitat availability modifiers. Finally, we calculate comparative metrics across different impact scenarios. This framework explicitly separates climate and land use-driven habitat suitability from disturbance-driven habitat availability, allowing for attribution of biodiversity impacts to specific drivers.

We conducted all modelling and analyses in R 4.4.2 (R Core Team, 2024) using RStudio 2024.9.0.375 (Posit Team, 2025) unless otherwise indicated. All analyses were conducted for the European continent (EPSG:3035 coordinate reference system) at a spatial resolution of 10×10 km grid cells aligned with the statistically downscaled GLOBIOM land use maps based on the ACCREU adaptation scenarios developed under Task 2.2. Our temporal coverage spans the decades of 2020, 2030, 2040, and 2050, under several **climate and mitigation matched scenarios (RCP2.6; RCP4.5; RCP7.0)**, and three agricultural adaptation scenarios (low; reference (medium); high) as included in GLOBIOM outputs. These adaptation scenarios refer to the following levels of agricultural sector adaptation to changing environmental conditions (See **ACCREU Deliverable 2.2**):

- The high adaptation scenario represents a future where farmers have a high adaptive capacity to climate change. Significant investments are made to reduce the vulnerability of agricultural systems to climate impacts, including proactive measures and advanced technology to increase yields under climate change, more efficient irrigation systems, expansion of sustainable irrigation, and increased trade from less climate-affected areas
- The reference scenario represents the medium adaptation scenario that aligns with the underlying assumptions for the development of the agriculture and forestry sector under the socioeconomic pathway SSP2.
- The low adaptation scenario represents a future where farmers have less access to technical options and therefore, the agricultural sector has limited adaptive capacity to climate change. In this scenario, irrigation systems are poorly maintained, which lowers their efficiency. Crop switching and land use adjustments happen slowly and on a smaller scale.

4.2.2 Habitat suitability modelling

4.2.2.1 Habitat suitability under climate and land-use scenarios

We captured the combined impact of future climate and land use on individual species distributions by coupling a species distribution modelling approach with the ibis.iSDM modelling tool (Jung, 2023a) and refinement of suitable habitat (Brooks et al., 2019; Pereira et al., 2024; Visconti et al., 2024, 2016). By refining a species distribution by its species-specific habitat requirements, we capture the availability of natural and modified land directly available to the species. This enables us to capture both climatically driven shifts in the distribution of European species and their attributed LULUCF impacts in terms of land-use change. This integrated approach allows for a better understanding of how land-use changes and management practices affect species habitat suitability beyond what climate-only SDMs can provide.

We focused on species that had (1) sufficient species occurrence records (for a full data preparation routine, see Supplementary Materials of Chapman et al. (2025)), and (2) species-specific available habitat preference information (IUCN Red List database or EEA databases). We excluded non-native species (based on Nature Directives listings) and fully aquatic species (to focus on terrestrial and semi-aquatic taxa), focusing on species that are listed in the EU Habitat and Birds directive, as well as species of relevance to the EU pollinator initiative. For each species, we extracted and formatted habitat preferences and converted them to spatial priors aligned with the land-use classification system. For additional nuance, we also incorporated weights into habitat preferences based on their suitability classification: "Suitable"/"Preferred" habitats received full weight (1.0), "Marginal"/"Occasional" habitats received reduced weight (0.5). Finally, we incorporated species-specific suitable elevation ranges where available (Brooks et al., 2019). Otherwise, the full elevation range was used.

Using projections from the downscaled GLOBIOM land use maps of the ACCREU adaptation scenarios (**ACCREU Deliverable 2.2**), we estimated the corresponding (matched GCM–RCP) future climate-only species projections using climate forcing data from ISIMIP, which were temporally aggregated to a decadal scale (data available here). Specifically, we trained and projected for each species and GCM-RCP combination, a total of 4 different Bayesian (e.g., regularized point process regressions) and machine learning (e.g., Extreme Gradient Descent Boosting). Furthermore, we constructed for each model 3 different folds utilizing spatial block cross-validation approaches (Roberts et al., 2017). Contemporary and future predictions were first averaged through a weighted ensemble calculation, by maximizing a True Skill Statistic (TSS) calculated on a threshold map, first across folds and then across GCMs. To constrain future projections, we created a 'mcp_dispersal' variant, which constrains the projected habitat suitability by the minimum convex polygon covering all observations and a negative exponential kernel with an average dispersal estimate per taxonomic group following Thuiller et al. (2019). All modelling was conducted using the ibis.iSDM R-package (Jung, 2023a), with hyperparameters and model contributions varied depending on data availability per species to further limit overfitting. The resulting projections capture the climatic niche (unit 0-1) of a species for each SSP and adaptation.

Finally, for each species, we calculated within the current and future climatic niche the amount of suitable habitat, integrating information on downscaled land-use change for each SSP-RCP scenario combination and species-specific habitat preferences. This was done using the ibis.insights R package (Jung, 2023b), adopting an approach by Visconti et al. (2016). We note that the linkage between species ranges and land use is dependent on the accuracy and availability of habitat preference information. Particularly for permanent croplands, full impacts on habitat availability can be underestimated, as species-specific coefficients are not always available.

4.2.2.2 Integrating wildfire & sea level rise risk projections

Building on the species-specific habitat availability as projected in 4.2.2.1, we then used a *post hoc* integrated mapping approach to investigate the potential effects of wildfires and sea level rise on habitat availability. First, we preprocessed the wildfire risk maps produced in this deliverable (**Chapter 2**). We rasterized and transformed the wildfire vector datasets to a fraction of burned area per 10×10 km grid cell, and the number of fire events per grid cell, per decade, maintaining the original projection (EPSG: 3035). The full preprocessing methodology can be found in **Appendix E**. These projections represent the expected fractional burned area per grid cell under three SSP-RCP scenarios (SSP1/RCP2.6, SSP2/RCP4.5, SSP3/RCP7.0). We derived our coastal inundation due to sea level rise (SLR) projections from our custom, modified bathtub approach model used in **Chapter 3** (**Appendix D**). The data set consisted of a multi-band raster file, representing the fractional coastal area of each 10×10 km grid cell expected to be inundated under three sea level rise scenarios (RCP 2.6, RCP 4.5, RCP 7.0) for each decade from 2020 to 2050.

We integrated wildfire and sea level rise impacts on species distributions following a systematic mathematical framework. For each species, climate scenario, and decade, we calculated adjusted habitat availability values. For fire-adjusted habitat availability:

$$H_{fire}(x,y) = \left(0, H_{climate}(x,y) - (F(x,y) * \alpha)\right) \#(4.1)$$

For sea level rise-adjusted habitat availability:

$$H_{slr}(x,y) = \left(0, H_{climate}(x,y) - (S(x,y) * \alpha)\right) \#(4.2)$$

For combined impacts:

$$H_{combined}(x,y) = max\left(0, H_{climate}(x,y) - (F(x,y) * \alpha) - (S(x,y) * \alpha)\right) \#(4.3)$$

Where: $H_{climate}(x,y)$ is the baseline climate-driven habitat availability at location (x,y); $F(x,y)$ is the fractional burned area at location (x,y); $S(x,y)$ is the fractional inundated area at location (x,y); α is an impact scale factor (set to 1.0 in our analysis); $H_{fire}(x,y)$, $H_{slr}(x,y)$, and $H_{combined}(x,y)$ are the resulting adjusted habitat availability values. This approach assumes that areas affected by wildfire or sea level rise experience a proportional reduction in habitat availability, with a zero floor to prevent negative availability values. The impact scale factor α allows for calibration of impact intensity, though in our implementation, we used the full impact (α = 1.0). For the combined impact scenario, we applied both fire and sea level rise impacts additively, again with a zero floor.

For each species, scenario, impact type, and decade, we calculated the total suitable habitat area using the sum of habitat availability values across all cells, converted to area units in km²:

$$A_{suitable} = \sum_{x,y} H(x,y) * a_{cell} \#(4.4)$$

Where: $A_{suitable}$ is the total suitable habitat area in km²; $H(x,y)$ is the habitat availability value at location (x,y); and a_{cell} is the area of each grid cell in km². This approach accounts for both the extent and quality of habitat, as cells with partial availability contribute proportionally to the total suitable area.

We make several assumptions about the integrated post hoc impacts of wildfire and sea level rise on habitat availability, which could be improved upon in the future for enhanced empirical modelling. For wildfire, we aggregated wildfire events *per* decade, which, given the short-term nature of individual fire events, may obscure shorter-term impacts on biodiversity patterns. Further, we assumed that there would be a decline in suitable habitat after exposure to fire. However, empirical evidence suggests species-specific responses to wildfire (**Chapter 2**). Similarly, we also did not model coastal species' ability to migrate inland as a response to SLR. A further limitation is that we treat wildfires and sea level rise as independent from one another, though any impacts may have interactive effects.

4.2.2.3 Ecological metric calculation

We report two complementary ecological metrics for our overall analysis, each of which has different meanings, but together offer a more complete ecological understanding. First, we report **total habitat change relative to the decade 2020 (%),** which measures range expansion/contraction, crucial for overall species persistence. We established 2020 as a baseline year and calculated both absolute and relative changes for each subsequent decade:

$$\Delta A = A_t - A_{2020} \#(4.5)$$

$$\Delta A\% = \left(\frac{A_t}{A_{2020}} - 1\right) * 100 \#(4.6)$$

Where: ΔA is the absolute change in suitable habitat area (km²); $\Delta A\ \%$ is the percentage change in suitable habitat area; A_t is the suitable habitat area at decade t; A_{2020} is the suitable habitat area in the baseline year 2020. Next, we calculated **mean availability change relative to 2020 (%),** which measures habitat quality shifts, an important indicator for species population viability within the species range.

$$A_{suitable} = \sum_{x,y} S(x,y) * a_{cell} \#(4.7)$$

Where a_{cell} is the area of each grid cell in km². Reporting both total and mean habitat availability allows us to identify important ecological scenarios, and each metric can inform different conservation priorities with regards to a specific climate change adaptation scenario.

4.3 Results & Discussion

4.3.1 Species assessment coverage

Our assessment covered 754 species across Europe, of which the majority consisted of birds (39.3 %), Lepidoptera (butterflies; 12.7 %), and mammal (9.2 %) species (Table 5). The full species list can be found in **Appendix E**.

Table 5: Taxonomic summary table of species considered in our analysis. The table shows the major ecological group, the number of species considered within each group, and the percentage representation of each group within the larger dataset.

Group	Species count	Percent of total (%)
Birds	296	39.3
Lepidoptera	96	12.7
Mammals	69	9.2
Dicots (other)	58	7.7
Hymenoptera	57	7.6
Reptiles	42	5.6
Amphibians	36	4.8
Beetles	21	2.8
Monocots (other)	18	2.4
Molluscs	13	1.7
Mosses	12	1.6
Ferns	8	1.1
Grasses	7	0.9
Orthoptera	7	0.9
Legumes	3	0.4
Odonata	3	0.4
Dicot herbs	2	0.3
Arachnids	1	0.1
Arthropods (other)	1	0.1
Insect other	1	0.1
Liverworts	1	0.1
Lycophytes	1	0.1
True bugs	1	0.1
Total	**754**	**100**

4.3.2 Additional impacts of sea level rise and wildfire

We calculated total suitable habitat change (%) and mean habitat availability (%) from 2020 decade baseline, for three climate and land use scenarios, plus the additional impacts of wildfire and sea level rise, and three agriculture adaptation strategies (low, medium/reference, high) (**Figure E1 in Appendix E**). We found that the addition of wildfires and sea level rise impacts in our impact model modestly influenced the calculated metrics (largest impact < 0.04 %; Figure 31). This indicates that climate and land use changes remain the dominant drivers of habitat availability for the **modeled species** at the continental scale, although we recognize the uncertainty with regards to spatial and temporal scales (see discussion).

However, we believe these modest impacts reflect methodological constraints rather than the true ecological significance of these disturbances. Our integration approach applies a direct proportional reduction to habitat availability based on the fraction of each grid cell affected by wildfire or inundation. This straightforward approach allows for consistent application across diverse taxa but may underestimate impacts for several reasons. First, our species pool excludes certain highly vulnerable groups (e.g., aquatic species affected by post-fire sedimentation, dune specialists impacted by coastal erosion) due to data limitations. Second, our framework cannot yet capture complex species-specific responses to wildfire and sea level rise disturbances. For example, the positive responses of certain beetle and reptile species to wildfire documented in our meta-analysis (**Chapter 2**), or the potential for coastal species to migrate with shifting habitats under sea level rise when space allows.

The spatial and temporal resolution of our disturbance layers may further dilute apparent impacts. At 10 km resolution, localized but severe wildfire or inundation effects are averaged across larger areas, potentially masking significant local habitat loss. Similarly, while modeled sea level rise accurately represents permanent inundation, it cannot capture dynamic coastal processes like erosion, salt intrusion, and storm surge that may affect much larger areas.

Despite these limitations, we retained the integrated impact approach for three reasons: (1) it establishes a methodological framework for multi-threat assessment that can be refined as more detailed data becomes available; (2) it acknowledges the reality that biodiversity faces concurrent rather than isolated threats; and (3) the relative importance of these disturbances is likely to increase as climate change intensifies fire regimes and accelerates sea level rise. For our subsequent analyses, we report habitat availability metrics calculated from all impacts (climate, land-use, wildfire, and sea level rise), with the understanding that most continental-scale effects are currently attributed to climate and land use changes.

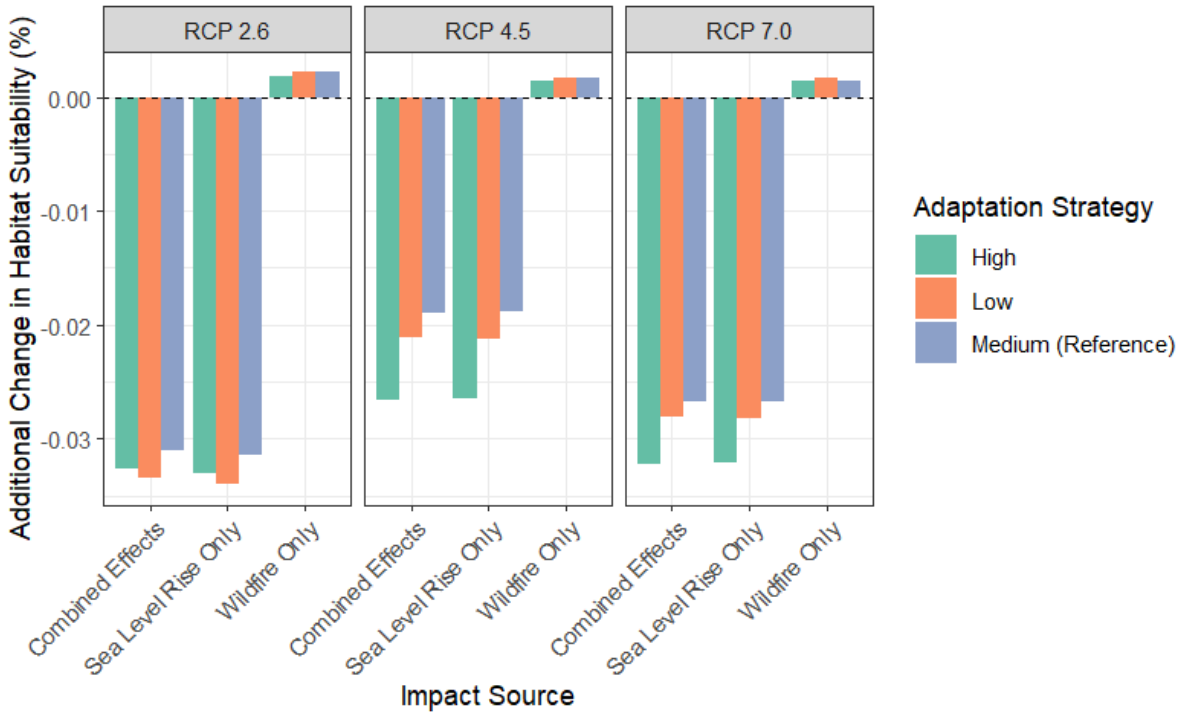

Figure 31: Additional change in habitat availability due to wildfires, sea level rise, and both combined, beyond climate and land use change. Negative values indicate additional habitat loss beyond those of climate change and land use.

4.3.3 Overall habitat availability

We projected that by 2050, there will be substantial projected losses in total suitable area (> 6 %, Figure 32A) and mean habitat availability (habitat quality, > 3%, Figure 32B) across all climate scenarios (RCPs) and adaptation strategies. We interpret the losses of total suitable area as less physically suitable habitat amount for a species to persist. We interpret the losses in mean availability as the decline in *quality* of the remaining habitat to support many species.

For change in total suitable area (%, Figure 32A), under RCP 2.6 we found the largest losses in total suitable habitat by 2050, with progressively smaller losses under RCP 4.5 and RCP 7.0. Across all climate scenarios, **low adaptation strategies resulted in the greatest loss of suitable habitat area by 2050** (-6.50 to -6.85 %) under RCP 2.6. Medium (reference) and high adaptation strategies consistently preserve more total suitable habitat area, with high adaptation resulting in less area loss (-6.15 %), compared to low adaptation under RCP 7.0. This means that under low adaptation scenarios, there is less suitable habitat area available for species to inhabit, indicating range contraction over time. From these results, we can imply that stronger agricultural adaptation measures could mitigate species range constrictions across all climate futures.

For mean habitat availability (%, Figure 32B), which we interpret as an indicator of habitat quality, our findings reveal that most severe habitat quality declines occur under RCP 4.5, reach -5.71 % losses by 2050. Across RCPs, under the **low adaptation** scenario, we found the **slowest decline in *mean availability***, as compared to medium/reference and high adaptation scenarios. Under RCP 2.6, declines in mean suitable habitat follow adaptation strategy intensity, where lower declines in mean availability are found at **low adaptation** (-3.22 %), and steepest declines under high adaptation (-4.37 %). For RCP 4.5 and RCP 7.0, mean habitat availability shows comparable declines between medium/reference (-4.37 to -5.27%) and (-4.43 to -5.18 %) high adaptation scenarios.

Together, our findings reveal a critical trade-off in adaptation strategies over time. Low adaptation preserves higher-quality habitat but in a reduced area. Medium/Reference and high adaptation strategies maintain larger total habitat area but include more suboptimal land. This area-quality trade-off may have important conservation implications, and warrants further investigation.

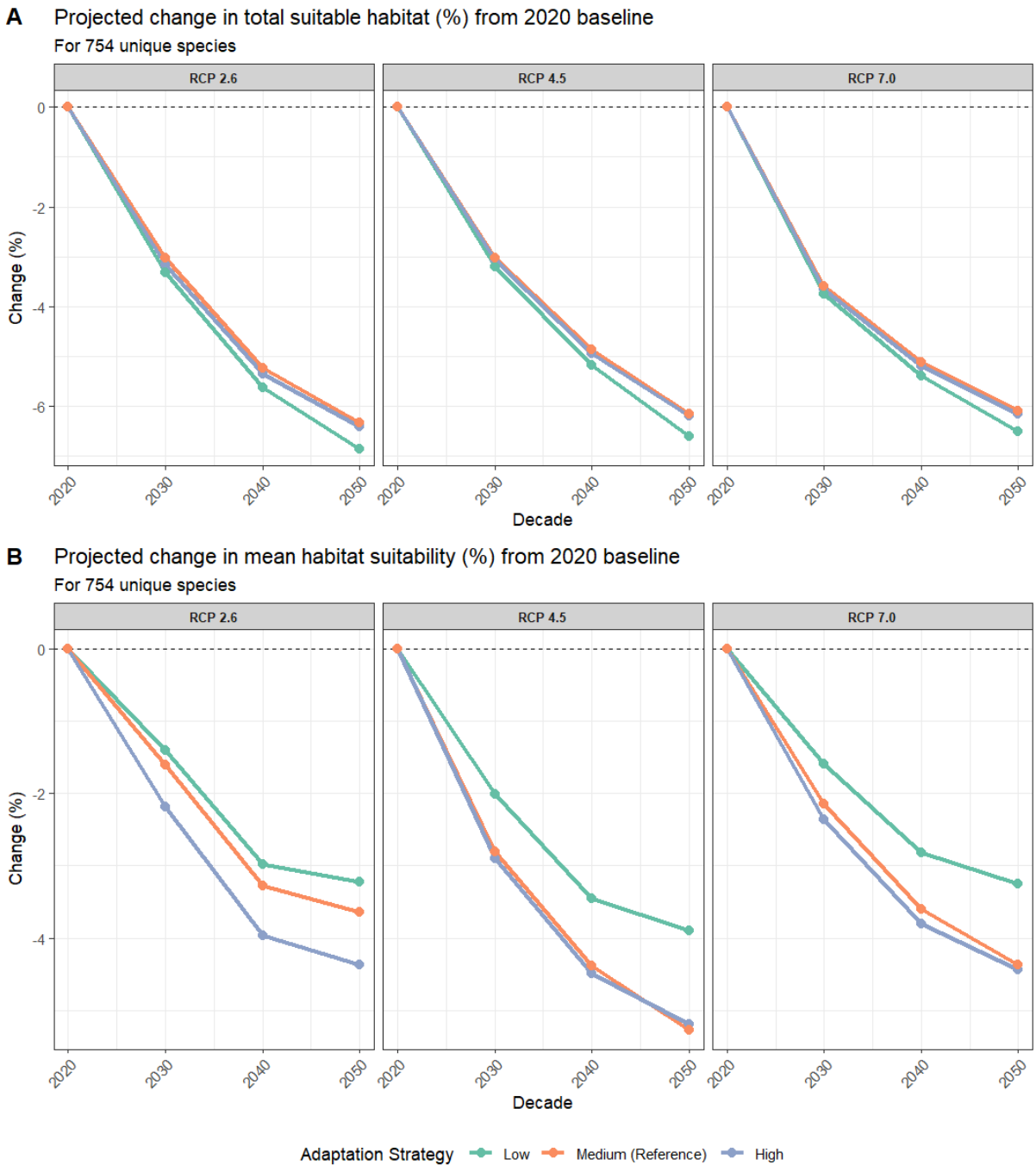

Figure 32: Projected decadal change in total suitable area and habitat availability for 754 species under different impacts and adaptation scenarios from the 2020 decade baseline. (A) Change in total suitable area (%) for all species combined from a 2020 baseline under three RCP scenarios (2.6, 4.5, 7.0) and three agricultural adaptation strategies (High, Low, Reference). Impact scenarios include climate, land use, wildfire, and sea level rise impacts. (B) Mean change in habitat availability (%) from the 2020 baseline for the same set of species and scenarios.

The overall mean habitat availability results (Figure 32B) show large variations around the mean, indicating large variances in species-specific responses. (Figure 33). This means that species-specific habitat availability is largely different from overall mean habitat availability, implying that species-specific responses are not uniform, which is typical for biodiversity projections. The overall mean masks variations between species or taxonomic groups, so it is essential to disaggregate indices by taxonomic groups.

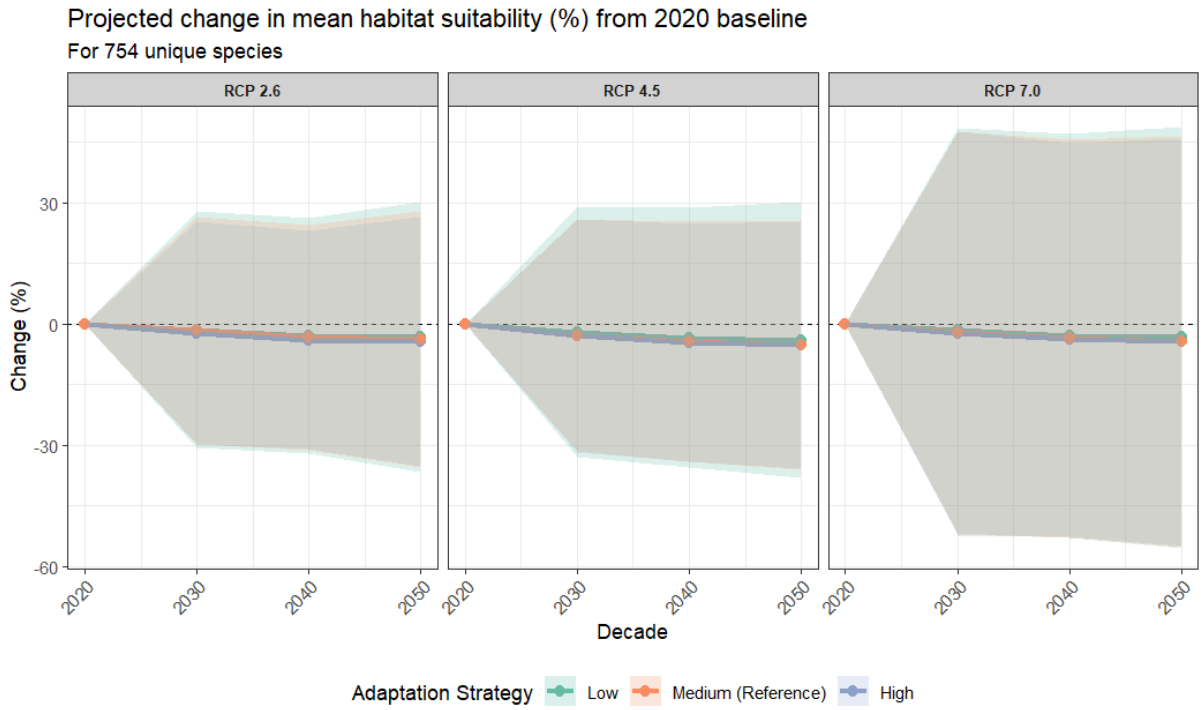

Figure 33: Mean change in habitat availability (%) from the 2020 baseline for 754 species under different impacts and adaptation scenarios from the 2020 decade baseline. The results consider three RCP scenarios (2.6, 4.5, 7.0) and three adaptation strategies (High, Low, Reference). All scenarios include impacts of climate, land use, wildfire, and sea level rise. Error ribbons show ± 1 standard deviation from the mean.

4.3.4 Taxa-specific habitat availability

Figure 34 illustrates projected changes in suitable habitat for diverse taxonomic groups across climate scenarios and agricultural adaptation measures by 2050. **Most taxonomic groups show declining suitable habitat across all climate scenarios**, with the severity of habitat loss typically increasing from RCP 2.6 to RCP 7.0.

Notably, several groups protected under the EU Birds and Habitats Directives show consistent vulnerability. Birds (protected under Directive 2009/147/EC) demonstrate increasing habitat loss with climate severity, from approximately 4.78- 5.10 % under RCP 2.6 and 5.96- 6.31 % under RCP 7.0. Amphibians and reptiles (Annex II, IV species under Directive 92/43/EEC) show consistent declines across all scenarios, though amphibians display a counter-intuitive pattern of slightly reduced impacts under more severe climate scenarios. Mammals, many of which are priority species under the Habitats Directive, show relatively consistent habitat losses of 7.86-8.00 % regardless of climate scenario, suggesting persistent impacts regardless of emission pathway. Among invertebrates, pollinator groups Lepidoptera, which include several protected butterfly species listed in Annex II and IV of the Habitats Directive, and Hymenoptera (wild bees) show increasing habitat loss with climate severity, from minimal change under RCP 2.6 to losses exceeding 6% under RCP 7.0.

Within each RCP scenario, agricultural adaptation measures, which are designed to maintain production rather than biodiversity, affect taxonomic groups differently. For directive-protected vertebrates, birds and reptiles show greater habitat losses under high agricultural adaptation scenarios, while amphibians generally experience reduced losses under higher adaptation. Divergent responses are apparent in plant groups too, where grasses, mosses, and other dicots showing greater habitat losses under high agricultural adaptation, whereas ferns generally show little no habitat availability differences between adaptation scenarios. These divergent responses highlight **potential conflicts between agricultural intensification and conservation objectives for certain protected species groups.**

Notably, pollinator groups Hymenoptera (bees) and Lepidoptera (butterflies) show strong differentiation across adaptation levels, with medium (reference) and high adaptation resulting in significantly greater habitat losses. For both pollinator groups under RCP 7.0, the difference between low adaptation (2.56-2.88 %) and high adaptation (5.86-6.06 %) is particularly pronounced, suggesting that intensive agricultural adaptation strategies may negatively impact pollinator habitat and, therefore, impact pollination ecosystem services. We explore pollinator species distributions and potential impacts on crop pollination ecosystem services further in **Chapter 5**.

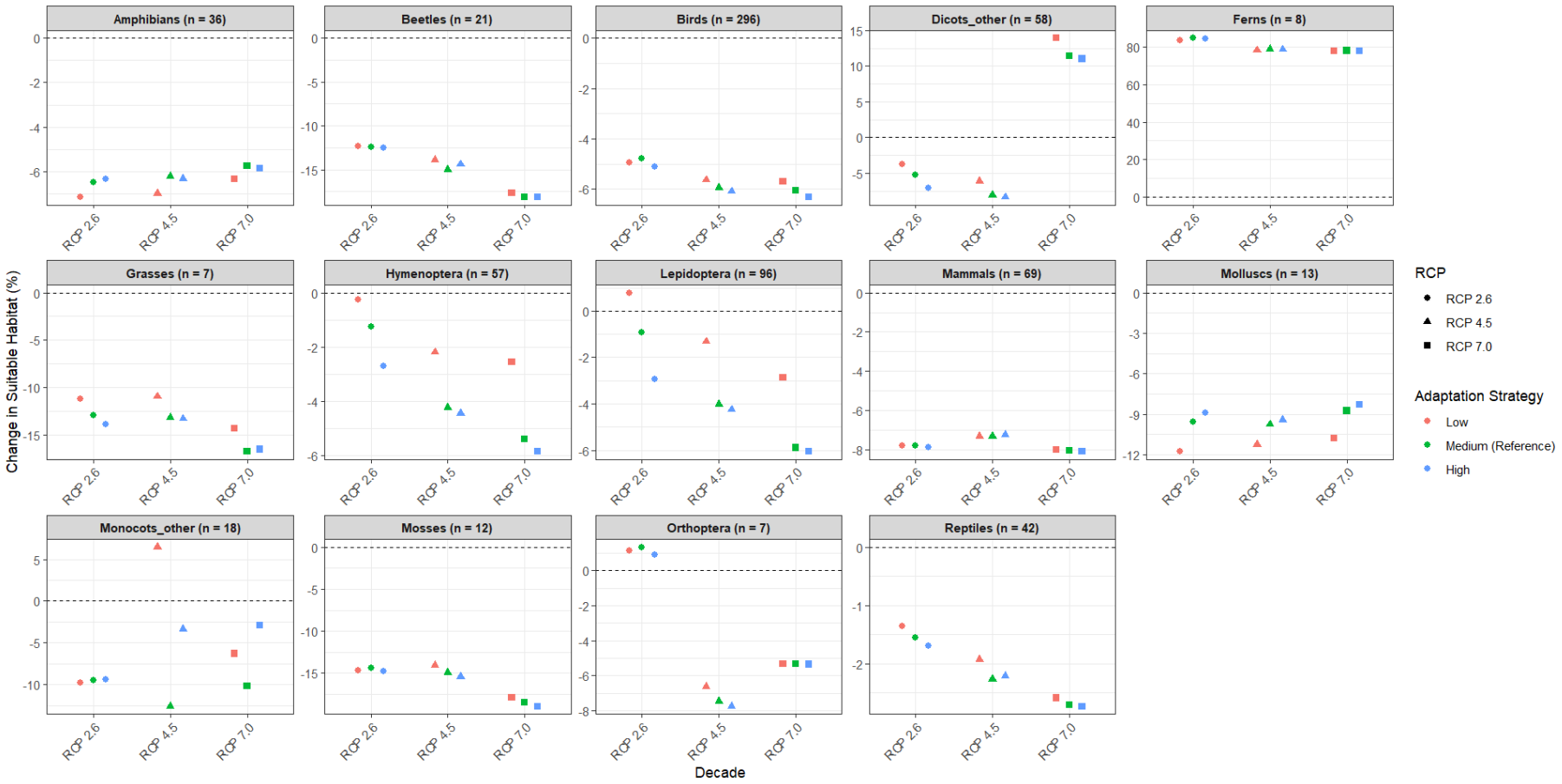

Figure 34: Taxonomic group impact assessment showing mean percent change in total suitable habitat in 2050 compared to 2020 baseline. Groups are displayed by climate scenario (RCP 2.6, 4.5, and 7.0) and adaptation strategy (Low, Medium/Reference, High). Adaptation strategies represent different levels of proactive agricultural measures to address climate impacts, from limited response (Low) to comprehensive implementation of climate-resilient approaches (High). This figure excludes groups with < 5 species for statistical robustness: Arachnids (n = 1); Arthropods Other (n = 1); Insects Other (n =1), Liverworts (n = 1); Lycophtes (n = 1); True bugs (n = 1); Saxifragaceae dicots (n = 2); Legumes (n = 3); Odonata (n = 3).

4.4 Conclusion/Key takeaways

Our integrated assessment methodology advances biodiversity impact modeling by explicitly accounting for multiple interacting threats, including climate change, land-use dynamics, wildfire, and sea level rise. This multi-threat approach reveals that most taxonomic groups face a declining suitable habitat by 2050, with impact patterns varying significantly across taxa. The clear escalation of habitat loss with increasing emission scenarios underscores that climate mitigation remains fundamental for biodiversity conservation across Europe.

Our findings demonstrate critical trade-offs between agricultural adaptation and biodiversity protection. Agricultural strategies designed to maintain agricultural productivity often increase habitat losses, particularly for pollinators like Hymenoptera and Lepidoptera. This is especially concerning given pollination's essential ecosystem service value. The pronounced impacts on pollinator groups may threaten both biodiversity and food security, highlighting an urgent need for pollinator-specific research and conservation measures within agricultural landscapes. The varied responses across taxonomic groups, particularly those protected under the EU Birds and Habitats Directives, indicate that effective conservation planning must incorporate taxonomic differences in climate sensitivity and responses to agricultural practices.

While our 10×10 km resolution assessment captures continent-scale patterns effectively, we acknowledge limitations in representing fine-scale habitat heterogeneity and potential underestimation of sea level rise and wildfire impacts. Further, the decadal time steps we select may miss important inter-decadal variability, and the analysis endpoint of 2050 may miss critical longer-term impacts. Despite these constraints, our results provide robust evidence that biodiversity-friendly agricultural adaptation approaches are urgently needed, especially for taxonomic groups showing high sensitivity to intensive farming practices. By identifying specific impact patterns across taxa, climate scenarios, and adaptation pathways, this assessment provides a scientific foundation for developing targeted conservation strategies that reconcile agricultural adaptation with biodiversity protection in a changing climate.

5 Impacts on non-market ecosystem services: the case of crop pollination

5.1 Introduction

Biodiversity and ecosystem services are intrinsically linked, with species diversity underpinning many of the processes that benefit human societies. This relationship is particularly evident in crop pollination, where wild insects directly support agricultural production (Gallai et al., 2009; Leonhardt et al., 2013; Rubinigg Michael, 2024). As global change reshapes European landscapes, understanding their effects on pollinators and the services they provide becomes increasingly urgent for food security.

Building on **Chapter 4's** finding that pollinator groups (Hymenoptera, Lepidoptera) face pronounced vulnerability to global change, with suitable habitat declining by 2050, we examine the implications of the biodiversity changes for crop pollination value for agricultural services. To address this critical need, we focused on quantifying crop pollination as a key regulating ecosystem service, defined here as the fertilization of crops by insects that maintain or increase crop production (Vallecillo et al., 2018). We focus on crop pollination because it provides a direct, measurable link between biodiversity and agricultural economic outcomes.

Our approach employs Species Distribution Models (SDMs) rather than direct abundance measurements due to the continental scale of our analysis and data limitations. While abundance data would ideally provide more precise service delivery estimates, SDMs allow us to project habitat availability for pollinator species across multiple future scenarios (Jung, 2023a), offering valuable insights into potential service supply under changing conditions. By integrating these habitat availability projections with crop distribution data, we build upon existing frameworks for assessing both the spatial distribution and economic value of pollination services across Europe.

This chapter specifically addresses the following Task 2.4 objectives, both directly and indirectly:

- Assessing the combined effect of climate change and land-use changes estimated in T2.2, using the ibis.iSDM modelling tool, on the availability of any given land area for European species, specifically those listed in the Habitats and Birds Directive of the EU and for which management-related cost estimates can be made, **with a focus on pollinator insects**.
- The non-market values of biodiversity and ecosystem services will be assessed by applying state-of-the-art valuation methods for non-market goods, such as stated and revealed preference methods of environmental evaluation and benefit transfer approaches, **with a focus on crop pollination.**
- We will account for both the use and non-use values individuals gain or lose from marginal changes in ecosystem services, **with a focus on crop pollination.**

The monetary evaluation of pollination services provides a bridge between ecological research and policy implementation, helping to incorporate natural capital into economic decision-making frameworks while highlighting the tangible consequences of biodiversity loss.

5.2 Conceptual framework

We developed a spatially explicit accounting framework to quantify crop pollination services across Europe under various climate and adaptation scenarios. Our approach aligns with the System of Environmental-Economic Accounting Ecosystem Accounting (SEEA EA) by distinguishing between ecosystem service capacity, potential, and actual flow, which are essential distinctions for understanding the spatial dynamics of pollination services. The methodology emphasizes the integration of biophysical assessment with economic valuation and builds upon that of the Knowledge Innovation Project on Integrated Natural Capital Accounting (KIP INCA) undertaken by European Commission services (EUROSTAT, JRC, DG Environment, DG Research and Innovation) and the European Environment Agency.

Specifically, our methodology is based on the KIP INCA crop pollination evaluation assessment (Vallecillo et al., 2018), which combines spatially explicit crop production data with pollinator habitat availability maps to calculate the realized benefits of pollination services in terms of physical and monetary flows. Our framework captures the full chain of ecosystem service delivery through three interconnected components.

First, we assess **pollination demand** as the area of crops requiring animal pollination weighted by their dependency coefficients. These coefficients represent the proportion of yield attributable to animal pollination, with examples ranging from 0% for wind-pollinated crops to 65% for highly dependent crops like sunflowers. This demand component represents the economic activities that could benefit from pollination services.

Second, we quantify **pollination potential** as the capacity of certain areas to potentially support wild pollinator populations, represented by habitat availability indices (0-1) derived from SDMs. This potential represents the ecosystem's capability to provide pollination services, regardless of whether crops requiring pollination are present.

Third, we calculate the **actual flow** of pollination services as the spatial intersection between potential and demand. This intersection approach recognizes that pollination services are only realized where both suitable pollinator habitat and pollinator-dependent crops co-exist within the foraging range of pollinators. The actual flow is measured in both physical terms (pollinated area) and monetary terms (economic value of pollination contribution).

This three-component structure enables us to identify spatial mismatches between pollination supply and demand, while providing the accounting metrics needed for natural capital valuation and ecosystem service assessment under changing conditions.

5.3 Methods

5.3.1 Crop pollination demand

We quantified **crop pollination demand** as the proportional extent of crops dependent on pollination across Europe. This measures how much area theoretically requires pollination, weighted by dependency coefficients. It represents the maximum potential service requirement if all conditions were ideal and is independent of whether pollinating insects are present. We selected this method over using total crop area because it more accurately represents the ecological service requirement by accounting for varying degrees of pollinator reliance.

Our multi-step methodological framework integrates GLOBIOM crop production data for 17 crop types (see **ACCREU Deliverable 2.2**), with crop pollinator dependency indices (PDIs), and aggregates the results to standardized administrative units. We used crop distribution data for simulated units from the GLOBIOM model (vector points), which provides spatial projections of **area, production, and revenue** for crops under various scenarios, estimated from several general climate circulation models (GFDL, IPSL, MPI, UKESM). For this analysis, we calculated the ensemble mean across climate models to account for model uncertainty.

We assigned pollinator dependency indices to each crop (Table 6), representing the proportion of crop yield dependent on wild insect pollination. By weighting crop areas by dependency indices, we account for varying degrees of pollinator reliance across crops. We note here that GLOBIOM does not yet account for some highly pollinator-dependent crops, such as fruits; thus, any estimation we provide here underestimates the true extent of pollinator-dependent crops in Europe. While this represents a limitation in the assessment of total pollination demand, our methodology provides valuable insights into the dynamics of field crop pollination requirements, which constitute a significant component of European agriculture.

Table 6: GLOBIOM crop types and their Pollination Dependency Index (PDI), which represents the proportion of crop yield dependent on wild insect pollinators.

Crop	Pollination Dependency Index (PDI)	Dependence Categories	Note
Barley	0*	None	Wind-pollinated; no insect pollination requirement
Dry bean	0.25*	Modest	Benefits from insect pollination
Chickpea	0.25*	Modest	Benefits from insect pollination
Corn	0*	None	
Cotton	0.05#	Little	Estimated, usually self-pollinating
Groundnut	0.05*	Little	
Millet	0*	None	
Potato	0*	None	
Rapeseed	0.25*	Modest	Partial self-pollination capability
Rice	0*	None	
Soybean	0.25*	Modest	Can self-pollinate, benefits from insect pollination
Sorghum	0*	None	
Sugarcane	0*	None	
Sunflower	0.65*	Great	
Sweet potato	0*	None	
Wheat	0*	None	Wind-pollinated; no insect pollination requirement
Other	0*	None	Mixed/unspecified crop types, conservative estimate

*(Bugin et al., 2022); #(Muhammad et al., 2020)

For each crop type in each spatial unit point, we calculated the **crop pollination demand (ha)** and **crop pollination potential revenue (USD)** as:

$$D_{area} = \sum_{c} A_c \cdot d_c \#(5.1)$$

$$D_{value} = \sum_{c} R_c \cdot d_c \#(5.2)$$

Where D_{area} is pollination demand (ha); D_{value} is the potential pollination value (USD); A_c is the area of crop c (ha); R_c is the revenue from crop c (USD) from the crop data; and d_c is the dependency coefficient for crop c (proportion of yield attributable to insect pollination, Table 6).

So far, the crop data and demand calculations were for polygon point data, representing values for a single simulation unit. Therefore, we needed to process the crop data to spatial units that are capable of integration with crop pollinator SDM data, and to facilitate multi-scale analysis relevant to different policy and management levels. To do this, we implemented a hierarchical spatial aggregation approach using the European Union's Nomenclature of Territorial Units for Statistics (NUTS) classification. Briefly, we first spatially joined crop point data to NUTS3 (smallest administrative units) regions. For each crop type and scenario combination, we aggregated values to NUTS3 regions, maintaining unweighted crop-specific PDIs (d_c; as they are constants for each crop type). For each NUTS3 region, crop-scenario combination, and year, we aggregate data through summation:

$$NUTS3\ TotalArea = \sum_{i=1}^{m} Area_m \#(5.3)$$

where m represents all crop points within a NUTS3 region. We performed similar summations for revenue, and pollination metrics. We then calculated derivative metrics for each region:

$$Revenue\ per\ hectare = \frac{Total\ Revenue\ (USD)}{Total\ Area\ (ha)} \#(5.4)$$

$$Pollination\ Fraction = \frac{Pollination\ Demand\ (ha)}{Total\ Area\ (ha)} \#(5.5)$$

$$Pollination\ Value\ per\ hectare = \frac{Pollination\ Value\ (USD)}{Total\ Area\ (ha)} \#(5.6)$$

To ensure comprehensive coverage, we implement a zero-filling procedure for regions without crop data, ensuring all administrative units appear in the final dataset.

Thereafter, we aggregated all metrics upward to the country level (NUTS3 → NUTS2; NUTS2 → NUTS1; NUTS1 → NUTS0). We selected this bottom-up approach to preserve fine-scale spatial patterns while enabling policy-relevant national and European summaries. At each aggregation level, we calculated:

1. Sum of total metrics across all constituent lower-level regions:

$$NUTS_{higher}Total\ Area = \sum_{j=1}^{k} NUTS_{lower}Total\ Area_j \#(5.7)$$

2. Weighted average of dependency indices, using area as the weighting factor:

$$NUTS_{higher}DependencyIndex = \frac{\sum_{j=1}^{k} DependencyIndex_j * TotalArea_j}{\sum_{j=1}^{k} TotalArea_j} \#(5.8)$$

3. Recalculation of all derivative metrics using the aggregated totals
4. Tracking of region and point counts to maintain data provenance information

This approach allows for consistent analysis across administrative scales while preserving the relationship between pollination demand and agricultural production. The resulting multi-level dataset enables analysis of crop pollination requirements at scales ranging from local administrative units to entire countries, supporting targeted conservation planning for pollination services across Europe under various climate and adaptation scenarios. For this study, we report all results at the country (NUTS0) level, and provide all other NUTS level datasets in the shared repository (contact authors for access).

5.3.2 Crop pollination potential

To map crop pollination potential across Europe, we utilized individual species distribution models (SDMs) for key pollinator groups Lepidoptera (Butterflies) and Hymenoptera (Bees) from ACCREU-developed SDMs (See Section 4.2.2, and Table 7). Along with Coleoptera and Diptera (not modelled here due to data limitations), Lepidoptera and Hymenoptera represent the dominant taxa providing pollination services to crops in Europe (Moldoveanu et al., 2024; Potts et al., 2016; Reverté et al., 2023; Wardhaugh, 2015).

Table 7: Summary of wild insect pollinator groups (Hymenoptera, Lepidoptera) considered in our analysis. For each represented Genus, we provided the count of species for that Genus in brackets.

Pollinator Group	Species count	% of Total Pollinators	Represented Genus (Species count per genus)
Hymenoptera (Bees)	96	62.75	*Andrena (10); Bombus (11); Chelostoma (1); Colletes (2); Dufourea (1); Epeolus (2); Halictus (2); Hoplitis (3); Hylaeus (2); Lasioglossum (2); Macropis (1); Megachile (3); Nomads (12); Osmia (1); Panurgus (2); Sphecodes (1); Stelis (1)*
Lepidoptera (Butterflies)	57	37.25	*Anthocharis (1); Apatura (1); Aricia (1); Arytrura (1); Cacyreus (1); Clossiana (1); Coenonympha (6); Colias (1); Cupido (1); Danaus (1); Erannis (1); Erebia (20); Eriogaster (1); Euchloe (2); Euphydryas (2); Gegenes (1); Glyphipterix (1); Hipparchia (7); Laeosopis (1); Lampides (1); Lasiommata (1); Leptidea (1); Leptotes (1); Lignyoptera (1); Lopinga (1); Lycaena (3); Lysandra (1); Melanargia (2); Melitaea (4); Nymphalis (2); Oeneis (1); Papilio (2); Parnassius (2); Pelopidas (1); Pieris (1); Polyommatus (4); Pontia (1); Proserpinus (1); Pseudophilotes (2); Pyrgus (6); Vanessa (3); Xestia (1); Xylomoia (1); Zerynthia (1)*
Total	**153**	**100 %**	

The SDMs provide species-specific habitat availability indices, represented as a fraction of suitable habitat per 10 km^2 grid cell across Europe for different climate and adaptation scenarios. From these, we calculated **species-weighted habitat availability across all pollinator species** for each 10 km^2 grid cell, providing a measure of overall pollinator potential (0-1). We first calculated species richness, the absolute count of species with suitable habitat in each grid cell, as:

$$R = \sum_{i=1}^{n} I\left(s_i > t\right) \#(5.9)$$

where R is species richness and I is an indicator function that equals 1 when species i has availability above threshold t (set at 0.0). Thereafter, for each grid cell, we calculated species-weighted habitat availability as:

$$S_{mean} = \frac{\sum_{i=1}^{R} s_i \cdot I\left(s_i > t\right)}{\sum_{i=1}^{R} I\left(s_i > t\right)} \#(5.10)$$

where S_{mean} is the mean habitat availability for the grid cell, s_i is the habitat availability of species i, I is the indicator function as defined above, and R is the total number of pollinator species in the grid cell (species richness).

For reporting purposes, we reclassified each grid cell into ecologically meaningful categories of pollination potential, based on mean habitat availability (Vallecillo et al., 2018): Negligible (< 0.1) indicates little to no availability for pollinators and therefore no pollination potential; Low (0.1-0.2) indicates little availability for pollinators and low pollination potential; Medium (0.2-0.3) and High (0.3) indicate areas of 'prime' habitat availability for pollinators, and therefore higher pollination potential. This classification allows for clearer communication of results while maintaining ecological relevance in the availability gradients.

To allow integration of pollination potential information (rasters) with crop demand (vectors aggregated at NUTS3 up to NUTS 0), we intersected the pollination rasters with NUTS3 administration borders using a hierarchical spatial sampling approach. Beginning at NUTS3, for each administrative region, we extracted pollinator availability values at the NUTS3 region centroids. For regions where centroids failed (e.g., small regions not aligned with raster cells), we extracted all valid values within the regions bounding box, calculated the mean of these values as the regions' pollinator potential, and if no valid values were available, we used the global mean or a conservative default value (0.1). This methodology ensured complete spatial coverage while accounting for geographic variability in the vector boundaries (NUTS) and pollinator distributions.

For NUTS level, we calculated the area (in hectares) in each availability class for all time periods and scenarios. We focused our analysis on areas with medium and high availability (>0.2), representing prime pollinator habitat. For each country and scenario, we calculated the percent change from the 2020 baseline.

5.3.3 Actual flow of crop pollination – physical and monetary

Actual pollination flow represents the ecosystem service that contributes to agricultural production. This captures the spatial intersection between crop demand and available pollinator supply. The flow only occurs where both crops needing pollination and pollinators exist together. We calculated actual pollination flow (realized pollination) as the product of pollination demand and pollinator potential at each location, following the supply-use spatial correspondence principle established in ecosystem service assessment literature. For each administrative unit:

$$F_{area} = D_{area} \cdot S_{norm} \#(5.11)$$

$$F_{value} = D_{value} \cdot S \#(5.12)$$

where: F_{area} is the realized pollination area (ha); F_{value} is the realized pollination value (USD); and S is the habitat availability for pollinators (i.e., pollinator potential) (0-1). This formulation explicitly accounts for the spatial mismatch between pollinator habitat and agricultural areas that often limits service delivery in real-world systems.

5.4 Results & Discussion

5.4.1 Crop pollination demand

Here, we report the change in **effective area requiring pollination services (ha)**, accounting for the varying dependency levels of different crops (Table 6). This metric directly corresponds to the economic value calculations, making it more consistent with economic impact assessments than reporting total area (already reported in ACCREU Deliverable D2.2). It is crucial to note that the GLOBIOM model only includes a subset of pollinator-dependent field crops (e.g., sunflower, soybean, rapeseed), while excluding many important pollinator-dependent fruits and nuts. **Therefore, these results should be interpreted as changes in field crop pollination demand rather than total agricultural pollination requirements**.

The overall extent of pollinator-dependent crop area demand across Europe **declines** by 2050 relative to 2020 (Figure 35 A). This decline varies in magnitude across climate and adaptation scenarios, ranging from -26.97 % to -30.40 % % under high adaptation, to -40.67 % to -41.99 % under low adaptation scenarios. Notably, the rate of decline is moderated by adaptation intensity, where high adaptation scenarios show the least decline, while low adaptation scenarios exhibit the steepest reduction. The consistent decline in overall pollinator-dependent crop area demand indicates a net reduction in field crop pollination demand across Europe. **However, this should not be interpreted as the reduced importance of pollinators for European agriculture, as many high-value fruit and nut crops that rely heavily on pollinators are not captured in this analysis.**

When disaggregated by crop dependency (high, moderate, low), we found striking differences in how crop categories with different pollinator dependencies respond to climate and adaptation scenarios (Figure 35 B). High dependency crops (65 %), here sunflower oil, show substantial declines across all scenarios. These crops exhibit the most severe losses by 2050 under low adaptation scenarios (-40.70 % to -42.01 % reduction), with the decline somewhat moderated under high adaptation (-27.00 % to -30.44 % reduction). This represents a significant reduction in crops that are most sensitive to pollinator services. Moderate dependency crops (25 %) show an increase across all scenarios, ranging from 13.98 % to over 76.05 % by 2050. This increase becomes more pronounced with higher emission scenarios (greater under RCP 70 than RCP 26) and higher adaptation intensity. We find that the increase in medium-dependent crops over time is primarily driven by expansion in soybean cultivation, offsetting declines in rapeseed (**Appendix F Figure F1**, not shown here). Low dependency crops (5 %) show minimal changes overall, with slight increases (0.33 to 1.98 %) under low adaptation scenarios and small decreases under medium (-1.40 to -3.25 %) and high (-3.21 to -5.52 %) adaptation scenarios.

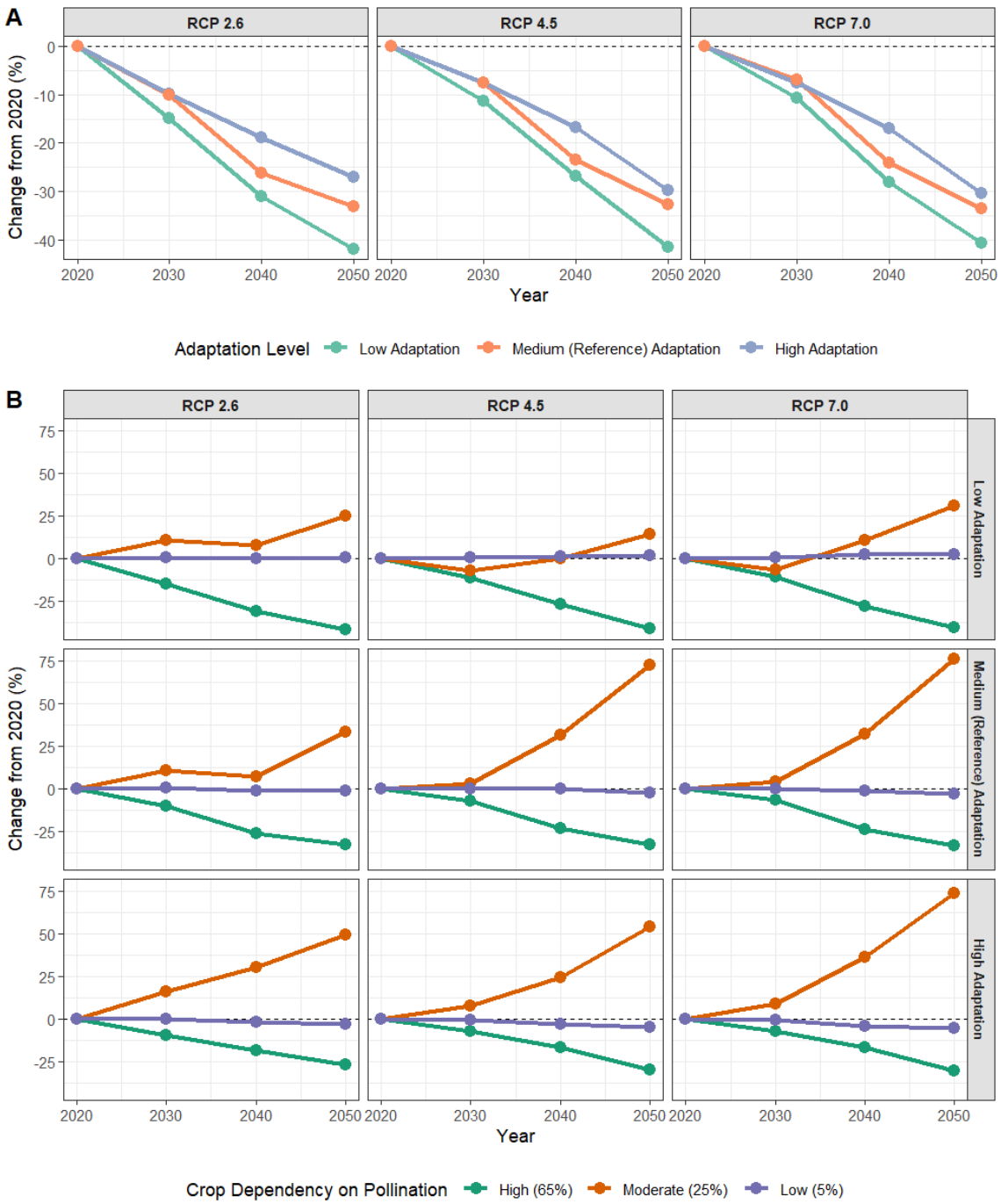

*Figure 35: Change in field crop pollination demand area from 2020 by climate scenario (RCP) and adaptation level for (A) combined pollinator-dependent crops across Europe, and (B) Grouped by crop dependency High (65 %; Sunflower), Moderate (25 %; Rapeseed, Soybean, Dry bean, Chickpea); and Low (5 %; Cotton, Groundnut). Effective area (calculated as total crop area * pollination dependency index) is the relative area of crops depending on pollination services, accounting for their varying dependency levels on pollination.*

Figure 36 illustrates the geographic variation in pollination demand changes across European countries by 2050, relative to 2020 baseline conditions. Countries with consistent increases across most scenarios include Portugal, Sweden, and Ireland (particularly under RCP 4.5 and 7.0), with high adaptation generally producing the largest increases in pollinator-dependent crop area.

Several countries exhibit mixed crop pollination demand responses: Serbia's demand increases except under low adaptation, North Macedonia shows the largest increases under high adaptation, Italy shows strong increases only under RCP 7.0 high adaptation, and the UK increases under RCP 4.5 and 7.0 for medium and low adaptation scenarios. Countries with minimal changes include Albania, Switzerland, Slovenia, the Netherlands, Finland, and Cyprus. All other modelled countries show consistent decreases across all scenarios, with the most severe declines observed in Croatia, Spain, Lithuania, Estonia, and Belgium.

The differential response of crop pollination-dependency categories (low, moderate, high) to climate change and adaptation scenarios reveals potential shifts in European agriculture systems. However, these findings must be considered with important caveats. Our model does not include Mediterranean fruit crops, berry production in Northern Europe, or orchard crops throughout the continent, all of which are highly pollinator-dependent and economically significant.

Within the modeled field crops, the north-south and east-west divide in pollination demand changes suggests differential capacity for adaptation. Northern European countries like Sweden and Ireland show increases in modeled pollinator-dependent crops, potentially indicating improved availability for crops like soybean under warming conditions (not shown here, **Appendix F Figure F1**). Conversely, traditional crop-producing regions in Continental and Eastern Europe show consistent decreases, suggesting challenges in maintaining current field crop systems.

The differential effectiveness of adaptation measures across countries is particularly noteworthy. For countries like Ireland, Greece, and North Macedonia, high adaptation corresponds to the largest increases in pollinator-dependent crop area. Conversely, in countries like Belgium, Spain, and Lithuania, even high adaptation cannot prevent substantial declines. This suggests that adaptation effectiveness is context-dependent, likely influenced by local climate conditions, agricultural systems, and socioeconomic factors.

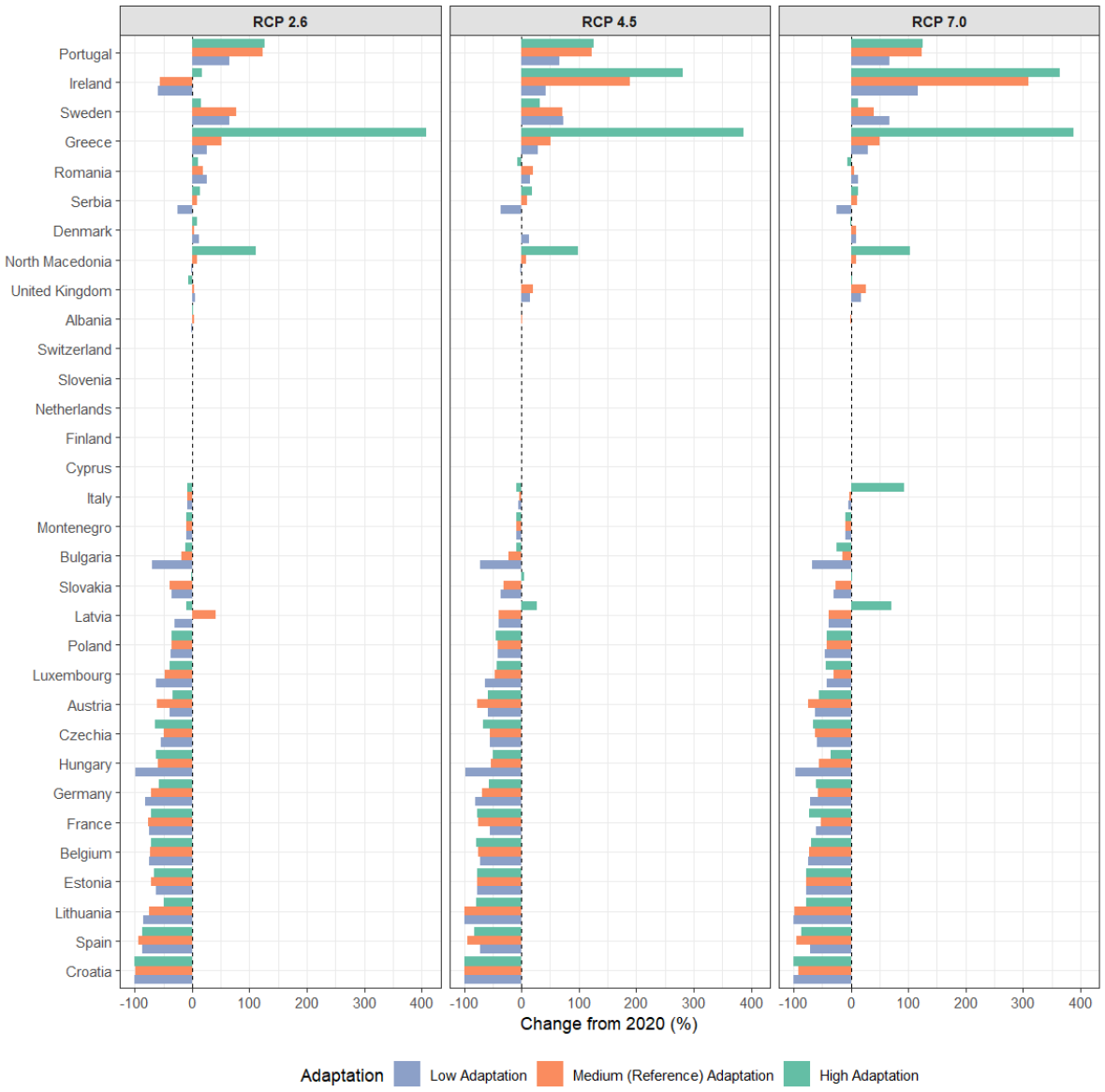

Figure 36: Change in field crop pollination demand area (%) by 2050 from 2020 by climate scenario (RCP) and adaptation level for combined pollinator-dependent crop area demand across European countries. Crop pollination demand is the effective area requiring pollination services. Excludes Liechtenstein, Malta, Kosovo, and Norway.

5.4.2 Crop pollination potential

We used the SDMs of 153 unique pollinator bee and butterfly species to calculate pollinator habitat (i.e., environmental) availability over time, across scenarios. Our analysis reveals significant changes in pollinator habitat availability across Europe between 2020-2050 under various climate and adaptation scenarios (Figure 37; Figure 38). To better report trends, we discuss changes in crop pollinator potential extent in terms of change from 2020 (%; Figure 38), rather than actual numbers (Figure 37).

Areas with high pollinator habitat availability (>0.3) consistently declined across all scenarios and adaptation strategies, with losses ranging from 11.8-14.3 % under the most optimistic RCP scenario (RCP2.6 low emission scenario) to more than 18% under the most pessimistic scenario (RCP7.0 high emission scenario) by 2050. The intensity of climate change strongly influences the magnitude of habitat availability changes. Under RCP2.6, high availability losses remain relatively contained (-11.8 % to – 14.3 %). Under RCP4.5 (intermediate emissions), these losses accelerate to -15.6 % - -17.7 %. Under RCP7.0, we observe the most severe losses in high availability habitat (-16.0 % to -18.3 %). **The substantial loss of prime pollinator habitat within three decades demonstrates the increasing impacts on pollinator habitats under more extreme climate change.** Notably, within each RCP scenario, higher agricultural adaptation intensities correspond to greater losses in high availability areas. **This reveals a negative relationship between agricultural adaptation strategies and prime habitat for pollinators.**

Under all scenarios, medium availability areas (0.2-0.3) increase slightly (0.3-4.3 %) from 2020, with larger gains under more intense climate scenarios (RCP 7.0; 3.3-4.3 %) and smaller gains under less intense climate scenarios (RCP 2.6; 0.3-1.2 %). This increase diminishes as adaptation intensity rises from low to high, suggesting that higher adaptation measures lead to a slower increase in medium suitable areas. Both low (0.1-0.2) and negligible (<0.1) availability areas show consistent increases across all scenarios, with gains of 5.4-13.0% for low availability and 1.8-2% for negligible availability areas by 2050. For low availability areas specifically, higher adaptation intensity leads to greater increases across all climate scenarios. This suggests that agricultural adaptation may be converting high or medium availability habitat to low availability habitat rather than preserving high-quality pollinator habitats.

These patterns show a “downgrading” of habitat quality throughout Europe, with high availability areas converting to medium and low availability. This suggests a general shift toward poorer habitat conditions for pollinators throughout Europe, rather than an abrupt loss. This pattern is consistent with climate-driven changes in vegetation composition (De Pauw et al., 2021; Rumpf et al., 2022), phenology (Hacket-Pain and Bogdziewicz, 2021), and resource availability (Harris et al., 2024) that affect habitat availability for pollinators. The consistent decline in high availability pollinator habitats across all scenarios represents a significant concern for pollinator conservation in Europe. These areas likely serve as core habitats and population sources for many pollinator species. Their loss may have cascading effects on pollinator population dynamics and community composition.

The projected changes in pollinator habitat availability have direct implications for crop pollination services. Areas experiencing substantial losses in high-quality pollinator habitat may face increased pollination deficits, potentially affecting crop yields and food security. The spatial redistribution of pollinator habitat quality may create new mismatches between pollination demand (crop production areas) and supply (areas with suitable pollinator habitat), requiring adaptive management of agricultural landscapes to maintain pollination services.

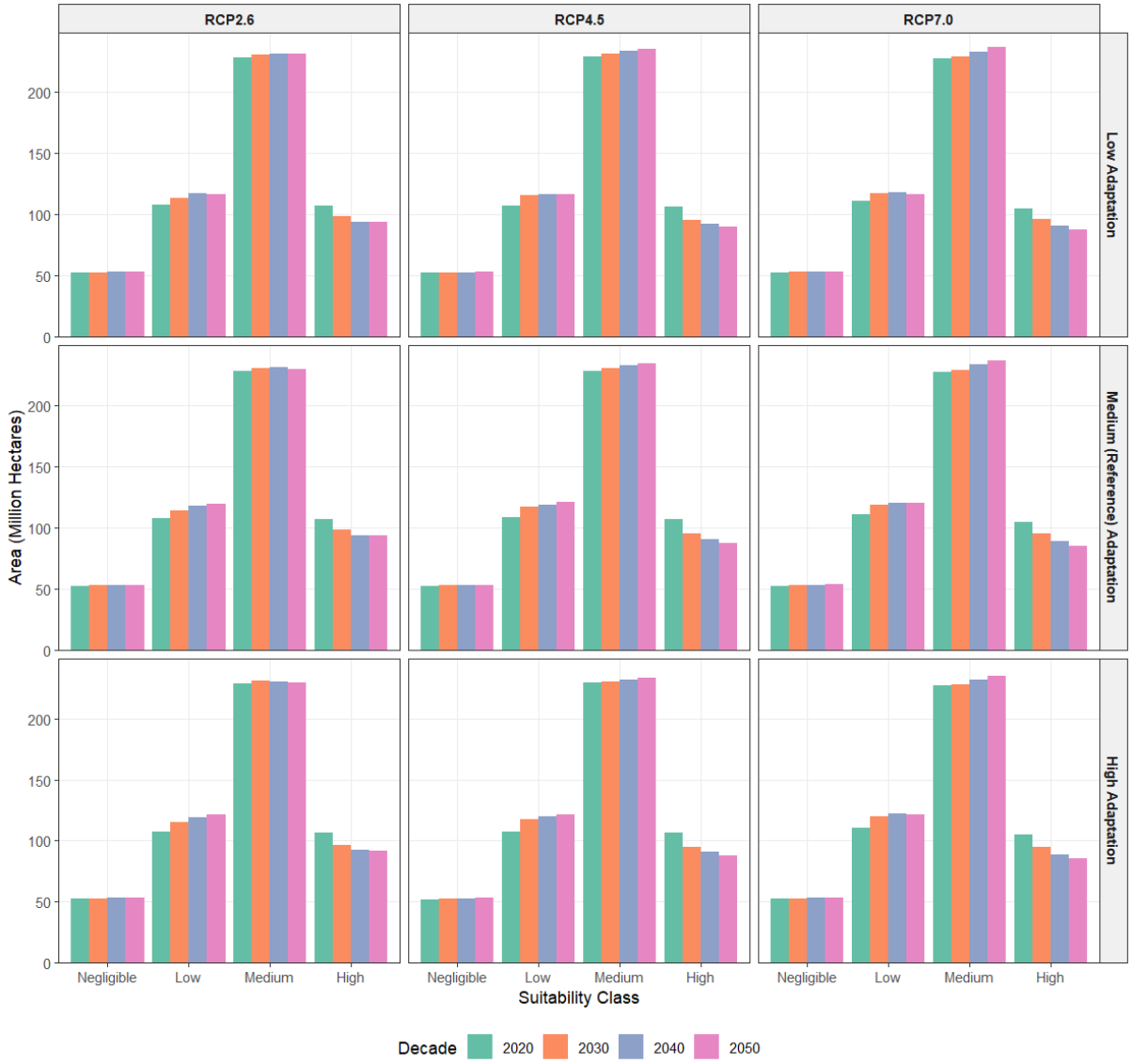

Figure 37: Suitable habitat area extent for pollinators across Europe (million ha), by pollinator-dependency class, under several climate (RCP 2.6; 4.5; 7.0) and adaptation (high, medium/reference, low) scenarios. Pollinator dependency classes are based on the mean habitat availability, where "High" (>0.3) indicates high availability for pollinators, "Medium" (0.2-0.3) indicates moderate availability, "Low" (0.1-0.2) indicates low availability, and "Negligible" (< 0.1) indicates little to no availability.

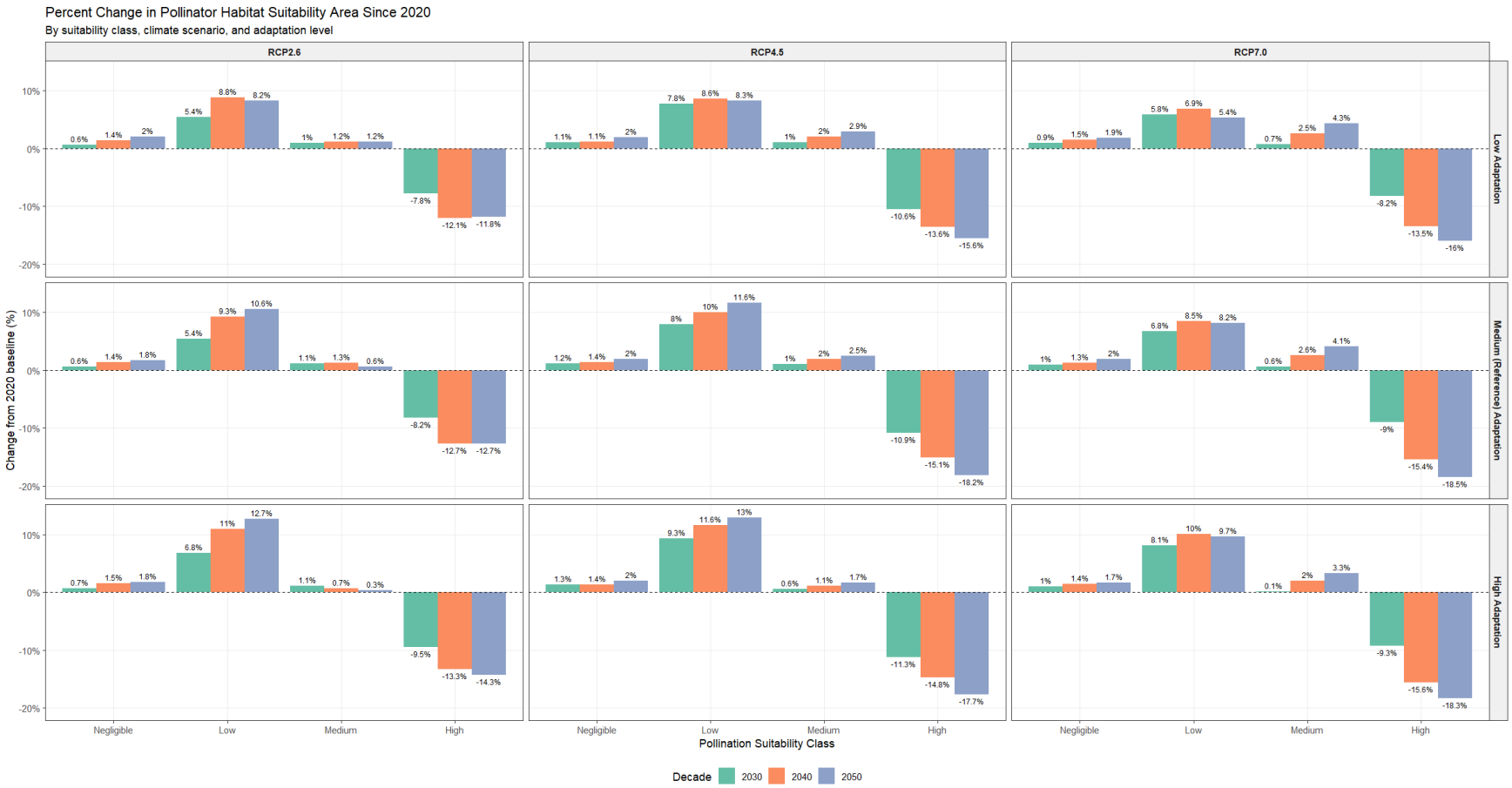

Figure 38: Percent change in suitable habitat area extent for pollinators, by pollinator-dependency class, relative to 2020 baseline conditions under several climates (RCP 2.6; 4.5; 7.0) and adaptation (high, medium/reference, low) scenarios. Pollinator dependency classes are based on the mean habitat availability, where "High" (>0.3) indicates high availability for pollinators, "Medium" (0.2-0.3) indicates moderate availability, "Low" (0.1-0.2) indicates low availability, and "Negligible" (< 0.1) indicates little to no availability.

By analyzing the percent change in high and medium pollinator availability in 2050 compared to 2020, we find a distinct geographic pattern in pollinator habitat changes (Figure 39). The countries showing consistent increases (Montenegro, Switzerland, Albania, Kosovo) share mountainous topography, suggesting that elevation and topographic complexity may buffer pollinator habitats against climate change impacts. In contrast, the countries experiencing the most severe losses are considered lowland areas (Luxembourg, Belgium, Netherlands). This highland-lowland divide may reflect how topographic heterogeneity provides microclimate refugia for pollinators. Czechia also exhibits substantial losses, which is a concern given its importance as a producer of pollinator-dependent arable crops e.g., oilseeds (rapeseed and sunflower) (Bernas et al., 2021; CZSO (The Czech Statistical Office), 2021).

Several countries exhibit surprising patterns that warrant further investigation. The Netherlands shows severe losses under most scenarios but a counterintuitive increase under RCP 7.0 (9.09-18.18 %), possibly indicating threshold effects where extreme climate conditions benefit certain pollinator habitats. Similarly, Denmark shows increases under RCP2.6 (~10 %) but massive declines under RCP 7.0 (40-50 %), highlighting how climate response can be non-linear. The UK's consistent gains despite being a heavily developed island nation suggest unique factors that warrant further investigation.

The distribution of losses creates particular concern for European agriculture. Many of Europe's agricultural powerhouses (Germany, France, Belgium, Netherlands) face substantial declines in pollinator habitat. These countries produce significant portions of Europe's pollination-dependent crops, including fruits, vegetables, and oilseeds. The projected pollinator habitat losses in these regions could create 'agricultural vulnerability hotspots' where pollination deficits may significantly impact food production and security.

These country-specific patterns suggest the need for tailored conservation approaches. For countries showing increases, protection of these emerging pollinator strongholds should be prioritized. For those facing severe losses, aggressive habitat restoration and pollinator-friendly farming practices will be essential. The results also highlight potential 'conservation opportunity zones' in countries like Hungary and Serbia that maintain or increase pollinator habitat despite climate pressures, making them valuable for transboundary conservation initiatives.

The stark differences between RCP scenarios for countries like Portugal and Denmark underscore how climate mitigation could significantly affect pollinator conservation outcomes. For these climate-sensitive nations, strong emissions reductions could mean the difference between maintaining or losing critical pollination services, providing additional justification for ambitious climate action at both national and EU levels.

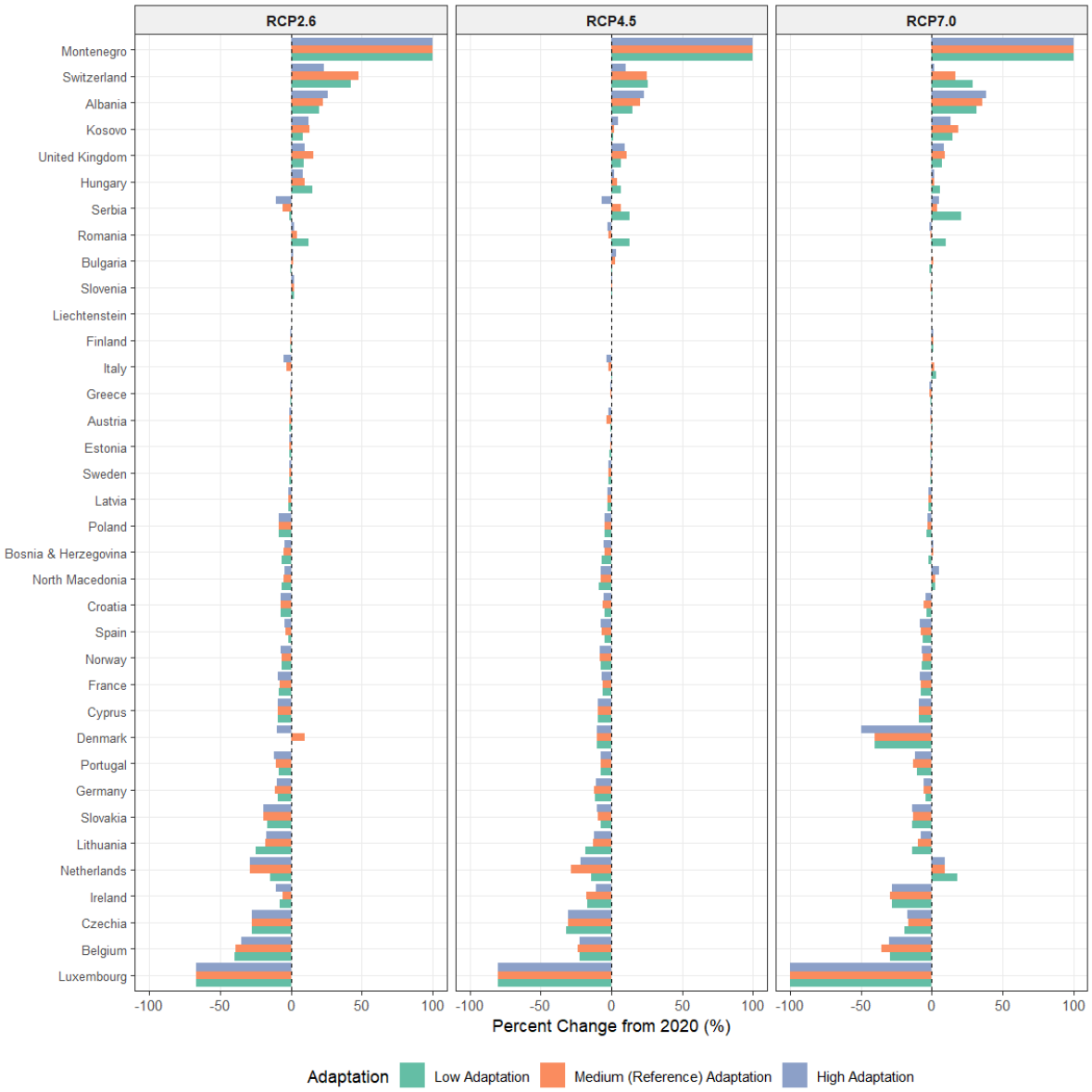

Figure 39: Percent change in high (> 0.3) and medium (0.2-0.3) pollinator habitat availability/quality in 2050 compared to a 2020 baseline for all modelled European countries.

5.4.3 Actual flow of crop pollination

Realized pollination area represents the actual spatial extent where pollination services are delivered in agricultural landscapes. Ecologically, it quantifies the intersection between pollinator habitat (supply) and pollinator-dependent crops (demand), capturing where functional pollination occurs rather than where it potentially could occur. Economically, it represents the productive agricultural land that receives pollination services, directly contributing to crop yields and economic output. Within the SEEA EA framework, realized pollination area constitutes the "actual ecosystem service flow" in physical terms, which is a core component of ecosystem accounting that measures the tangible biophysical interaction between ecosystems and agricultural production systems.

Figure 40 illustrates the realized pollination area across Europe from 2020 to 2050 under different climate and adaptation scenarios. The results show a consistent decline in total realized pollination area over time across all scenarios, with the steepest losses occurring under low adaptation pathways. By 2050, the realized pollination area under RCP 7.0 with low adaptation (3.38 million ha) declines by approximately 46.6 % compared to 2020 levels (6.32 million ha), while high adaptation scenarios show more moderate reductions of 36.8 % (3.99 million ha).

The composition of crops receiving pollination services is dominated by three major crops (sunflower, rapeseed, and soybean), which collectively account for most realized pollination area. In 2020, sunflower represented the largest share (58.80 %), followed by rapeseed (38.20 %) and then soybean (2.13 %). By 2050, notable shifts occur in this composition, particularly under high adaptation scenarios where soybeans' relative contribution increases substantially (9.55-12.00 %). This suggests that agricultural adaptation strategies that include crop switching and technological improvements may favor soybean cultivation under changing climate conditions.

Interestingly, the differences in realized pollination area across RCP scenarios (2.6, 4.5, and 7.0) are relatively modest compared to the pronounced effects of adaptation levels. This indicates that **agricultural adaptation strategies may have a greater influence on maintaining pollination services than the specific climate pathway, at least within the timeframe examined.**

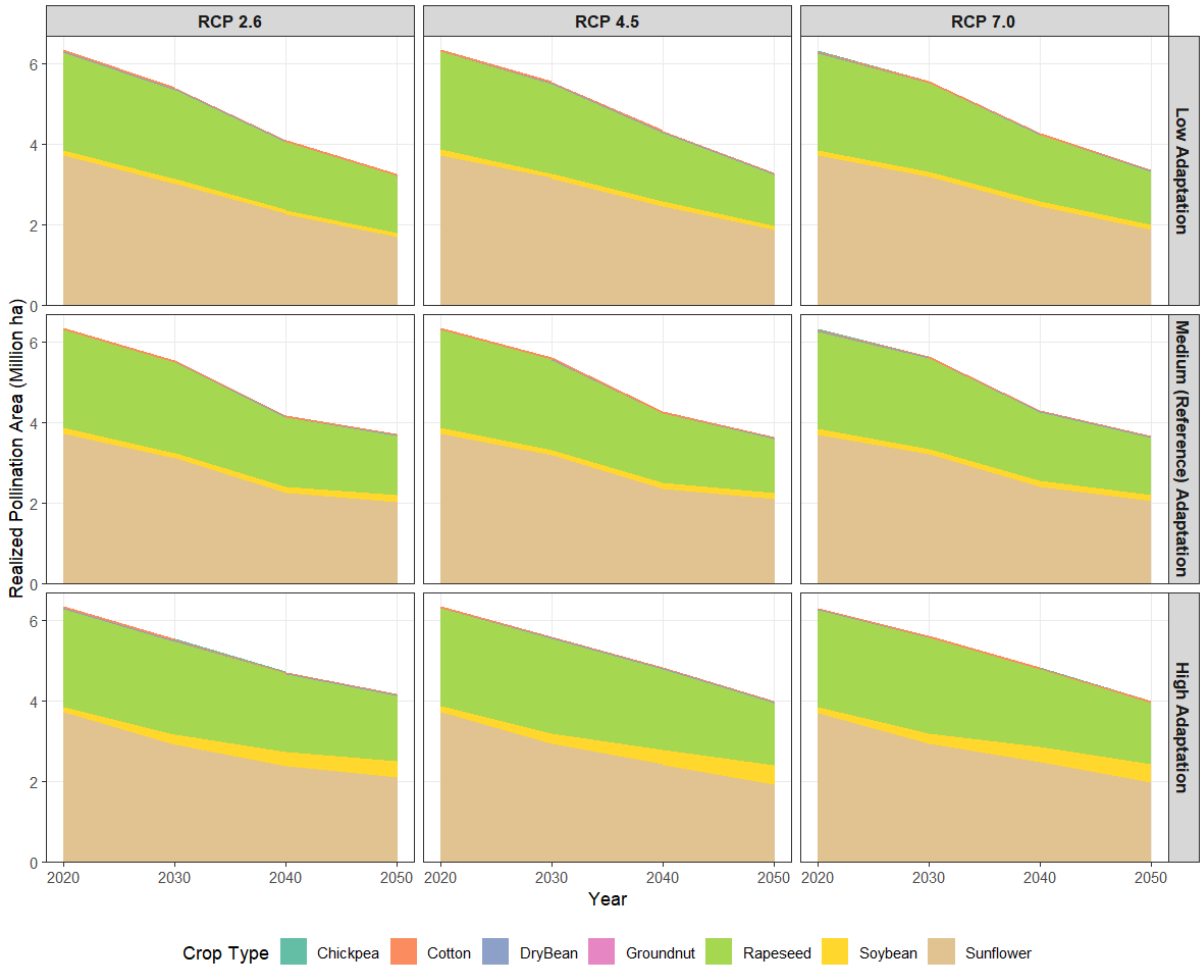

Figure 40: European-wide total realized pollination flow (area, million ha) over time per pollinator-dependent field crop type. The realized pollination flow is the intersection between pollinator habitat (supply) and pollinator-dependent crops (demand).

Figure 41 presents the percent change in realized pollination area between 2020 and 2050 for individual European countries across climate and adaptation scenarios. The results reveal striking spatial heterogeneity in pollination service dynamics across Europe. Most countries (18) show decreases in realized pollination area by 2050 across all scenarios, with the magnitude of decline generally **greater under low adaptation pathways** compared to high adaptation. This reinforces the EU-wide finding that **adaptation measures can substantially mitigate losses in pollination services**.

However, several countries exhibit more complex patterns. Denmark, for instance, shows counterintuitive gains under low adaptation and losses under high adaptation across all RCP scenarios. This unusual pattern may reflect shifts in crop distribution under different adaptation pathways, where limited adaptation options may favor pollinator-dependent crops in Denmark's specific agricultural context. Serbia demonstrates dramatic losses under low adaptation but gains under high adaptation, illustrating the potential effectiveness of targeted adaptation measures in certain geographic contexts.

A small group of countries shows consistent gains in realized pollination area across all scenarios. Romania exhibits the largest increases under RCP 2.6, particularly with low adaptation measures. Sweden shows most substantial gains under RCP 4.5, while the UK achieves optimal outcomes under reference (medium) adaptation rather than high adaptation.

Two countries display exceptional increases: Ireland shows gains of over 300 % under high adaptation for RCP 4.5 and 7.0, while Greece exhibits extreme increases of 387 % under high adaptation for RCP 2.6. These dramatic increases likely reflect significant shifts in agricultural systems under high adaptation, potentially including expansion of irrigation for pollinator-dependent crops in these regions.

These diverse country-level responses highlight the complex interactions between climate change, adaptation strategies, and local agricultural contexts. High adaptation, which includes advanced technologies, improved irrigation systems, and strategic crop switching, delivers substantially different outcomes across Europe's diverse agroecological zones. The observed patterns suggest that **adaptation strategies must be tailored to specific regional conditions rather than applied uniformly across Europe to effectively maintain pollination services under climate change.**

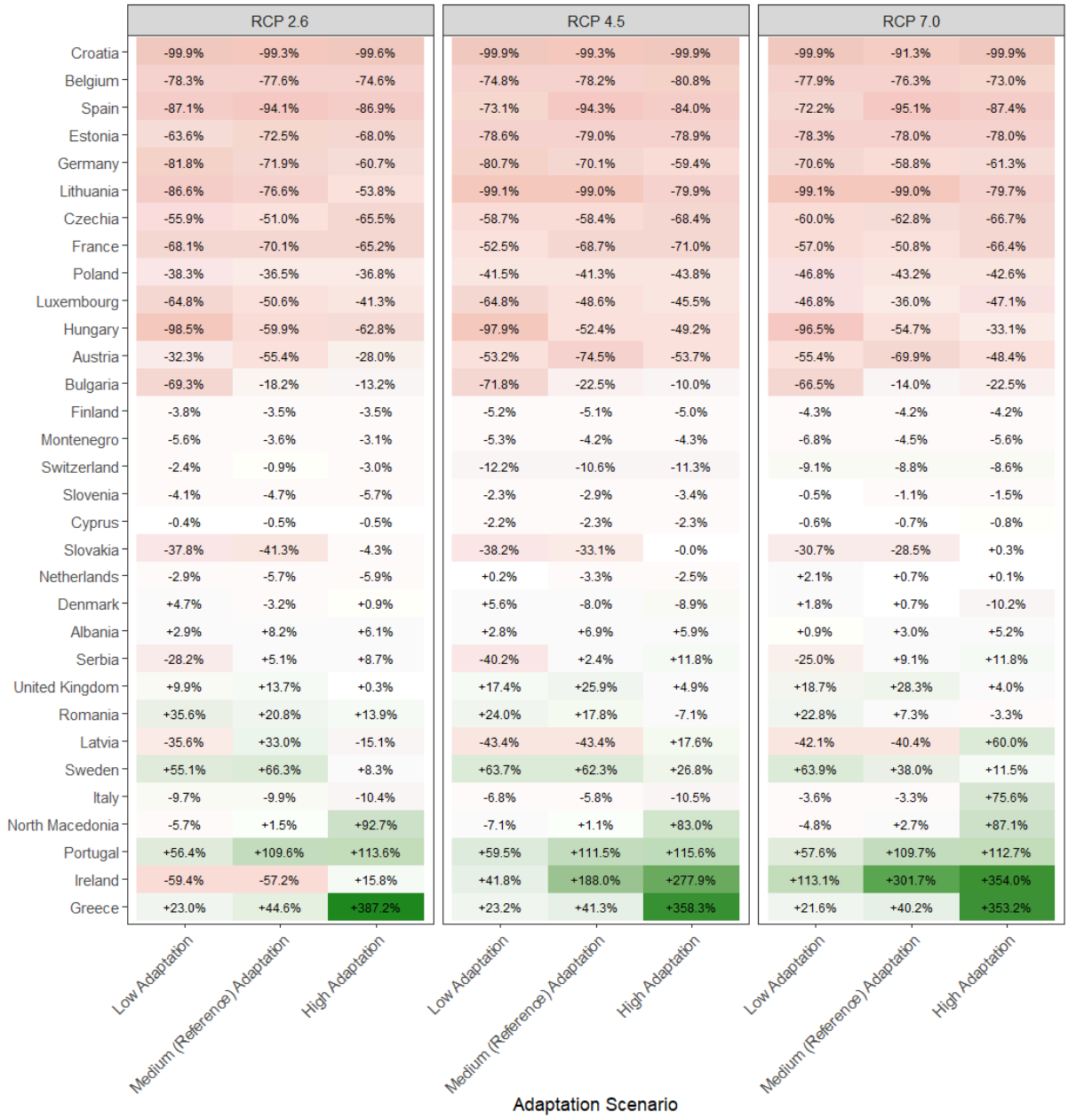

Figure 41: Percent change in the actual pollination flow by country, measured by realized pollination area (million ha) for the 2020-2050 period. Areas shaded in red show a decrease, areas in green show an increase.

5.4.4 Monetary evaluation of crop pollination

The monetary evaluation of crop pollination translates the physical flow of pollination services into economic terms, representing the financial contribution of this ecosystem service to agricultural production. Ecologically, it quantifies the portion of crop value directly attributable to pollinator activity, reflecting both the dependency of crops on pollinators and the effectiveness of pollination delivery. Economically, it provides a tangible measure of natural capital contribution to human welfare, enabling cost-benefit analyses of conservation measures and adaptation strategies. Within the SEEA EA framework, realized pollination value constitutes the monetary component of ecosystem service flow accounts, connecting ecosystem assets to economic activities and supporting the integration of natural capital into standard economic accounting.

Figure 42 illustrates the projected realized economic value of crop pollination across Europe from 2020 to 2050 under different climate and adaptation scenarios. Our baseline(2020) estimated economic value of pollination services is approximately **5.23 billion USD annually**. This value differs from previously published estimates, which report substantially larger figures: 22 billion euros (Gallai et al., 2009), 7 to 18 billion USD per year from 1991 to 2018 (Rubinigg Michael, 2024), 14.6 billion EUR per year from 1991 to 2009 (Leonhardt et al., 2013). The discrepancy between our estimated value and the previous estimates can be attributed primarily to the methodological scope limitations in our assessment framework. Previous studies incorporated high-value, highly pollinator-dependent crops such as fruit and nuts. Our analysis was deliberately restricted to crops modelled within the GLOBIOM framework, which excludes high-value horticultural crops that significantly contribute to previous estimates. This approach ensures consistent integration with our climate-land use scenarios and provides a standardized baseline for analyzing relative changes across temporal projections. While producing lower absolute values than comprehensive assessments, our methodology offers analytical consistency when comparing climate scenarios and adaptation pathways, which constitutes the primary objective of our assessment.

Looking at our temporal projections, we found that the total economic value of pollination services consistently declines across all scenarios, with values decreasing to **2.18 to 3.75 billion USD by 2050**, depending on the scenario. The steepest declines occur under low adaptation scenarios, where pollination value decreases by approximately 55.1 to 58.2 %. In contrast, high adaptation scenarios demonstrate more moderate reductions of 28.3 to 29.5 %, highlighting the importance of adaptive measures in preserving pollination services.

The composition of pollination value reveals that three crops of the largest flow (sunflower, rapeseed, and soybean) consistently account for most of the total pollination economic value across all scenarios. In 2020, sunflower contributed the largest share at approximately 2.86 billion USD (54.8 % of total value), followed by rapeseed (2.17 billion USD; 41.5 % of total value) and soybean (0.15 billion USD; 2.83 % of total value). However, this composition changes notably by 2050, particularly under high adaptation scenarios, where soybean's contribution increases by 13.4 to 15.8 %, while sunflower's relative contribution declines. Rapeseed shows resilience across scenarios, maintaining or even increasing its relative economic importance by 2050, particularly under high adaptation scenarios where it contributes 1.31 to 1.39 billion USD (35.1 to 37.6 % of total value). This economic realignment reflects both the changing distribution of these crops under different adaptation pathways and their relative market values.

The economic patterns largely mirror the physical flow trends discussed previously, but with important distinctions. While the physical pollination area shows relatively modest differences across RCP scenarios, the economic impacts display greater sensitivity to both climate pathways and adaptation levels. This suggests that the economic dimension of pollination services may be more vulnerable to climate change than the physical dimension alone, likely due to climate effects on crop yields and quality beyond simple area metrics.

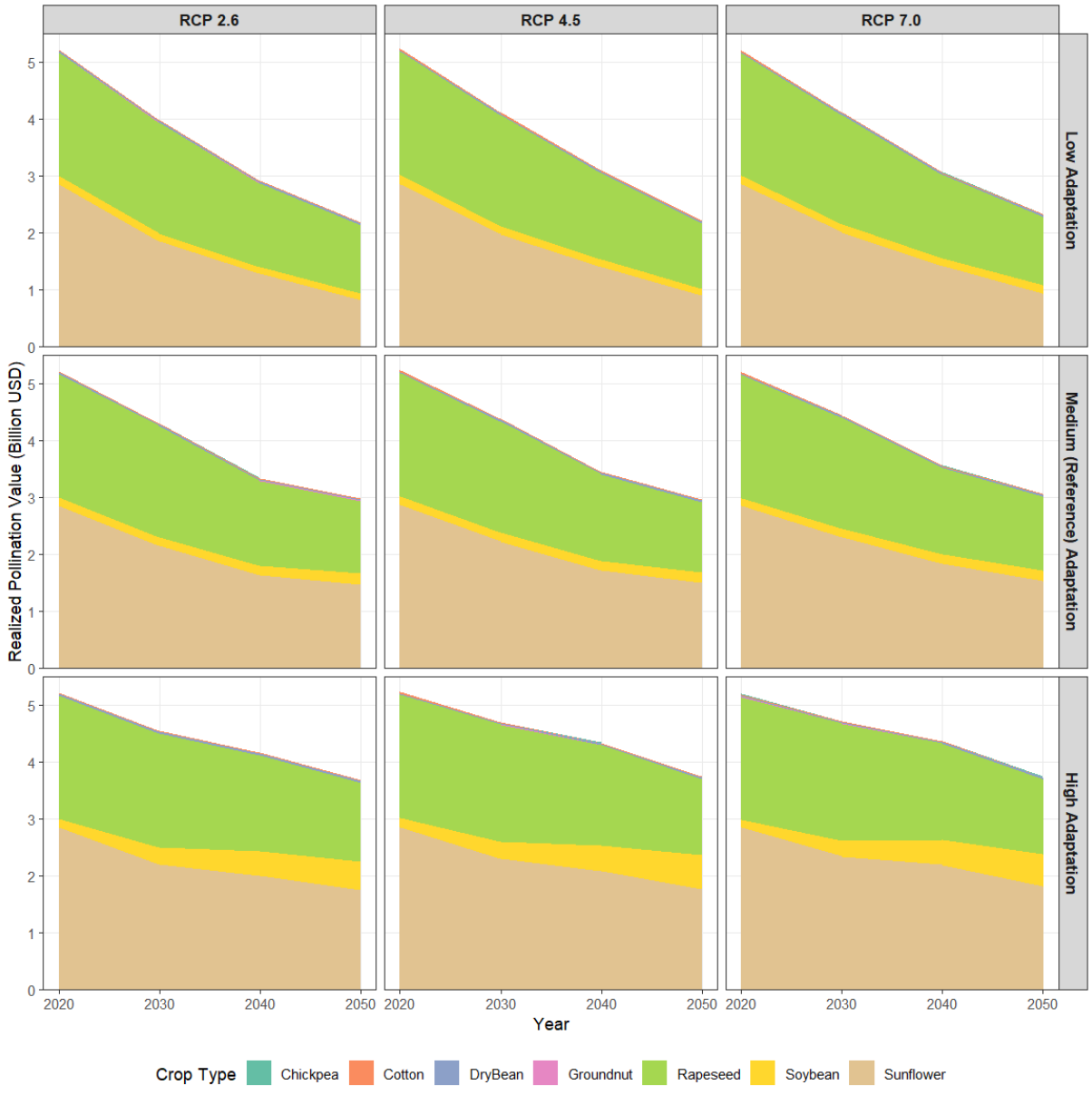

Figure 42: European-wide total realized pollination value (Billion USD) over time per pollinator-dependent field crop type from GLOBIOM outputs. The realized pollination value represents the financial contribution of this ecosystem service to agricultural production, accounting for both crop pollination supply and demand.

Figure 43 presents the percent change in realized pollination value between 2020 and 2050 for individual European countries across climate and adaptation scenarios, revealing striking economic disparities in impact and opportunity.

Most countries (17) experience decreases in pollination value by 2050 across all scenarios, with the magnitude of economic losses generally greater under low adaptation pathways. Hungary exemplifies this pattern with dramatic losses of 96-98% under low adaptation across all RCP scenarios, improving to 27-60% losses under high adaptation. Interestingly, Hungary's economic losses decrease from RCP 2.6 to RCP 7.0, suggesting that warmer conditions might benefit certain pollinator-dependent crops in this region when coupled with adaptation measures. Bulgaria shows similar patterns with major losses under low adaptation (74-77%) that improve substantially with higher adaptation (16-26%).

Several countries demonstrate scenario-dependent responses that highlight the critical role of adaptation strategies. Slovakia and Serbia show losses under low and medium adaptation but gains under high adaptation across all RCP scenarios. This pattern parallels their physical flow trends and underscores the economic returns on adaptation investments in these regions. Italy exhibits losses under most scenarios except for gains under RCP 7.0 with high adaptation, suggesting specific climate-adaptation interactions that benefit pollination services in this Mediterranean country.

A notable group of countries shows economic gains across nearly all scenarios, including Cyprus, the Netherlands, Switzerland, the UK, Romania, Portugal, North Macedonia, Ireland, and Greece. These countries generally demonstrated increases in physical pollination flow as well, but their economic gains are often proportionally larger, suggesting favorable price effects for pollinator-dependent crops in these regions. Romania shows the largest gains under RCP 2.6 with low adaptation measures, potentially benefiting from milder climate change with minimal disruption to existing agricultural systems. Portugal demonstrates increasing economic returns with increasing adaptation levels across all RCP scenarios, with optimal outcomes under RCP 4.5.

Ireland and Greece stand out with exceptional economic gains. Ireland shows massive increases of 213-272% under high adaptation for RCP 4.5 and 7.0, while Greece exhibits extraordinary gains of 510% under high adaptation for RCP 2.6, with similarly extreme increases under other scenarios (473% for RCP 4.5 and 466% for RCP 7.0). These values substantially exceed their physical flow increases, indicating that economic factors, likely to include crop prices and yield improvements from adaptation technologies, amplify the financial benefits of pollination services in these countries.

When compared to the physical flow results, the monetary valuation reveals amplified economic effects in both directions: **losses are often more severe and gains more substantial than the corresponding changes in physical pollination area**. This economic leverage effect highlights the critical importance of valuation in understanding the full implications of changing pollination services under global change.

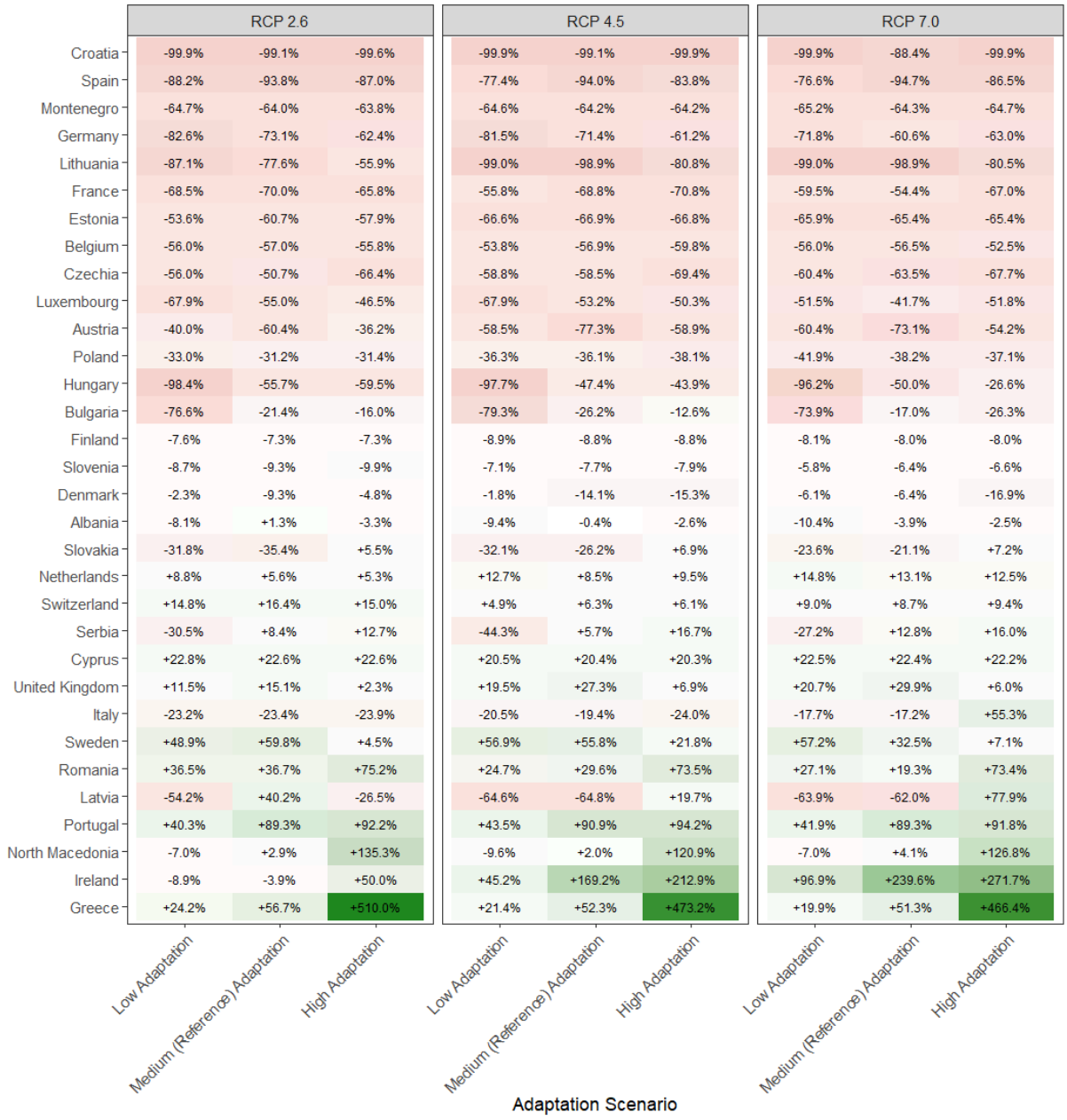

Figure 43: Percent change in realized economic crop pollination value (billion USD) in Europe, by country, for the 2020-2050 period. Areas shaded in red show a decrease, areas in green show an increase.

5.5 Conclusion/Key takeaways

Our analysis reveals a concerning "double pressure" on crop pollination in Europe through 2050. On one side, high-quality pollinator habitat is projected to decline by 12 % to more than 18% across Europe, with worse losses under higher emission scenarios. On the other side, the area of pollinator-dependent crops is projected to decline by 27-42%, but with important differences: highly pollinator-dependent crops (e.g., sunflower) show substantial decreases while moderately dependent crops (e.g., soybean) show increases. This creates a complex landscape where both pollinator supply and crop demand are shifting, often in opposite directions.

The economic value of crop pollination services, approximately **5.2 billion USD in 2020**, is projected to decline to between 2.2-3.8 billion USD by 2050, with agricultural adaptation strategies helping moderate these losses. Most striking is the uneven geographic impact, with many agricultural powerhouses facing severe losses while other countries could see dramatic increases in pollination services under certain adaptation scenarios. Crop pollination represents a critical ecosystem service that directly benefits agricultural production and food security across Europe. Without adequate pollination, yields of many important crops would decline significantly, affecting both farmer livelihoods and food availability.

Our analysis has several important limitations that point to the next critical steps for research. We focused on habitat availability rather than actual pollinator abundances, which are essential for service delivery, and our crop selection excluded high-value crops e.g., fruit and vegetables, that represent a substantial portion of pollinator-dependent agriculture in Europe. Additionally, our models don't account for potential adaptations by pollinators themselves or interactions with other stressors like pesticides and pathogens. The stark geographic differences in pollination service trajectories highlight the need for regionally tailored conservation strategies rather than one-size-fits-all approaches.

Future research should develop more integrated models that connect habitat quality to actual pollination delivery, validate projections through field observations, and design adaptation strategies that simultaneously support agricultural productivity and pollinator conservation, ensuring this essential ecosystem service continues to support European agriculture in a changing climate.

References

Amindin, A., Pourghasemi, H.R., Safaeian, R., Rahmanian, S., Tiefenbacher, J.P., Naimi, B., 2024. Predicting Current and Future Habitat Suitability of an Endemic Species Using Data-Fusion Approach: Responses to Climate Change. Rangeland Ecology & Management 94, 149–162. https://doi.org/10.1016/j.rama.2024.03.002

Antão, L.H., Weigel, B., Strona, G., Hällfors, M., Kaarlejärvi, E., Dallas, T., Opedal, Ø.H., Heliölä, J., Henttonen, H., Huitu, O., Korpimäki, E., Kuussaari, M., Lehikoinen, A., Leinonen, R., Lindén, A., Merilä, P., Pietiäinen, H., Pöyry, J., Salemaa, M., Tonteri, T., Vuorio, K., Ovaskainen, O., Saastamoinen, M., Vanhatalo, J., Roslin, T., Laine, A.-L., 2022. Climate change reshuffles northern species within their niches. Nat. Clim. Chang. 12, 587–592. https://doi.org/10.1038/s41558-022-01381-x

Arrogante-Funes, F., Mouillot, F., Moreira, B., Aguado, I., Chuvieco, E., 2024. Mapping and assessment of ecological vulnerability to wildfires in Europe. fire ecol 20, 98. https://doi.org/10.1186/s42408-024-00321-8

Augustynczik, A.L.D., Gusti, M., Deppermann, A., Nakhavali, M. (André), Jia, F., Di Fulvio, F., Havlík, P., 2025. Adapting forest management to climate change impacts and policy targets in the EU: Insights from the coupled GLOBIOM/G4M-i3PGmiX model. One Earth 8, 101313. https://doi.org/10.1016/j.oneear.2025.101313

Barbier, E.B., 2016. The protective service of mangrove ecosystems: A review of valuation methods. Marine Pollution Bulletin, Turning the tide on mangrove loss 109, 676–681. https://doi.org/10.1016/j.marpolbul.2016.01.033

Barbier, E.B., 2013. Valuing Ecosystem Services for Coastal Wetland Protection and Restoration: Progress and Challenges. Resources 2, 213–230. https://doi.org/10.3390/resources2030213

Barras, A.G., Braunisch, V., Arlettaz, R., 2021. Predictive models of distribution and abundance of a threatened mountain species show that impacts of climate change overrule those of land use change. Diversity and Distributions 27, 989–1004. https://doi.org/10.1111/ddi.13247

Bernas, J., Bernasová, T., Nedbal, V., Neugschwandtner, R.W., 2021. Agricultural LCA for Food Oil of Winter Rapeseed, Sunflower, and Hemp, Based on Czech Standard Cultivation Practices. Agronomy 11, 2301. https://doi.org/10.3390/agronomy11112301

Bieber, B.V., Vyas, D.K., Koltz, A.M., Burkle, L.A., Bey, K.S., Guzinski, C., Murphy, S.M., Vidal, M.C., 2023. Increasing prevalence of severe fires change the structure of arthropod communities: Evidence from a meta-analysis. Funct. Ecol. 37, 2096–2109. https://doi.org/10.1111/1365-2435.14197

Brander, L.M., Bräuer, I., Gerdes, H., Ghermandi, A., Kuik, O., Markandya, A., Navrud, S., Nunes, P.A.L.D., Schaafsma, M., Vos, H., Wagtendonk, A., 2012. Using Meta-Analysis and GIS for Value Transfer and Scaling Up: Valuing Climate Change Induced Losses of European Wetlands. Environ Resource Econ 52, 395–413. https://doi.org/10.1007/s10640-011-9535-1

Brooks, T.M., Pimm, S.L., Akçakaya, H.R., Buchanan, G.M., Butchart, S.H.M., Foden, W., Hilton-Taylor, C., Hoffmann, M., Jenkins, C.N., Joppa, L., Li, B.V., Menon, V., Ocampo-Peñuela, N., Rondinini, C., 2019. Measuring Terrestrial Area of Habitat (AOH) and Its Utility for the IUCN Red List. Trends in Ecology & Evolution 34, 977–986. https://doi.org/10.1016/j.tree.2019.06.009

Brotons, L., Herrando, S., Pons, P., 2008. Wildfires and the expansion of threatened farmland birds: the ortolan bunting *Emberiza hortulana* in Mediterranean landscapes. Journal of Applied Ecology 45, 1059–1066. https://doi.org/10.1111/j.1365-2664.2008.01467.x

Bugin, G., Lenzi, L., Ranzani, G., Barisan, L., Porrini, C., Zanella, A., Bolzonella, C., 2022. Agriculture and Pollinating Insects, No Longer a Choice but a Need: EU Agriculture's Dependence on Pollinators in the 2007–2019 Period. Sustainability 14, 3644. https://doi.org/10.3390/su14063644

Bunting, P., Rosenqvist, A., Hilarides, L., Lucas, R.M., Thomas, N., Tadono, T., Worthington, T.A., Spalding, M., Murray, N.J., Rebelo, L.-M., 2022. Global Mangrove Extent Change 1996–2020: Global Mangrove Watch Version 3.0. Remote Sensing 14, 3657. https://doi.org/10.3390/rs14153657

Chapman, M., Jung, M., Leclère, D., Boettiger, C., Augustynczik, A.L.D., Gusti, M., Ringwald, L., Visconti, P., 2025. Meeting European Union biodiversity targets under future land-use demands. Nat Ecol Evol 9, 810–821. https://doi.org/10.1038/s41559-025-02671-1

Chard, M., Foster, C.N., Lindenmayer, D.B., Cary, G.J., MacGregor, C.I., Blanchard, W., 2022. Time since fire influences macropod occurrence in a fire-prone coastal ecosystem. Austral Ecology 47, 507–518. https://doi.org/10.1111/aec.13127

Cimatti, M., Ranc, N., Benítez-López, A., Maiorano, L., Boitani, L., Cagnacci, F., Čengić, M., Ciucci, P., Huijbregts, M.A.J., Krofel, M., López-Bao, J.V., Selva, N., Andren, H., Bautista, C., Ćirović, D., Hemmingmoore, H., Reinhardt, I., Marenče, M., Mertzanis, Y., Pedrotti, L., Trbojević, I., Zetterberg, A., Zwijacz-Kozica, T., Santini, L., 2021. Large carnivore expansion in Europe is associated with human population density and land cover changes. Diversity and Distributions 27, 602–617. https://doi.org/10.1111/ddi.13219

Costanza, R., de Groot, R., Sutton, P., van der Ploeg, S., Anderson, S.J., Kubiszewski, I., Farber, S., Turner, R.K., 2014. Changes in the global value of ecosystem services. Global Environmental Change 26, 152–158. https://doi.org/10.1016/j.gloenvcha.2014.04.002

Cummings, S.R., Browner, W., Hulley, S.B., 2013. Conceiving the research question and developing the study plan., in: Designing Clinical Research. pp. 14–22.

CZSO (The Czech Statistical Office), 2021. Prague: Integrated Operational Program. European Union, Prague, Czech Republic.

Dasgupta, P., 2021. The economics of biodiversity: the Dasgupta review: full report, Updated: 18 February 2021. ed. HM Treasury, London.

Davidson, N.C., 2014. How much wetland has the world lost? Long-term and recent trends in global wetland area. Mar. Freshwater Res. 65, 934–941. https://doi.org/10.1071/MF14173

Davidson, N.C., Fluet-Chouinard, E., Finlayson, C.M., 2018. Global extent and distribution of wetlands: trends and issues. Mar. Freshwater Res. 69, 620–627. https://doi.org/10.1071/MF17019

de Groot, R., Brander, L., van der Ploeg, S., Costanza, R., Bernard, F., Braat, L., Christie, M., Crossman, N., Ghermandi, A., Hein, L., Hussain, S., Kumar, P., McVittie, A., Portela, R., Rodriguez, L.C., ten Brink, P., van Beukering, P., 2012. Global estimates of the value of ecosystems and their services in monetary units. Ecosystem Services 1, 50–61. https://doi.org/10.1016/j.ecoser.2012.07.005

De Pauw, K., Meeussen, C., Govaert, S., Sanczuk, P., Vanneste, T., Bernhardt-Römermann, M., Bollmann, K., Brunet, J., Calders, K., Cousins, S.A.O., Diekmann, M., Hedwall, P., Iacopetti, G., Lenoir, J., Lindmo, S., Orczewska, A., Ponette, Q., Plue, J., Selvi, F., Spicher, F., Verbeeck, H., Vermeir, P., Zellweger, F., Verheyen, K., Vangansbeke, P., De Frenne, P., 2021. Taxonomic, phylogenetic and functional diversity of understorey plants respond differently to environmental conditions in European forest edges. Journal of Ecology 109, 2629–2648. https://doi.org/10.1111/1365-2745.13671

Driscoll, D.A., Macdonald, K.J., Gibson, R.K., Doherty, T.S., Nimmo, D.G., Nolan, R.H., Ritchie, E.G., Williamson, G.J., Heard, G.W., Tasker, E.M., Bilney, R., Porch, N., Collett, R.A., Crates, R.A., Hewitt, A.C., Pendall, E., Boer, M.M., Gates, J., Boulton, R.L., Mclean, C.M., Groffen, H., Maisey, A.C., Beranek, C.T., Ryan, S.A., Callen, A., Hamer, A.J., Stauber, A., Daly, G.J., Gould, J., Klop-Toker, K.L., Mahony, M.J., Kelly, O.W., Wallace, S.L., Stock, S.E., Weston, C.J., Volkova, L., Black, D., Gibb, H., Grubb, J.J., McGeoch, M.A., Murphy, N.P., Lee, J.S., Dickman, C.R., Neldner, V.J., Ngugi, M.R., Miritis, V., Köhler, F., Perri, M., Denham, A.J., Mackenzie, B.D.E., Reid, C.A.M., Rayment, J.T., Arriaga-Jiménez, A., Hewins, M.W., Hicks, A., Melbourne, B.A., Davies, K.F., Bitters, M.E., Linley, G.D., Greenville, A.C., Webb, J.K., Roberts, B., Letnic, M., Price, O.F., Walker, Z.C., Murray, B.R., Verhoeven, E.M., Thomsen, A.M., Keith, D., Lemmon, J.S., Ooi, M.K.J., Allen, V.L., Decker, O.T., Green, P.T., Moussalli, A., Foon, J.K., Bryant, D.B., Walker, K.L., Bruce, M.J., Madani, G., Tscharke, J.L., Wagner, B., Nitschke, C.R., Gosper, C.R., Yates, C.J., Dillon, R., Barrett, S., Spencer, E.E., Wardle, G.M., Newsome, T.M., Pulsford, S.A., Singh, A., Roff, A., Marsh, K.J., Mcdonald, K., Howell, L.G., Lane, M.R., Cristescu, R.H., Witt, R.R., Cook, E.J., Grant, F., Law, B.S., Seddon, J., Berris, K.K., Shofner, R.M., Barth, M., Welz, T., Foster, A., Hancock, D., Beitzel, M., Tan, L.X.L., Waddell, N.A., Fallow, P.M., Schweickle, L., Le Breton, T.D., Dunne, C., Green, M., Gilpin, A.-M., Cook, J.M., Power, S.A., Hogendoorn, K., Brawata, R., Jolly, C.J., Tozer, M., Reiter, N., Phillips, R.D., 2024. Biodiversity impacts of the 2019–2020 Australian megafires. Nature. https://doi.org/10.1038/s41586-024-08174-6

Dullaart, J., Muis, S. (Sanne), Bloemendaal, N., Chertova, M., Couasnon, A., Aerts, J.C.J.H. (Jeroen), 2022. COAST-RP: A global COastal dAtaset of Storm Tide Return Periods. https://doi.org/10.4121/13392314.V2

Fayt, P., 2003. Insect prey population changes in habitats with declining vs. stable Three-toed Woodpecker Picoides tridactylus populations. Ornis Fenn 80, 182–192.

Fernandez-Anez, N., Krasovskiy, A., Müller, M., Vacik, H., Baetens, J., Hukić, E., Kapovic Solomun, M., Atanassova, I., Glushkova, M., Bogunović, I., Fajković, H., Djuma, H., Boustras, G., Adámek, M., Devetter, M., Hrabalikova, M., Huska, D., Martínez Barroso, P., Vaverková, M.D., Zumr, D., Jõgiste,

K., Metslaid, M., Koster, K., Köster, E., Pumpanen, J., Ribeiro-Kumara, C., Di Prima, S., Pastor, A., Rumpel, C., Seeger, M., Daliakopoulos, I., Daskalakou, E., Koutroulis, A., Papadopoulou, M.P., Stampoulidis, K., Xanthopoulos, G., Aszalós, R., Balázs, D., Kertész, M., Valkó, O., Finger, D.C., Thorsteinsson, T., Till, J., Bajocco, S., Gelsomino, A., Amodio, A.M., Novara, A., Salvati, L., Telesca, L., Ursino, N., Jansons, A., Kitenberga, M., Stivrins, N., Brazaitis, G., Marozas, V., Cojocaru, O., Gumeniuc, I., Sfecla, V., Imeson, A., Veraverbeke, S., Mikalsen, R.F., Koda, E., Osinski, P., Castro, A.C.M., Nunes, J.P., Oom, D., Vieira, D., Rusu, T., Bojović, S., Djordjevic, D., Popovic, Z., Protic, M., Sakan, S., Glasa, J., Kacikova, D., Lichner, L., Majlingova, A., Vido, J., Ferk, M., Tičar, J., Zorn, M., Zupanc, V., Hinojosa, M.B., Knicker, H., Lucas-Borja, M.E., Pausas, J., Prat-Guitart, N., Ubeda, X., Vilar, L., Destouni, G., Ghajarnia, N., Kalantari, Z., Seifollahi-Aghmiuni, S., Dindaroglu, T., Yakupoglu, T., Smith, T., Doerr, S., Cerda, A., 2021. Current Wildland Fire Patterns and Challenges in Europe: A Synthesis of National Perspectives. Air, Soil and Water Research 14, 11786221211028185. https://doi.org/10.1177/11786221211028185

Ferreira, D., Mateus, C., Santos, X., 2016. Responses of reptiles to fire in transition zones are mediated by bioregion affinity of species. Biodivers Conserv 25, 1543–1557. https://doi.org/10.1007/s10531-016-1137-3

Ferreira, D., Žagar, A., Santos, X., 2017. Uncovering the rules of (Reptile) species coexistence in transition zones between bioregions. Salamandra 53, 193–200.

Fluet-Chouinard, E., Stocker, B.D., Zhang, Z., Malhotra, A., Melton, J.R., Poulter, B., Kaplan, J.O., Goldewijk, K.K., Siebert, S., Minayeva, T., Hugelius, G., Joosten, H., Barthelmes, A., Prigent, C., Aires, F., Hoyt, A.M., Davidson, N., Finlayson, C.M., Lehner, B., Jackson, R.B., McIntyre, P.B., 2023. Extensive global wetland loss over the past three centuries. Nature 614, 281–286. https://doi.org/10.1038/s41586-022-05572-6

Franklin, M.J.M., Major, R.E., Bedward, M., Price, O.F., Bradstock, R.A., 2022. Forest avifauna exhibit enduring responses to historical high-severity wildfires. Biol. Conserv. 269. https://doi.org/10.1016/j.biocon.2022.109545

Fyllas, N.M., Koufaki, T., Sazeides, C.I., Spyroglou, G., Theodorou, K., 2022. Potential Impacts of Climate Change on the Habitat Suitability of the Dominant Tree Species in Greece. Plants 11, 1616. https://doi.org/10.3390/plants11121616

Gaget, E., Jung, M., Lewis, M., Hofhansl, F., Jane Graham, L., Warren-Thomas, E., Visconti, P., 2025. Reviewing and benchmarking ecological modelling practices in the context of land use. Ecography. https://doi.org/10.1002/ecog.07745

Gallai, N., Salles, J.-M., Settele, J., Vaissière, B.E., 2009. Economic valuation of the vulnerability of world agriculture confronted with pollinator decline. Ecological Economics 68, 810–821. https://doi.org/10.1016/j.ecolecon.2008.06.014

García-Duro, J., Cruz, O., Casal, M., Reyes, O., 2019. Fire as driver of the expansion of Paraserianthes lophantha (Willd.) I. C. Nielsen in SW Europe. Biol Invasions 21, 1427–1438. https://doi.org/10.1007/s10530-018-01910-w

Gerber, G., 2025. Wildfire and Biodiversity Meta-Analysis Dataset (European Forests). https://doi.org/10.5281/ZENODO.15800907

Ghermandi, A., Nunes, P.A.L.D., 2013. A global map of coastal recreation values: Results from a spatially explicit meta-analysis. Ecological Economics, Sustainable Urbanisation: A resilient future 86, 1–15. https://doi.org/10.1016/j.ecolecon.2012.11.006

Giorgis, M.A., Zeballos, S.R., Carbone, L., Zimmermann, H., Von Wehrden, H., Aguilar, R., Ferreras, A.E., Tecco, P.A., Kowaljow, E., Barri, F., Gurvich, D.E., Villagra, P., Jaureguiberry, P., 2021. A review of fire effects across South American ecosystems: the role of climate and time since fire. fire ecol 17, 11. https://doi.org/10.1186/s42408-021-00100-9

González, T.M., González-Trujillo, J.D., Muñoz, A., Armenteras, D., 2022. Effects of fire history on animal communities: a systematic review. Ecol. Processes 11. https://doi.org/10.1186/s13717-021-00357-7

Grau-Andrés, R., Moreira, B., Pausas, J.G., 2024. Global plant responses to intensified fire regimes. Global Ecology and Biogeography 33, e13858. https://doi.org/10.1111/geb.13858

Gusti, M., 2010. An algorithm for simulation of forest management decisions in the global forest model. Shtuchniy Intelekt 4, 45–49.

Gusti, M., Di Fulvio, F., Biber, P., Korosuo, A., Forsell, N., 2020. The Effect of Alternative Forest Management Models on the Forest Harvest and Emissions as Compared to the Forest Reference Level. Forests 11, 794. https://doi.org/10.3390/f11080794

Gutiérrez-Hernández, O., García, L.V., 2021. Chapter 11 - Relationship between precipitation and species distribution, in: Rodrigo-Comino, J. (Ed.), Precipitation. Elsevier, pp. 239–259. https://doi.org/10.1016/B978-0-12-822699-5.00010-0

Hacket-Pain, A., Bogdziewicz, M., 2021. Climate change and plant reproduction: trends and drivers of mast seeding change. Phil. Trans. R. Soc. B 376, 20200379. https://doi.org/10.1098/rstb.2020.0379

Hallegatte, S., Green, C., Nicholls, R.J., Corfee-Morlot, J., 2013. Future flood losses in major coastal cities. Nature Clim Change 3, 802–806. https://doi.org/10.1038/nclimate1979

Hardy, C.C., 2005. Wildland fire hazard and risk: Problems, definitions, and context. Forest Ecology and Management 211, 73–82. https://doi.org/10.1016/j.foreco.2005.01.029

Harris, C., Balfour, N.J., Ratnieks, F.L.W., 2024. Seasonal variation in the general availability of floral resources for pollinators in northwest Europe: A review of the data. Biological Conservation 298, 110774. https://doi.org/10.1016/j.biocon.2024.110774

Havlík, P., Schneider, U.A., Schmid, E., Böttcher, H., Fritz, S., Skalský, R., Aoki, K., Cara, S.D., Kindermann, G., Kraxner, F., Leduc, S., McCallum, I., Mosnier, A., Sauer, T., Obersteiner, M., 2011. Global

land-use implications of first and second generation biofuel targets. Energy Policy 39, 5690–5702. https://doi.org/10.1016/j.enpol.2010.03.030

Howard, J., Sutton-Grier, A., Herr, D., Kleypas, J., Landis, E., Mcleod, E., Pidgeon, E., Simpson, S., 2017. Clarifying the role of coastal and marine systems in climate mitigation. Frontiers in Ecology and the Environment 15, 42–50. https://doi.org/10.1002/fee.1451

Jonkman, S.N., Hillen, M.M., Nicholls, R.J., Kanning, W., Ledden, M. van, 2013. Costs of Adapting Coastal Defences to Sea-Level Rise— New Estimates and Their Implications. coas 29, 1212–1226. https://doi.org/10.2112/JCOASTRES-D-12-00230.1

Jung, M., 2023a. An integrated species distribution modelling framework for heterogeneous biodiversity data. Ecological Informatics 76, 102127. https://doi.org/10.1016/j.ecoinf.2023.102127

Jung, M., 2023b. ibis.insights: An R implementation of the InSiGHTS framework.

Khan, A.M., Li, Q., Saqib, Z., Khan, N., Habib, T., Khalid, N., Majeed, M., Tariq, A., 2022. MaxEnt Modelling and Impact of Climate Change on Habitat Suitability Variations of Economically Important Chilgoza Pine (Pinus gerardiana Wall.) in South Asia. Forests 13, 715. https://doi.org/10.3390/f13050715

Kim, T.N., Holt, R.D., 2012. The direct and indirect effects of fire on the assembly of insect herbivore communities: examples from the Florida scrub habitat. Oecologia 168, 997–1012. https://doi.org/10.1007/s00442-011-2130-x

Kindermann, G., Obersteiner, M., Sohngen, B., Sathaye, J., Andrasko, K., Rametsteiner, E., Schlamadinger, B., Wunder, S., Beach, R., 2008. Global cost estimates of reducing carbon emissions through avoided deforestation. Proc. Natl. Acad. Sci. U.S.A. 105, 10302–10307. https://doi.org/10.1073/pnas.0710616105

Kirwan, M.L., Temmerman, S., Skeehan, E.E., Guntenspergen, G.R., Fagherazzi, S., 2016. Overestimation of marsh vulnerability to sea level rise. Nature Clim Change 6, 253–260. https://doi.org/10.1038/nclimate2909

Krutilla, J.V., 1967. Conservation Reconsidered. The American Economic Review 57, 777–786.

Kummu, M., Taka, M., Guillaume, J.H.A., 2018. Gridded global datasets for Gross Domestic Product and Human Development Index over 1990–2015. Sci Data 5, 180004. https://doi.org/10.1038/sdata.2018.4

Leclère, D., Obersteiner, M., Barrett, M., Butchart, S.H.M., Chaudhary, A., De Palma, A., DeClerck, F.A.J., Di Marco, M., Doelman, J.C., Dürauer, M., Freeman, R., Harfoot, M., Hasegawa, T., Hellweg, S., Hilbers, J.P., Hill, S.L.L., Humpenöder, F., Jennings, N., Krisztin, T., Mace, G.M., Ohashi, H., Popp, A., Purvis, A., Schipper, A.M., Tabeau, A., Valin, H., Van Meijl, H., Van Zeist, W.-J., Visconti, P., Alkemade, R., Almond, R., Bunting, G., Burgess, N.D., Cornell, S.E., Di Fulvio, F., Ferrier, S., Fritz, S., Fujimori, S., Grooten, M., Harwood, T., Havlík, P., Herrero, M., Hoskins, A.J., Jung, M., Kram, T., Lotze-Campen, H., Matsui, T., Meyer, C., Nel, D., Newbold, T., Schmidt-Traub, G., Stehfest, E.,

Strassburg, B.B.N., Van Vuuren, D.P., Ware, C., Watson, J.E.M., Wu, W., Young, L., 2020. Bending the curve of terrestrial biodiversity needs an integrated strategy. Nature 585, 551–556. https://doi.org/10.1038/s41586-020-2705-y

Leonhardt, S.D., Gallai, N., Garibaldi, L.A., Kuhlmann, M., Klein, A.-M., 2013. Economic gain, stability of pollination and bee diversity decrease from southern to northern Europe. Basic and Applied Ecology 14, 461–471. https://doi.org/10.1016/j.baae.2013.06.003

Mason, S.C., Shirey, V., Ponisio, L.C., Gelhaus, J.K., 2021. Responses from bees, butterflies, and ground beetles to different fire and site characteristics: A global meta-analysis. Biological Conservation 261, 109265. https://doi.org/10.1016/j.biocon.2021.109265

Mattos, C.T., Ruellas, A.C.D.O., 2015. Systematic review and meta-analysis: What are the implications in the clinical practice? Dental Press J. Orthod. 20, 17–19. https://doi.org/10.1590/2176-9451.20.1.017-019.ebo

Mcleod, E., Chmura, G.L., Bouillon, S., Salm, R., Björk, M., Duarte, C.M., Lovelock, C.E., Schlesinger, W.H., Silliman, B.R., 2011. A blueprint for blue carbon: toward an improved understanding of the role of vegetated coastal habitats in sequestering CO2. Frontiers in Ecology and the Environment 9, 552–560. https://doi.org/10.1890/110004

Mcowen, C.J., Weatherdon, L.V., Bochove, J.-W.V., Sullivan, E., Blyth, S., Zockler, C., Stanwell-Smith, D., Kingston, N., Martin, C.S., Spalding, M., Fletcher, S., 2017. A global map of saltmarshes. Biodiversity Data Journal 5, e11764. https://doi.org/10.3897/BDJ.5.e11764

Menéndez, P., Losada, I.J., Torres-Ortega, S., Narayan, S., Beck, M.W., 2020. The Global Flood Protection Benefits of Mangroves. Sci Rep 10, 4404. https://doi.org/10.1038/s41598-020-61136-6

Moldoveanu, O.C., Maggioni, M., Dani, F.R., 2024. Environmental ameliorations and politics in support of pollinators. Experiences from Europe: A review. Journal of Environmental Management 362, 121219. https://doi.org/10.1016/j.jenvman.2024.121219

Moyo, S., 2022. Community Responses to Fire: A Global Meta-Analysis Unravels the Contrasting Responses of Fauna to Fire. Earth 3, 1087–1111. https://doi.org/10.3390/earth3040063

Muhammad, W., Ahmad, M., Ahmad, I., 2020. Pollination Behavior of Cotton Crop and Its Management, in: Ahmad, S., Hasanuzzaman, M. (Eds.), Cotton Production and Uses. Springer Singapore, Singapore, pp. 163–175. https://doi.org/10.1007/978-981-15-1472-2_10

Murray, N.J., Phinn, S.R., DeWitt, M., Ferrari, R., Johnston, R., Lyons, M.B., Clinton, N., Thau, D., Fuller, R.A., 2019. The global distribution and trajectory of tidal flats. Nature 565, 222–225. https://doi.org/10.1038/s41586-018-0805-8

Newton, A., Icely, J., Cristina, S., Perillo, G.M.E., Turner, R.E., Ashan, D., Cragg, S., Luo, Y., Tu, C., Li, Y., Zhang, H., Ramesh, R., Forbes, D.L., Solidoro, C., Béjaoui, B., Gao, S., Pastres, R., Kelsey, H., Taillie, D., Nhan, N., Brito, A.C., de Lima, R., Kuenzer, C., 2020. Anthropogenic, Direct Pressures on Coastal Wetlands. Front. Ecol. Evol. 8. https://doi.org/10.3389/fevo.2020.00144

Nicholls, R.J., Hinkel, J., Lincke, D., van der Pol, Thomas, 2019. Global Investment Costs for Coastal Defense through the 21st Century. Policy Research working paper no. WPS 8745 Washington, D.C. : World Bank Group.

Nicholls, R.J., Marinova, N., Lowe, J.A., Brown, S., Vellinga, P., de Gusmão, D., Hinkel, J., Tol, R.S.J., 2011. Sea-level rise and its possible impacts given a 'beyond 4°C world' in the twenty-first century. Philosophical Transactions of the Royal Society A: Mathematical, Physical and Engineering Sciences 369, 161–181. https://doi.org/10.1098/rsta.2010.0291

Nunes, 2006. Carabid (Coleoptera) Community Changes Following Prescribed Burning and the Potential Use of Carabids as Indicators Species to Evaluate the Effects of Fire Management in Mediterranean Regions. Silva Lusitana.

OECD, 2018. Cost-Benefit Analysis and the Environment: Further Developments and Policy Use. Organisation for Economic Co-operation and Development, Paris.

Olson, D.M., Dinerstein, E., Wikramanayake, E.D., Burgess, N.D., Powell, G.V.N., Allnut, T.F., Ricketts, T.H., Kura, Y., Lamoreux, J.F., Wettengel, W.W., Hedao, P., Kassem, K.R., 2001. Terrestrial ecoregions of the world: a new map of life on Earth. BioScience 51, 933–938.

Page, M.J., McKenzie, J.E., Bossuyt, P.M., Boutron, I., Hoffmann, T.C., Mulrow, C.D., Shamseer, L., Tetzlaff, J.M., Akl, E.A., Brennan, S.E., Chou, R., Glanville, J., Grimshaw, J.M., Hróbjartsson, A., Lalu, M.M., Li, T., Loder, E.W., Mayo-Wilson, E., McDonald, S., McGuinness, L.A., Stewart, L.A., Thomas, J., Tricco, A.C., Welch, V.A., Whiting, P., Moher, D., 2021. The PRISMA 2020 statement: an updated guideline for reporting systematic reviews. BMJ n71. https://doi.org/10.1136/bmj.n71

Passovoy, M.D., Fulé, P.Z., 2006. Snag and woody debris dynamics following severe wildfires in northern Arizona ponderosa pine forests. Forest Ecology and Management 223, 237–246. https://doi.org/10.1016/j.foreco.2005.11.016

Pereira, H.M., Martins, I.S., Rosa, I.M.D., Kim, H., Leadley, P., Popp, A., Van Vuuren, D.P., Hurtt, G., Quoss, L., Arneth, A., Baisero, D., Bakkenes, M., Chaplin-Kramer, R., Chini, L., Di Marco, M., Ferrier, S., Fujimori, S., Guerra, C.A., Harfoot, M., Harwood, T.D., Hasegawa, T., Haverd, V., Havlík, P., Hellweg, S., Hilbers, J.P., Hill, S.L.L., Hirata, A., Hoskins, A.J., Humpenöder, F., Janse, J.H., Jetz, W., Johnson, J.A., Krause, A., Leclère, D., Matsui, T., Meijer, J.R., Merow, C., Obersteiner, M., Ohashi, H., De Palma, A., Poulter, B., Purvis, A., Quesada, B., Rondinini, C., Schipper, A.M., Settele, J., Sharp, R., Stehfest, E., Strassburg, B.B.N., Takahashi, K., Talluto, M.V., Thuiller, W., Titeux, N., Visconti, P., Ware, C., Wolf, F., Alkemade, R., 2024. Global trends and scenarios for terrestrial biodiversity and ecosystem services from 1900 to 2050. Science 384, 458–465. https://doi.org/10.1126/science.adn3441

Posit Team, 2025. RStudio: Integrated Development Environment for R.

Potts, S.G., Imperatriz-Fonseca, V., Ngo, H.T., Biesmeijer, J.C., Breeze, T.D., Dicks, L.V., Garibaldi, L.A., Hill, R., Settele, J., Vanbergen, A.J., 2016. The assessment report on pollinators, pollination and food production: summary for policymakers. Secretariat of the Intergovernmental Science-Policy Platform on Biodiversity ….

Puig-Gironès, R., Brotons, L., Pons, P., Franch, M., 2023. Examining the temporal effects of wildfires on forest birds: Should I stay or should I go? For. Ecol. Manage. 549. https://doi.org/10.1016/j.foreco.2023.121439

R Core Team, 2024. R: A Language and Environment for Statistical Computing.

Rao, N.S., Ghermandi, A., Portela, R., Wang, X., 2015. Global values of coastal ecosystem services: A spatial economic analysis of shoreline protection values. Ecosystem Services, Marine Economics and Policy related to Ecosystem Services: Lessons from the World's Regional Seas 11, 95–105. https://doi.org/10.1016/j.ecoser.2014.11.011

Reguero, B.G., Beck, M.W., Bresch, D.N., Calil, J., Meliane, I., 2018. Comparing the cost effectiveness of nature-based and coastal adaptation: A case study from the Gulf Coast of the United States. PLoS ONE 13, e0192132. https://doi.org/10.1371/journal.pone.0192132

Reguero, B.G., Beck, M.W., Schmid, D., Stadtmüller, D., Raepple, J., Schüssele, S., Pfliegner, K., 2020. Financing coastal resilience by combining nature-based risk reduction with insurance. Ecological Economics 169, 106487. https://doi.org/10.1016/j.ecolecon.2019.106487

Reverté, S., Miličić, M., Ačanski, J., Andrić, A., Aracil, A., Aubert, M., Balzan, M.V., Bartomeus, I., Bogusch, P., Bosch, J., Budrys, E., Cantú-Salazar, L., Castro, S., Cornalba, M., Demeter, I., Devalez, J., Dorchin, A., Dufrêne, E., Đorđević, A., Fisler, L., Fitzpatrick, Ú., Flaminio, S., Földesi, R., Gaspar, H., Genoud, D., Geslin, B., Ghisbain, G., Gilbert, F., Gogala, A., Grković, A., Heimburg, H., Herrera-Mesías, F., Jacobs, M., Janković Milosavljević, M., Janssen, K., Jensen, J., Ješovnik, A., Józan, Z., Karlis, G., Kasparek, M., Kovács-Hostyánszki, A., Kuhlmann, M., Le Divelec, R., Leclercq, N., Likov, L., Litman, J., Ljubomirov, T., Madsen, H.B., Marshall, L., Mazánek, L., Milić, D., Mignot, M., Mudri-Stojnić, S., Müller, A., Nedeljković, Z., Nikolić, P., Ødegaard, F., Patiny, S., Paukkunen, J., Pennards, G., Pérez-Bañón, C., Perrard, A., Petanidou, T., Pettersson, L.B., Popov, G., Popov, S., Praz, C., Prokhorov, A., Quaranta, M., Radchenko, V.G., Radenković, S., Rasmont, P., Rasmussen, C., Reemer, M., Ricarte, A., Risch, S., Roberts, S.P.M., Rojo, S., Ropars, L., Rosa, P., Ruiz, C., Sentil, A., Shparyk, V., Smit, J., Sommaggio, D., Soon, V., Ssymank, A., Ståhls, G., Stavrinides, M., Straka, J., Tarlap, P., Terzo, M., Tomozii, B., Tot, T., Van Der Ent, L., Van Steenis, J., Van Steenis, W., Varnava, A.I., Vereecken, N.J., Veselić, S., Vesnić, A., Weigand, A., Wisniowski, B., Wood, T.J., Zimmermann, D., Michez, D., Vujić, A., 2023. National records of 3000 European bee and hoverfly species: A contribution to pollinator conservation. Insect Conserv Diversity 16, 758–775. https://doi.org/10.1111/icad.12680

Rey, L., Kéry, M., Sierro, A., Posse, B., Arlettaz, R., Jacot, A., 2019. Effects of forest wildfire on inner-Alpine bird community dynamics. PLoS ONE 14. https://doi.org/10.1371/journal.pone.0214644

Roberts, D.R., Bahn, V., Ciuti, S., Boyce, M.S., Elith, J., Guillera-Arroita, G., Hauenstein, S., Lahoz-Monfort, J.J., Schröder, B., Thuiller, W., Warton, D.I., Wintle, B.A., Hartig, F., Dormann, C.F., 2017. Cross-validation strategies for data with temporal, spatial, hierarchical, or phylogenetic structure. Ecography 40, 913–929. https://doi.org/10.1111/ecog.02881

Rosenberger, R.S., Loomis, J.B., 2017. Benefit Transfer, in: Champ, P.A., Boyle, K.J., Brown, T.C. (Eds.), A Primer on Nonmarket Valuation, The Economics of Non-Market Goods and Resources. Springer Netherlands, Dordrecht, pp. 431–462. https://doi.org/10.1007/978-94-007-7104-8_11

Rossi, J.L., Chatelon, F.J., Marcelli, T., 2020. Fire Intensity, in: Manzello, S.L. (Ed.), Encyclopedia of Wildfires and Wildland-Urban Interface (WUI) Fires. Springer International Publishing, Cham, pp. 391–397. https://doi.org/10.1007/978-3-319-52090-2_51

Rubinigg Michael, 2024. Socioeconomic data on pollinators. https://doi.org/10.13140/RG.2.2.23481.68969

Rumpf, S.B., Gravey, M., Brönnimann, O., Luoto, M., Cianfrani, C., Mariethoz, G., Guisan, A., 2022. From white to green: Snow cover loss and increased vegetation productivity in the European Alps. Science 376, 1119–1122. https://doi.org/10.1126/science.abn6697

Santos, X., Mateos, E., Bros, V., Brotons, L., Mas, E., Herraiz, J.A., Herrando, S., Miño, À., Olmo-Vidal, J.M., Quesada, J., Ribes, J., Sabaté, S., Sauras-Yera, T., Serra, A., Vallejo, V.R., Viñolas, A., 2014. Is response to fire Influenced by dietary specialization and mobility? A comparative study with multiple animal assemblages. PLoS ONE 9, 88224.

Sasmito, S.D., Murdiyarso, D., Friess, D.A., Kurnianto, S., 2016. Can mangroves keep pace with contemporary sea level rise? A global data review. Wetlands Ecol Manage 24, 263–278. https://doi.org/10.1007/s11273-015-9466-7

Schiavina, M., Freire, S., MacManus, K., 2023. GHS-POP R2023A - GHS population grid multitemporal (1975-2030). https://doi.org/10.2905/2FF68A52-5B5B-4A22-8F40-C41DA8332CFE

Schuerch, M., Spencer, T., Temmerman, S., Kirwan, M.L., Wolff, C., Lincke, D., McOwen, C.J., Pickering, M.D., Reef, R., Vafeidis, A.T., Hinkel, J., Nicholls, R.J., Brown, S., 2018. Future response of global coastal wetlands to sea-level rise. Nature 561, 231–234. https://doi.org/10.1038/s41586-018-0476-5

Sgardelis, S.P., Pantis, J.D., Argyropoulou, M.D., Stamou, G.P., 1995. Effects of Fire on Soil Macroinvertebrates in a Mediterranean Phryganic Ecosystem. Int. J. Wildland Fire 5, 113-121,. https://doi.org/10.1071/wf9950113.

Spencer, T., Schuerch, M., Nicholls, R.J., Hinkel, J., Lincke, D., Vafeidis, A.T., Reef, R., McFadden, L., Brown, S., 2016. Global coastal wetland change under sea-level rise and related stresses: The DIVA Wetland Change Model. Global and Planetary Change 139, 15–30. https://doi.org/10.1016/j.gloplacha.2015.12.018

Swengel, A.B., Swengel, S.R., 2007. Benefit of permanent non-fire refugia for Lepidoptera conservation in fire-managed sites. J Insect Conserv 11, 263–279. https://doi.org/10.1007/s10841-006-9042-9

Taillardat, P., Thompson, B.S., Garneau, M., Trottier, K., Friess, D.A., 2020. Climate change mitigation potential of wetlands and the cost-effectiveness of their restoration. Interface Focus 10, 20190129. https://doi.org/10.1098/rsfs.2019.0129

Thuiller, W., Guéguen, M., Renaud, J., Karger, D.N., Zimmermann, N.E., 2019. Uncertainty in ensembles of global biodiversity scenarios. Nat Commun 10, 1446. https://doi.org/10.1038/s41467-019-09519-w

Toivanen, 2014. Emulating natural disturbances in boreal Norway spruce forests: Effects on ground beetles (Coleoptera, Carabidae. Forest Ecology and Management.

Ury, E.A., Yang, X., Wright, J.P., Bernhardt, E.S., 2021. Rapid deforestation of a coastal landscape driven by sea-level rise and extreme events. Ecological Applications 31, e02339. https://doi.org/10.1002/eap.2339

Vafeidis, A.T., Nicholls, R.J., McFadden, L., Tol, R.S.J., Hinkel, J., Spencer, T., Grashoff, P.S., Boot, G., Klein, R.J.T., 2008. A New Global Coastal Database for Impact and Vulnerability Analysis to Sea-Level Rise. Journal of Coastal Research 244, 917–924. https://doi.org/10.2112/06-0725.1

Vafeidis, A.T., Schuerch, M., Wolff, C., Spencer, T., Merkens, J.L., Hinkel, J., Lincke, D., Brown, S., Nicholls, R.J., 2019. Water-level attenuation in global-scale assessments of exposure to coastal flooding: a sensitivity analysis. Nat. Hazards Earth Syst. Sci. 19, 973–984. https://doi.org/10.5194/nhess-19-973-2019

Vallecillo, S., La Notte, A., Polce, C., Zulian, G., Alexandris, N., Ferrini, S., Maes, J., 2018. Ecosystem services accounting. Part I, Outdoor recreation and crop pollination. (No. EUR 29024 EN; JRC110321). Publications Office of the European Union, Luxembourg.

van der Werf, G.R., Randerson, J.T., Giglio, L., Van Leeuwen, T.T., Chen, Y., Rogers, B.M., Mu, M., Van Marle, M.J.E., Morton, D.C., Collatz, G.J., Yokelson, R.J., Kasibhatla, P.S., 2017. Global fire emissions estimates during 1997–2016. Earth Syst. Sci. Data 9, 697–720. https://doi.org/10.5194/essd-9-697-2017

van Zelst, V.T.M., Dijkstra, J.T., van Wesenbeeck, B.K., Eilander, D., Morris, E.P., Winsemius, H.C., Ward, P.J., de Vries, M.B., 2021. Cutting the costs of coastal protection by integrating vegetation in flood defences. Nat Commun 12, 6533. https://doi.org/10.1038/s41467-021-26887-4

Versluijs, M., Eggers, S., Mikusiński, G., Roberge, J.-M., Hjältén, J., 2020. Foraging behavior of the eurasian three-toed woodpecker (Picoides tridactylus) and its implications for ecological restoration and sustainable boreal forest management. Avian Conserv. Ecology 15, 1–11. https://doi.org/10.5751/ACE-01477-150106

Viechtbauer, W., 2010. Conducting Meta-Analyses in *R* with the **metafor** Package. J. Stat. Soft. 36. https://doi.org/10.18637/jss.v036.i03

Visconti, P., Bakkenes, M., Baisero, D., Brooks, T., Butchart, S.H.M., Joppa, L., Alkemade, R., Di Marco, M., Santini, L., Hoffmann, M., Maiorano, L., Pressey, R.L., Arponen, A., Boitani, L., Reside, A.E., Van Vuuren, D.P., Rondinini, C., 2016. Projecting Global Biodiversity Indicators under Future Development Scenarios: Projecting biodiversity indicators. CONSERVATION LETTERS 9, 5–13. https://doi.org/10.1111/conl.12159

Visconti, P., Jung, M., Leclere, D., Ringwald, M., Chapman, L., Gusti, M., Balkovi\vc, J., Ondo, I., Maney, C., Fjardo, J., Harrison, M., Faustino, C., Hill, S., Lessa Derci Augustynczik, A., Di Fulvio, F., Deppermann, A., Kesting, M., Witzke, P., Havlik, P., 2024. BIOCLIMA: Assessing Land use, Climate and Biodiversity impacts of land-based climate mitigation and biodiversity policies in the EU. https://doi.org/10.10.2779/37660

Wardhaugh, C.W., 2015. How many species of arthropods visit flowers? Arthropod-Plant Interactions 9, 547–565. https://doi.org/10.1007/s11829-015-9398-4

Yamazaki, D., Ikeshima, D., Tawatari, R., Yamaguchi, T., O'Loughlin, F., Neal, J.C., Sampson, C.C., Kanae, S., Bates, P.D., 2017. A high-accuracy map of global terrain elevations. Geophysical Research Letters 44, 5844–5853. https://doi.org/10.1002/2017GL072874